UNIVERSITY OF OKLAHOMA

GRADUATE COLLEGE

KINETIC STUDIES ON THE ROLE OF HYDROGEN-BONDING INTERACTIONS IN THE TiO_2 PHOTOOXIDATION OF SMALL POLAR ORGANIC COMPOUNDS IN AQUEOUS SOLUTION

A DISSERTATION

SUBMITTED TO THE GRADUATE FACULTY

in partial fulfillment of the requirements for the

Degree of

DOCTOR OF PHILOSOPHY

By

CAROLINA SALAZAR-BALLESTEROS
Norman, Oklahoma
2009

KINETIC STUDIES ON THE ROLE OF HYDROGEN-BONDING INTERACTIONS IN THE TiO_2 PHOTOOXIDATION OF SMALL POLAR ORGANIC COMPOUNDS IN AQUEOUS SOLUTION

A DISSERTATION APPROVED FOR THE
DEPARTMENT OF CHEMISTRY AND BIOCHEMISTRY

BY

Dr. George Richter-Addo, Chair

Dr. Mark A. Nanny

Dr. Kenneth M. Nicholas

Dr. Richard W. Taylor

Dr. Robert L. White

ACKNOWLEDGEMENTS

I would like to express my most sincere gratitude to my major professor, Dr. Mark A. Nanny, for providing me with an interesting project and for his guidance and encouragement throughout its completion. I would also like to extend my gratitude to the other members of my committee, Drs. Kenneth M. Nicholas, Richard W. Taylor, Robert L. White and my former advisor, Dr. George Richter-Addo (chair of my committee as well). Thank you for your helpful suggestions and for the time you have devoted to me.

I would like to deeply thank my parents, Luis René Salazar and Sara Ballesteros, and my sisters, Adriana and Laura, for their endless love, faith, and support. This accomplishment is as much theirs as it is mine.

I owe special thanks to my friends Olajumoke Olowu, Jun Yi (Eva), and Praveen Gadad. Thank you for lending your helping hands and for giving me the strength to hang on.

Very special thanks go out to Mr. Thornton Carpenter and Mr. Ricky Frnka, technical support specialists at Shimadzu. Your act of kindness meant more than words can say. You were God-sent angels to me.

Additionally, I would like to thank NASA for providing the funding for this research. I also recognize that my graduate studies at the University of Oklahoma would not have been possible without the financial assistance of the Department of Chemistry and Biochemistry (teaching assistantships) and the School of Civil Engineering and Environmental Science (research assistantships).

Finally, I want to thank my Heavenly Father who has given me strength with his love and who answered my prayers.

TABLE OF CONTENTS

LIST OF TABLES

APPENDICES

LIST OF FIGURES

ABSTRACT

Drinking and hygiene water sustainability is a current concern due to the rapid pace of global urbanization and the vast coverage gap between urban and rural areas worldwide. Therefore, water recycling has become a necessity to alleviate the fragile state of most of the planet's water resources and has prompted the search for viable and efficient alternatives for wastewater treatment. In response to this search, Advanced Oxidation Processes (AOP), like UV/TiO_2 heterogeneous photocatalysis, have arisen and are being extensively investigated.

The general goal of this research was to study, characterize, and model the TiO_2-mediated photocatalytic degradation (PCD) of small polar organic compounds (SPOC) as a function of typical water parameters (pH, carbonate-bicarbonate alkalinity, and ionic strength) in order to determine possible base-case conditions that may translate into an efficient photocatalytic method for a final water polishing step. Similarly, we aimed to find experimental evidence that may indicate the important role that hydrogen-bonding interactions may play in the photooxidation of SPOC at the catalyst surface.

Our results showed that the fastest initial degradation rates of model SPOC (isopropanol and acetone) occurred in a pH range 6.04 - 8.61 were the optimal conditions for adsorption through hydrogen-bonding to the TiO_2 surface and optimum concentration of hydroxyl radicals coincided.

The kinetic data that resulted from the effect of carbonate-bicarbonate alkalinity in the application of TiO_2 heterogeneous photocatalysis for the oxidation of acetone and isopropanol showed that the extent of inhibition on their initial rates of degradation varied according to the type of anions and radicals ($CO_3^{-\bullet}$/ $HCO_3^{\bullet}$) present in the

photocatalytic systems. Although it is known that the carbonate anion adsorbs to a less extent on the TiO_2 surface than bicarbonate anion, the higher ability for scavenging of hydroxyl radicals of the former had a more detrimental effect on the photodegradation rates of our target compounds at the pH of 10.35. The inhibitory effect of carbonate anions on the photodegradation of isopropanol and acetone was suppressed at the highly basic pH of 12.0.

Under the joint effect of pH and ionic strength, the PCD rates of isopropanol and acetone were susceptible to changes in the Brönsted acid/base character of the TiO_2 surface site speciation and depicted the greater enhancement with the increase in ionic strength at pH 6.04 (for isopropanol) and 8.61 (for acetone). Further support to the role of hydrogen-bonding interactions on the PCD of our model SPOC was obtained from the study of 1:1 binary mixtures, since isopropanol, the substrate bearing the best hydrogen-bonding capacities, degraded predominantly in our systems.

Although the construction of a ranking of degradation at the TiO_2 surface on the basis of hydrogen-bonding abilities was not possible with the addition of a third model compound (dimethylsulfoxide), the overall data collected in our studies showed a good correlation between the enhancement in the PCD reaction rates of the model SPOC and the increase in the Brönsted acid/base character of the surface speciation.

Keywords: TiO_2 heterogeneous photocatalysis, pH, carbonate-bicarbonate alkalinity, ionic strength, hydrogen-bonding interactions, small polar organic compounds, isopropanol, acetone, dimethylsulfoxide.

CHAPTER 1

Introduction

1.1. The surface of titanium dioxide and the interface with aqueous solution

1.1.1. Water chemisorption

It is known that both common forms of titanium dioxide (TiO_2), anatase and rutile, have the 6-3 crystal configuration. That is, in the bulk of each solid the titanium ion is surrounded by six oxygen neighbors, while three titanium atoms coordinate to each oxygen atom [Parfitt, 1976]. Contrary to the interior situation, vacant coordination sites are present on the crystal surface. Therefore, when water (as vapor or liquid) enters in contact with the TiO_2 surface the coordination sphere in the Ti^{4+} ion is filled with chemisorbed water [Boehm, 1971; Bourikas et al., 2001]. Once this step occurs, the surface has the ability to dissociate a proton from the water molecule adsorbed on the metal site resulting in the transfer of a proton to the neighbor surface oxide ion (the bridging two-coordinated O^{2-}). This process results in the formation of two types of surface hydroxyl groups [1]: one on the metal site having monodentate attachment (i.e., singly-coordinated or terminal OH group) and another on the oxide site which is bidentate (i.e., doubly-coordinated or bridging OH group) [Boehm, 1971; Bourikas et al., 2001]. This model of surface hydroxylation has general validity and has been confirmed by infrared studies [Griffiths and Rochester, 1977; Jackson and Parfitt, 1971; Jones and Hockey, 1971a, 1971b, 1972; Lewis and Parfitt, 1966; Munuera and Stone, 1971; Primet et al., 1971; Rochester, 1986; Suda and Morimoto, 1987a; Yates, 1961]. Although the

[1] As stated by Boehm (1971) the bonding in TiO_2, as well as in most other metal oxides, is not purely ionic. Therefore, it is valid to speak of OH groups instead of OH^- ions.

process is described for the (001) face of anatase in Figure 1.1, the model is applicable to other crystal faces in both anatase and rutile [Boehm, 1971; Henderson, 1996].

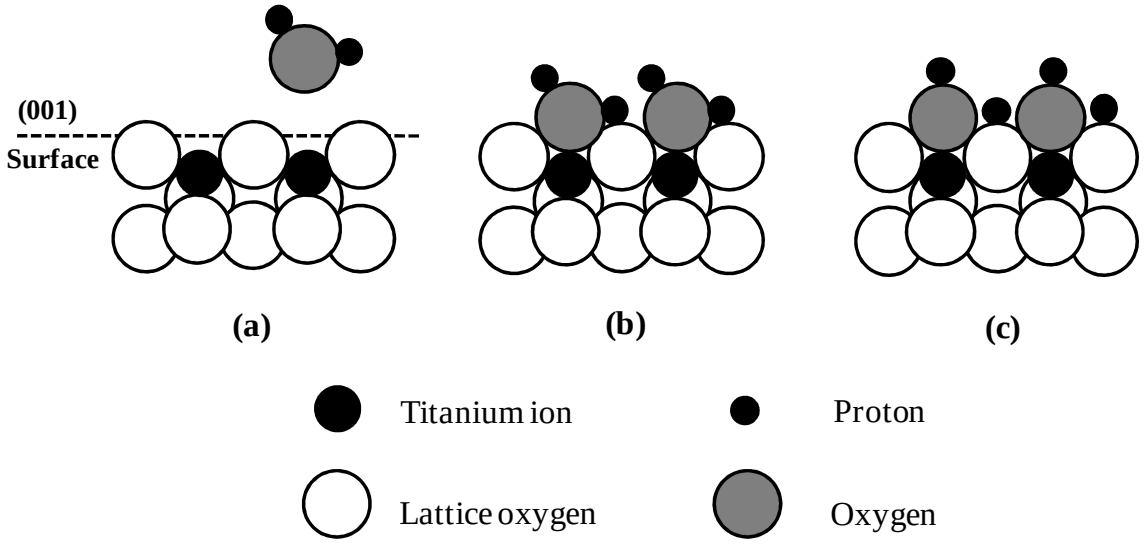

Figure 1.1. Structure of the anatase (001) face (a) hydroxyl-free surface, (b) chemiadsorption of water, (c) dissociation of water to form two distinct hydroxyl groups; (reproduced from Turchi and Ollis (1990), p. 179, Figure 1).

Due to the different coordination environments, the surface hydroxyl groups are expected to show different chemical behavior. Boehm (1971) suggested that the doubly-coordinated surface hydroxyl group has an acidic character, while the singly-coordinated OH group is predominantly basic in character and may participate in ligand exchange reactions with other anions. These differences in chemical behavior have been used to develop experimental procedures that would appear to yield the number of available OH surface groups.

Van Veen et al. (1985) used a fluoride exchange reaction method to determine the number of basic, singly-coordinated OH groups in a TiO_2 sample from Degussa (P25

TiO_2 [2]). They reported a value of 0.14 mmol g^{-1} (or 1.7 sites nm^{-2}) and confirmed that the F^- exchange is in fact with basic hydroxyl groups only by following the infrared spectrum bands of both types of surface hydroxyl groups.

On the other hand, base adsorption experiments were used to determine the number of acidic OH groups in TiO_2 [Boehm, 1971; Rodríguez et al., 1996]. From the adsorption isotherms of KOH on TiO_2 (P25 type) Rodríguez et al. (1996) calculated that the number of acidic groups available at the surface was 2.97 $x10^{-6}$ mol m^{-2} (or 1.79 sites nm^{-2}).

1.1.2. The primary charging behavior of TiO_2

The mechanism by which the surface charge of titanium dioxide in contact with aqueous solution is established is due to a two step process: the hydroxylation due to dissociative water chemisorption followed by simple ionization of the surface hydroxyl groups. The mechanism of the first step was already explained but the effect on the local effective charge of individual surface species will be described as follows.

In ionic structures the principle of electroneutrality implies that the charge of a cation is compensated by the charge of the surrounding anions [Boehm, 1971; Hiemstra et al., 1989]. According to Pauling's principle the degree of neutralization of charge can be expressed per bond. This leads to the definition of formal bond valence (ν) as the charge (z) of cation divided by its coordination number (CN). On the surface of TiO_2 there is a lack of neutralization of charge due to insaturation of the coordination sphere of Ti^{4+} ions. According to Pauling's electrostatic valence rule, to neutralize the charge of

[2] The most common commercial brand of TiO_2 used in photocatalytic studies is the P25 type from Degussa Corp.

Ti^{4+} ions (z = +4, CN = 6, ν = +2/3) the singly- and doubly-coordinated anions on the surface should have the "ideal charges" of -2/3 and -4/3, respectively [Boehm, 1971; Hiemstra et al., 1989]. The charge -1 of each of the hydroxide anions formed after dissociative water chemisorption comes nearer to the "ideal values" and, therefore, the hydroxylation brings more stability to the exposed surface [Boehm, 1971; Hiemstra et al., 1989]. From the above it derives that for a proper book keeping of charges residual values must be given to individual surface species formed after dissociative water chemisorption. That is, the singly-coordinated surface group is designated as $\equiv Ti\text{-}OH^{1/3-}$, while the doubly-coordinated hydroxyl site is depicted as $\equiv Ti_2\text{-}OH^{1/3+}$ (the latter group will be shorthanded to $\equiv OH^{1/3+}$ for convenience) [Hiemstra et al., 1989].

As we already mentioned, the other contribution to surface charge comes from the proton equilibria between the surface hydroxyl groups and the contacting solution. Almost two decades ago, Hiemstra et al. (1989) formulated a multisite complexation (MUSIC) model that accounted for the proton adsorption reactions of all three types of surface oxygen groups that may occur on the surface of TiO_2: singly- ($TiO^{4/3-}$), doubly- ($Ti_2O^{2/3-}$), and triply- (Ti_3O^{0}) coordinated [3] [Hiemstra et al., 1989; Hiemstra and Riemsdijk, 1991].

Making use of a combination of crystallographic data and physical chemical considerations, Hiemstra et al. (1989) predicted that although each type of surface group may adsorb in principle two protons, the affinity constants associated to the protonation steps on one type of surface group differ by approximately 14 log K units. This

[3] The triply-coordinated oxygen plays no part in the dissociative water chemisorption process because the oxygen is tri-coordinated to the metal ion as are all the oxygen atoms inside the lattice. Therefore, it does not have undersaturation.

prediction has the consequence that species such as $Ti_2OH_2^{4/3+}$ [4] and $TiO^{4/3-}$ will not be present at the interface of TiO_2 with aqueous solutions [Hiemstra et al., 1989]. In addition, the protonation of the tri-coordinated group is not possible in the normal pH range (log K = 7.5; Hiemstra et al., 1989). Therefore, the charging behavior of TiO_2 is only due to the proton equilibria [5]:

$$\equiv Ti\text{-}OH_2^{2/3+} \leftrightarrow \equiv Ti\text{-}OH^{1/3-} + H^+ \qquad K_{a1} \qquad (1.1)$$

$$\equiv OH^{1/3+} \leftrightarrow \equiv O^{2/3-} + H^+ \qquad K_{a2} \qquad (1.2)$$

Using the multisite model, Rodríguez et al. (1996) calculated the values of the intrinsic surface equilibrium constants for Degussa P25 TiO_2 [6] as $pK_{a1} = 5.38$ and $pK_{a2} = 7.60$. These values of the proton dissociation constants imply that neutral surface groups do not exist at the surface [Hiemstra et al., 1989]. However, the neutrality condition can be attained when the surface concentration of hydroxyl groups with the same residual charge but opposite in sign are equal. This condition is known as the point of zero charge (pH_{zpc} = 6.5 for P25 TiO_2; Rodríguez et al., 1996).

1.1.3. The electrical double layer

The picture of the solid/water interface of TiO_2 is not complete without describing the structure of the electrical double layer, which is schematically represented in Figure 1.2.

[4] According to the nomenclature adopted in this work the $Ti_2OH_2^{4/3+}$ would be shorthanded to $\equiv OH_2^{4/3+}$.
[5] H_s^+ is the local proton near the TiO_2 surface.
[6] This commercial brand of TiO_2 is commonly used in photocatalytic studies and it is employed in this research.

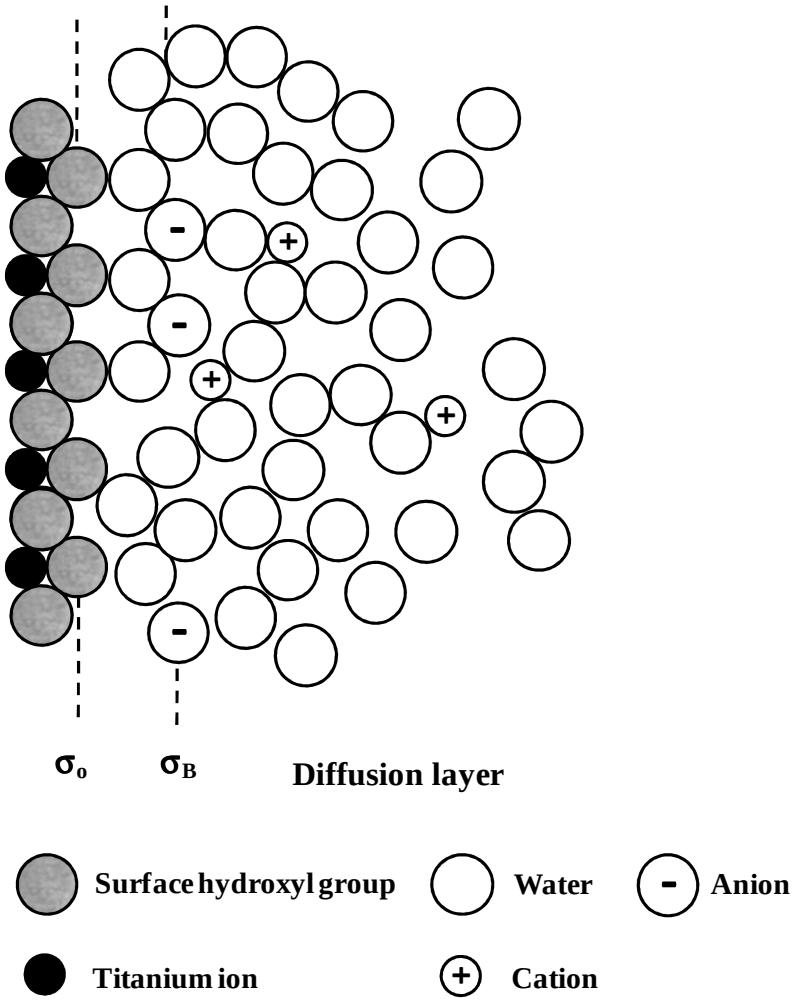

Figure 1.2. Schematic representation of the electrical double layer formed at the TiO_2/aqueous interface (reproduced from Bérubé and de Bruyn (1968), p. 99, Figure 7).

In this idealized planar surface model the surface hydroxyl groups constitute the plane of surface charge, σ_o. The σ_o plane is followed by an oriented layer of water molecules which is normally referred as the Stern layer. Bérubé and de Bruyn (1968) proposed that the surface hydroxyl groups impose order in the surrounding liquid through hydrogen-bonding and the thickness of this ordered structure of the Stern layer can be extended by intermolecular hydrogen-bonding of the adsorbed water molecules. This

view is supported by experimental evidence obtained from infrared [Lewis and Parfitt, 1966; Yates; 1961], gas adsorption [Dawson, 1967; Jurinak, 1964], and heats of adsorption [Hollabaugh and Chessick, 1961] studies regarding the multilayer adsorption of water on TiO_2.

From the above evolves that the opposing ordering forces of the Stern layer and the bulk solution (or diffuse layer) create a transition region characterized by a great disorganization of the liquid medium [Bérubé and de Bruyn, 1968]. It is proposed that this region is the focal point for the establishment of the electrical double layer and is pictured as the σ_B plane in Figure 1.2. It is in this plane where the hydrated ions of the contacting electrolyte solution locate to counterbalance the surface charge of TiO_2 [Bourikas et al., 2001]. Yates et al. (1974) suggested that this counterbalance effect is due to the formation of "ion pairs" between the electrolyte ions and the charged surface hydroxyl groups with the agency of the structured water molecules.

According to this approach, the "ion pairs" are considered as outer sphere complexes without forming strong chemical bonds with the surface hydroxyl groups [Bourikas et al., 2001]. Only those ions that may participate in ligand exchange reactions with the singly coordinated hydroxyl group may penetrate the Stern layer and form inner sphere complexes [Hiemstra et al., 1991]. Bérubé and de Bruyn (1968) suggested that the potential determining ions (H^+ and OH^-) reach the σ_o plane because they can hydrogen-bond to the water molecules forming the Stern layer.

From this basic model of the double layer it derives that due to the distance between the two electrostatic planes, σ_o and σ_B, the TiO_2/aqueous interface can be seen as a plate condenser. The analysis and mathematical treatment of the electrical double layer

as a condenser are given in several publications and it will not be presented here [Boddy, 1965; Danielli et al., 1973; Morrison, 1971].

The model of the electrical double layer described above in combination with the multisite complexation model have been used to calculate theoretical values of surface charge densities of the potential determining ions and the potential at the σ_B plane. These values have shown to be consistent with experimental data obtained from acid/base titrations and electrokinetic potential determinations on TiO_2 suspensions [Hiemstra and Van Riemsdijk, 1991; Rodríguez et al., 1996; Yates et al., 1974].

1.2 Primary events in heterogeneous photocatalysis and formation of hydroxyl radicals

The initiating event in heterogeneous photocatalysis processes is the excitation of the catalyst by a photon ($\lambda \leq 388$ nm) with energy equal or greater than the band gap energy of TiO_2 ($E_{bg} \cong 3.2$ eV) [De Lasa et al., 2005]. This photoexcitation generates mobile electrons (e^-) in the conduction band (E_{CB}) and positive holes (h^+) in the valence band (E_{VB}) of the TiO_2 semiconductor [De Lasa et al., 2005]. Both species rapidly migrate to the surface. However, for the photocatalytic process to be productive the h^+ and e^- must rapidly participate in charge trapping processes at the TiO_2 particle surface before their recombination occurs, as depicted in Figure 1.3 [Fox and Dulay, 1993].

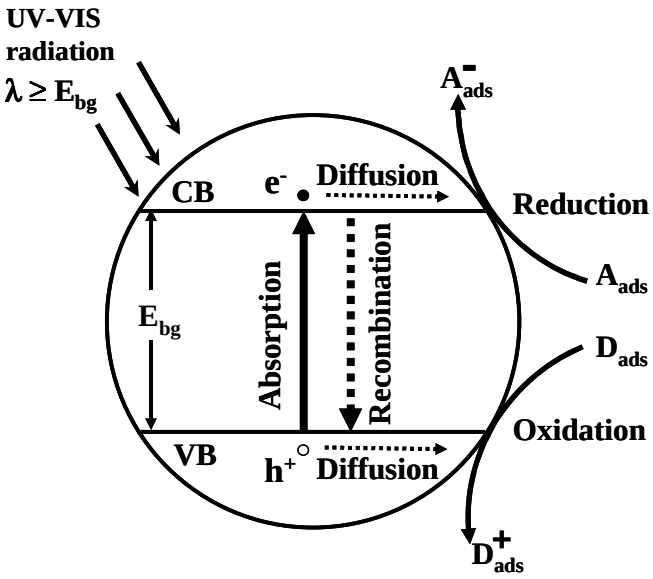

Figure 1.3. Schematic photoactivation of a TiO_2 particle followed by carrier trapping events (A: electron acceptor, D: electron donor, CB: conduction band, VB: valence band, E_{BG}: band-gap energy (reproduced from Öppenlander (2003), p. 67, Figure 3.17)

Considerable research has been devoted to determine the pathways by which initial trapping of photogenerated holes and electrons occur in TiO_2 particles and identify the subsequent reaction products. It is fairly well accepted that electrons are trapped at Ti^{4+} sites to form Ti^{3+} centers [Howe and Grätzel, 1985, 1987]. Howe and Grätzel (1987) observed that the electron paramagnetic resonance (EPR) signal attributed to the interstitial Ti^{3+} formed on irradiation in vacuo of a hydrated TiO_2 (anatase) sample was absent in the EPR spectrum taken when the irradiation was performed in the presence of oxygen. The results suggested that oxygen functions as a very efficient electron acceptor (A_{ads} in Figure 1.3) in photocatalytic systems [Howe and Grätzel, 1987]. Other gas-solid studies over highly hydroxylated TiO_2 also confirm the interaction of O_2 with the

conduction band electron (e_{CB}^-) which can be summarized in equation 1.3 and 1.4 [7] [Boonstra and Mutsaers, 1975; Gonzalez-Elipe et al., 1979; Munuera et al., 1979].

$$Ti^{4+} + e_{CB}^- \rightarrow Ti^{3+} \quad (1.3)$$

$$Ti^{3+} + (O_2)_{ads} \leftrightarrow (O_2^{-\bullet})_{ads} \quad (1.4)$$

It has been suggested that the process described above would be similar when the TiO_2 catalyst is suspended in an oxygenated aqueous solution [Herrman and Pichat, 1980]. In partial support of this view are the findings of Howe and Grätzel (1985) who reported EPR observations of the Ti^{3+} species on irradiation of colloidal TiO_2 dispersions in the presence of hole scavengers. Although oxygen adsorption studies in the aqueous phase are not possible, it is reasonable to suggest that if the Ti^{3+} centers are formed in aqueous photocatalytic systems then it is likely that electrons trapped near the surface of the TiO_2 particle are transferred to nearby O_2 molecules [Gerischer and Heller, 1991]. Therefore, in the absence of any other electron scavenger dissolved oxygen acts as the electron acceptor in aqueous TiO_2 slurries.

Far less clear are the charge trapping processes for the photogenerated holes in terms of where the hole traps are located in the TiO_2 particles. Using EPR spectroscopy to examine the paramagnetic species produced on a hydroxylated TiO_2 (anatase) sample upon UV irradiation, Howe and Grätzel (1987) proposed that the hole trap cannot be located on the surface layer itself but it may be at a lattice oxide anion immediately below the surface. Therefore, they described the subsurface hole trap as a (Ti^{4+}-$O^{-\bullet}$) radical, in accordance with other authors [Bahnemann et al., 1984a,b ; Henglein, 1988].

[7] The (ads) subscript indicates that the species are adsorbed on the TiO_2 surface.

Several other investigators suggested that the hole is trapped by surface hydroxyl groups present on the surface of TiO_2 and, therefore, the initial product of hole trapping is an adsorbed hydroxyl radical, $OH^{\bullet}$ [Anpo et al., 1985; Jaeger and Bard, 1979; Rajh et al., 1992; Turchi and Ollis, 1990]. Lawless et al. (1991) suggested that a $OH^{\bullet}$ radical adsorbed at the particle surface is indistinguishable from a hole trapped on a subsurface oxide anion. These authors used an experimental approach that consisted of oxidizing the hydroxylated TiO_2 particles suspended in aqueous solution with pulse radiolytically generated $OH^{\bullet}$ radicals in order to yield the "trapped holes" (i.e., the adsorbed $OH^{\bullet}$) on the surface. Lawless et al. (1991) studied the adsorption characteristics of the product of such reaction and observed a broad band centered at about 350 nm. Their observation was in close agreement with the spectral features for a hole trapped on a subsurface oxide anion as reported by Bahnemann and co-workers [Bahnemann et al., 1984a].

Based on these findings, the following resonance structure between the $OH^{\bullet}$ radical formed by hole trapping in a surface hydroxyl group and the hole trapped in a lattice oxide anion was proposed [8]:

$$\{\{Ti^{4+}\text{-}O^{2-}Ti^{4+}\}\text{-}OH^{\bullet} \leftrightarrow \{Ti^{4+}\text{-}O^{-\bullet}\text{-}Ti^{4+}\}\text{-}OH^{-}\} \qquad (1.5)$$

As can be inferred from equation 1.5, there is a prevailing view that the hydroxyl group acting as the hole trap is the terminal or singly-coordinated hydroxyl group due to its higher electron density [Micic et al., 1993; Rajh et al., 1992]. According to this view,

[8] The notation used in Equation 1.5 considers that the $OH^{\bullet}$ radical is formed by trapping of a hole in a surface hydroxyl anion. This notation considers the bonding in TiO_2 as purely ionic, although evidence for a covalent contribution is known [Parfitt, 1976]. Therefore, the residual charges assigned to surface hydroxyl groups as presented by the MUSIC model (using Pauling's rule) are not given. Unification of respective notations is lacking, hence they are used interchangeably in the literature.

the formation of hydroxyl radicals under basic and acidic pH conditions occurs according to Equations 1.6 and 1.7, respectively [9] [Salvador, 2007].

$$\equiv Ti_S^{4+} - OH^- + h_f^+ \rightarrow \equiv Ti_S^{4+}\text{-}OH^\bullet \quad (1.6)$$

$$\equiv Ti_S^{4+} - OH_2 + h_f^+ \rightarrow \equiv Ti_S^{4+}\text{-}OH^\bullet + H^+_{aq} \quad (1.7)$$

However, a number of researchers claim that this hypothesis is a misconception in TiO_2 photocatalysis [Monllor-Satoca, 2007; Salvador, 2007]. From the analysis of the electronic structure of adsorbed water on TiO_2, Salvador (2007) stated that hydroxyl groups specifically adsorbed on terminal (surface) Ti^{4+} ions cannot be photooxidized with free holes photogenerated under UV supra-band gap irradiation ($h\nu \geq 3.0$ eV). Therefore, the authors proposed that the only surface hole trap is the surface hydroxyl group associated with the O_s^{2-} terminal ion. Salvador (2007) explained that previous experimental evidence concerning the trapped hole as a subsurface ($Ti^{4+}\text{-}O^{-\bullet}$) radical should be reinterpreted as being associated to holes trapped at the bridging surface hydroxyl group. In a fashion similar to the previous hypothesis, this hydroxyl group can trap the photoproduced hole in its deprotonated or protonated form as depicted in Equations 1.8 and 1.9, respectively [10] [Salvador, 2007].

$$\equiv O_s^{2-} + h_f^+ \rightarrow \equiv O_s^{-\bullet} \quad (1.8)$$

$$\equiv O_s^{2-} + H^+_{aq} + h_f^+ \rightarrow \equiv OH_s^\bullet \quad (1.9)$$

[9] This notation assumes that the bonding in TiO_2 is purely ionic. h_f^+ indicates the free hole. The subscripts (s) and (aq) mean surficial ions and aqueous species, respectively.
[10] The product of hole trapping in Equation 1.8 is the conjugate base of the hydroxyl radical, the oxide radical anion.

1.3 Pathways of degradation in heterogeneous photocatalysis

The TiO_2-mediated photocatalytic oxidation of organic compounds in aqueous solution takes place through two mechanisms of interfacial hole transfer: direct and indirect.

The interfacial direct transfer mechanism occurs when the free holes reach the surface and are trapped by an organic solute specifically adsorbed on the TiO_2 surface. If the sorptive interactions of the organic substrate with the TiO_2 surface involve inner-sphere coordination with the underlying metal ion, the surface complex can sustain a direct charge transfer [Mao et al., 1991; Regazzoni et al., 1998; Sakata et al., 1984; Sun and Pignatello, 1995; Tunesi and Anderson, 1991]. Organic compounds capable of such strong interaction are those possessing ligand donor groups (e.g., carboxylic, hydroxyl, or amino groups) and the stereochemical configuration to form rings in their chelate complexes with the catalyst surface. The ligand groups in these molecules can displace the OH^- from a titanium center (i.e., the singly-coordinated surface hydroxyl group) [Regazzoni et al., 1998; Rodríguez et al., 1996; Stone et al., 1993; Vasudevan and Stone, 1996]. Photooxidation through direct electron transfer has been suggested for salicylic acid [Regazzoni et al., 1998; Tunesi and Anderson, 1991] and 2,4-dichlorophenoxyacetic acid [Sun and Pignatello, 1995]. The ability of the carboxylate group of these compounds to directly coordinate to Ti^{4+} ions facilitates the reaction. As an example, Regazzoni et al. (1998) proposed the following tentative surface complexation equilibria between salicylic acid and the TiO_2 surface.

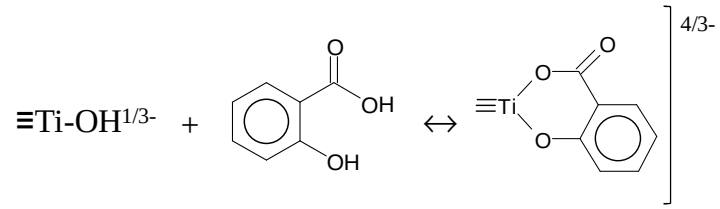

(1.10)

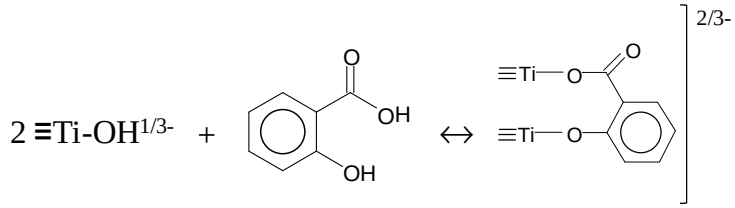

(1.11)

On the other hand, the interfacial indirect transfer mechanism takes place via a surface-bound $OH^{\bullet}$ radical (or its conjugate base) and a substrate that establishes a weak electronic interaction with the surface (i.e., outer-sphere forces). In this reaction model the hydroxyl radicals are considered as surface trapped holes, hence the name indirect transfer [Monllor-Satoca et al., 2007]. For this pathway, the adsorbed hydroxyl radical behaves like its free counterpart in that they tend to abstract hydrogen atoms or add to aromatic rings or double bonds in their reactions with organic compounds [Öppenlander, 2003; Sun and Pignatello, 1995]. A photodegradation mechanism through adsorbed hydroxyl radicals has been proposed for aliphatic hydrocarbons [Izumi et al., 1980], halogenated hydrocarbons [Kormann et al., 1991] and aromatic compounds like phenol [Okamoto et al., 1985; Tunesi and Anderson, 1991] and 4-chlorophenol [Tunesi and Anderson, 1991].

1.4 Adsorption and degradation pathways of isopropanol and acetone in TiO_2 photocatalytic systems

A combination of adsorption isotherms, infrared spectroscopy, temperature programmed desorption and gas chromatographic methods have been used to study the

adsorption of acetone and isopropanol in solid/gas systems employing both dehydroxylated and hydroxylated TiO_2 surfaces [Bickley et al., 1973; Coronado et al., 2003; El-Maazawi et al., 2000; Henderson, 2004; Kim et al., 1988; Munuera and Stone, 1971; Xu et al., 2003]. It has been demonstrated that acetone and isopropanol can be molecularly adsorbed in fully dehydroxylated TiO_2 surfaces. These adsorption modes occur through the formation of coordinate bonds with Ti^{4+} ions by utilizing the free electron pairs of the oxygen atoms in their respective functional groups [Bickley et al., 1973; Coronado et al., 2003; El-Maazawi et al., 2000; Henderson, 2004; Kim et al., 1988; Munuera and Stone, 1971; Xu et al., 2003]. These adsorption modes are shown in Figure 1.4. (a, b).

On the other hand, on partially hydroxylated [11] TiO_2 surfaces reversible physisorption of these two substrates also takes place and occurs by hydrogen-bonding with surface hydroxyl groups [Bickley et al., 1973; Munuera and Stone, 1971]. This mode of adsorption has also been reported for other aliphatic alcohols such as methanol, ethanol, and 1-propanol in TiO_2/gas studies [Hollabaugh and Chessick, 1961; Suda et al., 1987b]. Although it has been observed from infrared studies that after adsorption of the alcohol vapor on the hydroxylated surface the adsorption band due to free surface OH groups diminishes remarkably or completely disappears [Suda et al., 1987b], little has been said about specific structures for this bonding. Only Munuera and Stone (1971) proposed possible structures for the hydrogen-bonding of acetone and isopropanol in a partially hydroxylated TiO_2 surface involving the doubly coordinated OH group. These are presented in Figure 1.4 (c,d).

[11] A partially hydroxylated TiO_2 surface consists of isolated 5-coordinated Ti^{4+} ions, isolated O^{2-} ions and both types of surface hydroxyl groups.

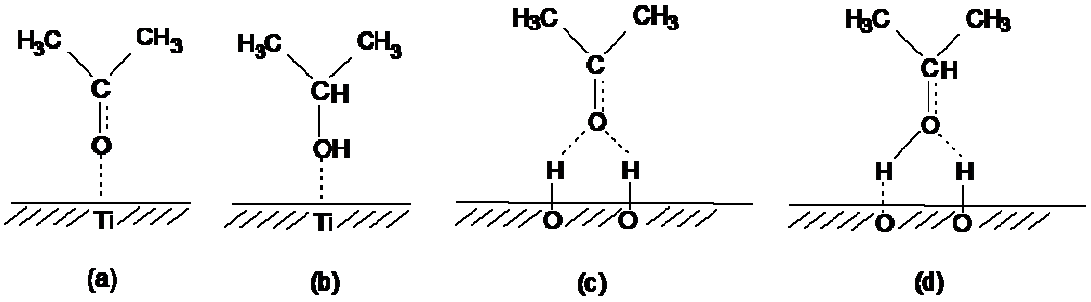

Figure 1.4. Proposed adsorption modes of acetone and isopropanol on a partially hydroxylated TiO_2 surface (reproduced from Munuera and Stone (1971), p. 213).

Contrary to the observations in solid/gas studies, in aqueous media the chemisorption of isopropanol and acetone should be negligible. In TiO_2/aqueous systems, isopropanol and acetone do not favorably compete with water for chemisorption to the TiO_2 surface. Therefore, alkoxyde complexes [12] (≡Ti-OR) or molecularly adsorbed species coordinated to the Ti^{4+} ions that have been observed at the TiO_2/gaseous interface are completely absent in TiO_2/aqueous systems. Mandelbaum et al. (1999) reported that no single feature that could reveal alcohol chemisorption on TiO_2 has been detected by ATR-FTIR. In addition, it is known from relative adsorption strength studies in TiO_2/gas systems that isopropanol does not displace the coordinatively adsorbed water and that water has the ability to dislodge acetone from its Ti^{4+} adsorption center [Bickley et al., 1973; Munuera and Stone, 1971].

In the light of the above, isopropanol and acetone are not expected to strongly bind to the TiO_2 surface in contact with their aqueous solution through adsorption modes (a) and (b) as shown in Figure 1.4. Similarly to the TiO_2/gas studies on fully

[12] The alkoxyde complex is formed by dissociative chemisorption of an alcohol. In a similar fashion to chemisorption of water, the molecularly adsorbed alcohol can dissociated to produce both a surface alkoxyde (≡Ti-OR) and a surface hydroxyl group [Suda et al., 1987].

prehydroxylated surfaces [Suda et al, 1987], in the aqueous media isopropanol and acetone exclusively adsorb through hydrogen-bonding to the primary layer of OH groups formed by dissociative water chemisorption on the TiO_2 surface.

Since it is known that at least two types of surface hydroxyl groups exist on a hydroxylated TiO_2 surface and that they undergo proton equilibria reactions [Boehm, 1971; Hiemstra and Van Riemsdijk, 1989], adsorption modes involving the singly- and double-coordinated OH groups in their protonated and deprotonated forms could be envisaged. Some structures may be proposed and are given in Figure 1.5.

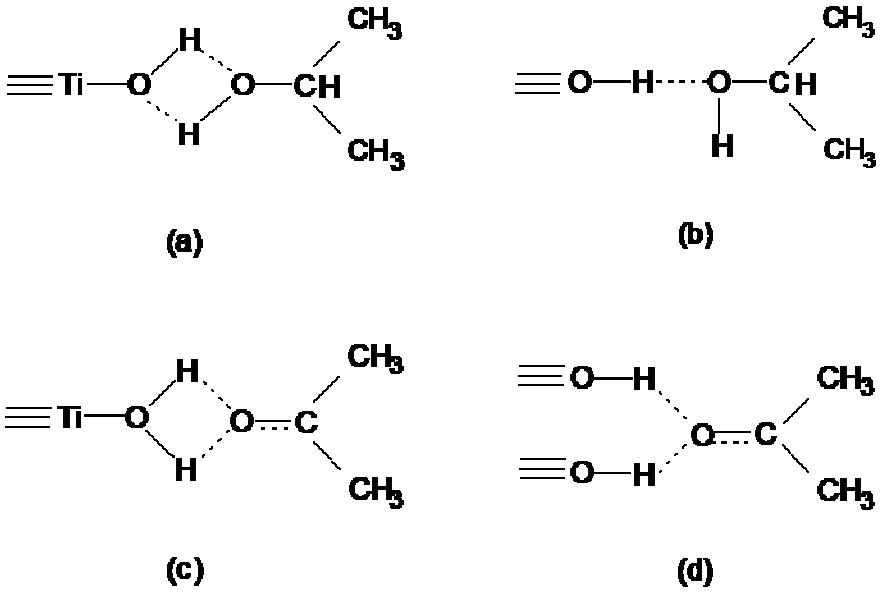

Figure 1.5. Possible hydrogen-bonding structures of isopropanol and acetone on the TiO_2 surface in contact with their aqueous solution (this work).

Since the adsorption of isopropanol and acetone may involve an outer sphere interaction with the TiO_2 surface through formation of hydrogen-bonds with surface hydroxyl groups, it is reasonable to suggest that their degradation pathway in TiO_2/aqueous systems occur via indirect electron transfer with adsorbed hydroxyl

radicals. Several authors have proposed the scheme of isopropanol photooxidation and it is summarized in Figure 1.6 [Cundall et al., 1976; Harvey et al., 1983; Sakaguchi et al., 2006; Ohko et al., 1997; Yamagata et al., 1988].

In this scheme, the photogenerated $OH^{\bullet}$ radical on the TiO_2 surface initiates the degradation reaction by abstracting a hydrogen atom from isopropanol. In a pulse radiolytic study of the site of $OH^{\bullet}$ radical attack on aliphatic alcohols in aqueous solution, Asmus et al. (1973) determined that abstraction of a hydrogen atom from the α-position seems in general to be preferred. Therefore, the initial step of isopropanol decomposition yields an α-alcohol radical (1-hydroxyl-1-methylethyl radical) that can decompose to acetone through three pathways [Ohko et al., 1997; Sakaguchi et al, 2006]: (1) liberation of a proton and electron transfer to the conduction band of TiO_2 (pathway I), a process known as current-doubling reaction, [13] (2) reaction with molecular oxygen to produce an unstable peroxo radical, the 1-hydroxy-1-methylethyl dioxyl radical (pathway II), and (3) reaction with hydroperoxyl ($HO_2^{\bullet}$) radical which can be formed through pathway II or through the protonation of the superoxide anion radical obtained in Equation 1.4 ($O_2^{-\bullet} + H^+ \leftrightarrow HO_2^{\bullet}$, $pK_a = 5$; Brinkley and Engel, 1998). These pathways of degradation have been proposed based on experimental evidence obtained by pulse radiolysis, spin trapping, photocurrent measurement, and product analysis [Ilan et al., 1976; Mandelbaum et al., 1999; Miyake et al., 1976; Yamagata et al., 1988].

[13] The whole current doubling reaction consists in that the alcohol donates two electrons to the semiconductor. One electron is donated to the valence band and the resultant radical with high electron potential injects another electron into the conduction band. In the case of isopropanol the first electron transfer occurs through the indirect process involving the hydroxyl radical [Mandelbaum et al., 1999; Yamagata et al., 1988]

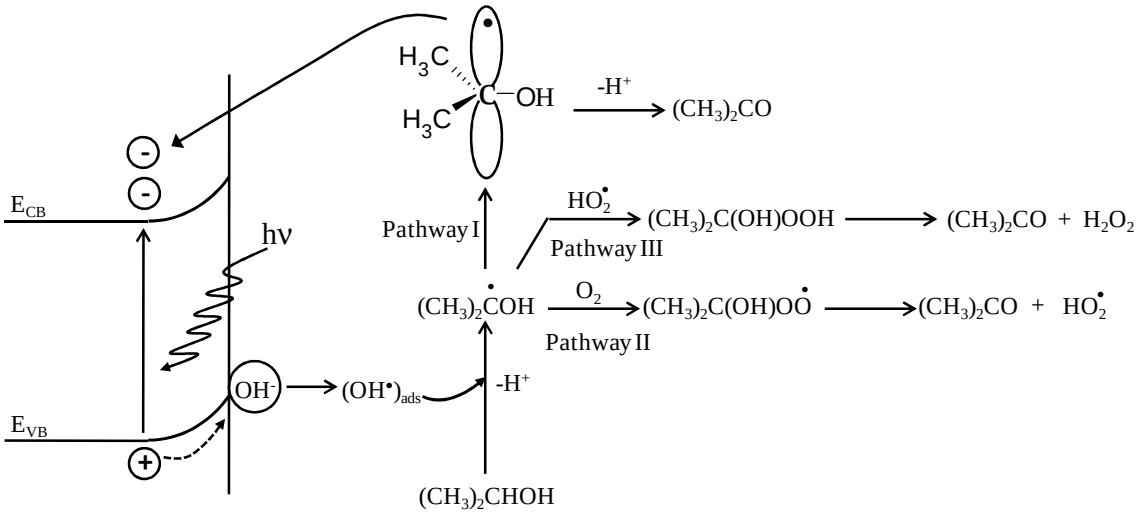

Figure 1.6. Reaction mechanism of isopropanol photooxidation on illuminated TiO_2 (partially reproduced from Yamagata et al. (1988), p. 3433, Figure 5).

For acetone, on the other hand, the following reaction scheme is consistent with observations from gas and ion chromatographic studies on its degradation through hydroxyl radicals produced by photolysis of hydrogen peroxide in aqueous solution [Stefan et al., 1996]. Since adsorbed hydroxyl radicals are believed to behave like its free counterpart [Sun and Pignatello, 1995] this reaction scheme may be applicable to UV/TiO_2 systems.

In a similar fashion to the case of isopropanol, the hydroxyl radical initiates the decomposition of acetone by hydrogen abstraction (Equation 1.12).

$$OH^{\bullet} + CH_3COCH_3 \rightarrow {}^{\bullet}CH_2COCH_3 + H_2O \qquad (1.12)$$

The acetonyl radical formed in Equation 1.12 reacts with molecular oxygen resulting in the production of a peroxyl radical.

$${}^{\bullet}CH_2COCH_3 + O_2 \rightarrow {}^{\bullet}OOCH_2COCH_3 \qquad (1.13)$$

The acetonylperoxyl radical can react by one of two routes. One route is a radical-radical reaction (Equation 1.14) followed by a β-scission (Equation 1.15).

$$2\ {}^{\bullet}OOCH_2COCH_3 \rightarrow 2\ {}^{\bullet}OCH_2COCH_3 + O_2 \quad (1.14)$$

$${}^{\bullet}OCH_2COCH_3 \rightarrow HCHO + {}^{\bullet}COCH_3 \quad (1.15)$$

The acetyl radical from Equation 1.15 can dissociate (Equation 1.16) or react with oxygen (Equation 1.18). This route generates formaldehyde and acetic acid.

$${}^{\bullet}COCH_3 \rightarrow CO + CH_3{}^{\bullet} \quad (1.16)$$

$$CH_3{}^{\bullet} + O_2 \rightarrow CH_3OO{}^{\bullet} \quad (1.17)$$

$${}^{\bullet}COCH_3 + O_2 \rightarrow {}^{\bullet}OOCOCH_3 \quad (1.18)$$

$$CH_3OO{}^{\bullet} + {}^{\bullet}OOCOCH_3 \rightarrow HCHO + CH_3COOH + O_2 \quad (1.19)$$

The second alternative route of the acetonylperoxyl radical is a six-membered atom rearrangement followed by a β-scission (Equation 1.20). Further reaction of the products thus formed generates acetic acid and formic acid (Equations 1.21 and 1.22).

$${}^{\bullet}OOCH_2COCH_3 \rightarrow [HOOCH_2COCH_2{}^{\bullet}] \rightarrow {}^{\bullet}CH_2OOH + CH_2CO \quad (1.20)$$

$$CH_2CO + H_2O \rightarrow CH_3COOH \quad (1.21)$$

$${}^{\bullet}CH_2OOH + O_2 \rightarrow HCOOH + HO_2{}^{\bullet} \quad (1.22)$$

1.5 Motivation and objectives of this research

The photocatalytic oxidation of small polar organic compounds (SPOC) like isopropanol and acetone by UV-illuminated TiO_2 has been more widely studied in the gas/solid [Bickley et al., 1973; Bickley and Jayanty, 1974; Brinkley and Engel, 1998;

Chang et al., 2004; Coronado et al., 2003a, b; Cunningham and Hodnett, 1981; El-Maazawi et al., 2000; Hager and Bauer, 1999; Henderson, 2004; Kozlov et al., 2003; Larson et al., 1995; Ohko et al., 1997; Peral and Ollis, 1992; Xu and Raftery, 2001a,b; Xu et al., 2003] than in the liquid/solid interface [Cundall et al., 1976; Cunningham and Srijaranai, 198; Harvey et al., 1983; Kado et al., 2001; Mandelbaum et al., 1999; Miyake et al, 1976; Sakaguchi et al., 2006; Yamagata et al., 1988]. This is probably due to the fact that they are major contaminants in indoor air and air streams. However, their presence in water, even at low concentrations, is also a concern and their removal to acceptable levels has already been reported as a challenge in an advanced water recovery system developed by NASA [14] [Verostko et al., 2000]. Therefore, a better understanding on the TiO_2-mediated photocatalytic oxidation of SPOC (e.g., isopropanol and acetone) is necessary if the ultimate goal is to apply this promising technique for the final polishing of waste- and graywater in order to attain hygiene and drinking water standards.

The research that has been devoted to the study of the photocatalytic decomposition of isopropanol in liquid systems expands to several aspects. Some of the studies in aqueous TiO_2-suspensions of isopropanol have focused on elucidating the mechanisms underlying the photodegradation reaction pathways in aqueous medium [Cunningham and Srijaranai, 1988; Mandelbaum et al., 1999; Miyake et al., 1976; Yamagata et al., 1988]. The knowledge gained from these studies promoted the use of photoinduced oxidation of isopropanol as a test reaction to determine the efficiency of different TiO_2 preparations or photocatalytic reaction systems [Harada et al., 1999; Villacres et al., 2003; Yamashita et al., 1998]. However, there is a lack of bench-scale studies on the effect of practical parameters in the photodecomposition of isopropanol

[14] National Aeronautics and Space Administration.

and acetone [Kado et al., 2001; Sakaguchi et al., 2006] that may contribute to the development of effective wastewater treatment conditions once this technique is translated to larger industrial or commercial size units.

It is interesting that the published literature makes no mention of what interactions play roles in the adsorption of isopropanol and acetone in TiO_2/aqueous systems. Some authors, for example, have suggested that since in aqueous media alcohols do not chemisorb to the catalyst surface the reaction between this type of substrate and the hydroxyl radicals takes place within the thin interfacial layer vicinal to the surface [Cunningham and Srijaranai, 1988; Mandelbaum et al., 1999]. However, nothing has been said about the role that hydrogen-bonding interactions may play on the photocatalytic degradation of isopropanol and its oxidation product, acetone, in aqueous systems.

The fact that these compounds do not strongly bind to the TiO_2 surface in contact with their aqueous solution by coordination to the Ti^{4+} ions does not preclude that their adsorption may take place on the layer of surface hydroxyl groups formed after water chemisorption. From studies on TiO_2/gas systems it is known that some extent of physical adsorption of isopropanol and other alcohols through hydrogen-bonding with surface OH groups occurs in pre-hydroxylated TiO_2 samples [Hollabaugh and Chessick, 1961; Munuera and Stone, 1971; Suda et al., 1987]. Therefore, in the case of TiO_2 in contact with an aqueous solution (and in the absence of any strongly bound species) a fully hydroxylated surface can be envisaged and hydrogen-bonding between isopropanol and the surface hydroxyl groups may be regarded as the only possible adsorption mode.

Although no studies of this kind have been done for acetone, a similar interaction can be suggested since this substrate has hydrogen acceptor capabilities.

In this dissertation research we undertake a systematic study on the photocatalytic degradation of small polar organic compounds that do not readily adsorb to the TiO_2 catalyst but bear hydrogen-bonding capabilities. Since numerical scales for solute hydrogen-bond acidity (α^H) and hydrogen-bond basicity (β^H) were constructed and published in the literature [Abraham, 1993], the α^H and β^H indexes will be used to analyze the photocatalytic degradation behavior of our model compounds based on their abilities to donate or accept a proton in a hydrogen-bond.

We will make use of the effects of typical water parameters (pH, carbonate/bicarbonate alkalinity, and ionic strength) on the surface hydroxyl speciation and their acid/base equilibria to elucidate the possible role of hydrogen-bonding interactions in the degradation of those model compounds in TiO_2 photocatalytic systems. Each water parameter will be the focus of a separate chapter. Kinetic data corresponding to the photodegradation of SPOC will be interpreted on the grounds of the multisite (MUSIC) model of the TiO_2 surface speciation which accounts for the presence of two types of surface hydroxyl groups possessing different Brönsted acid/base properties. This surface speciation model has not been applied to the interpretation of kinetic data describing the degradation of model compounds adsorbing by outer-sphere interactions.

Throughout these studies, isopropanol and acetone will be the two SPOC selected as model substrates. However, in Chapter 4 we will further test our hydrogen-bonding hypothesis by adding a third test compound (dimethylsulfoxide) in order to explore the

possibility of constructing a ranking of TiO_2-mediated photocatalytic degradation based on hydrogen-bonding empirical parameters (α^H and β^H).

The general goal of this research is to study, characterize and model the photocatalytic degradation of SPOC as a function of typical water parameters in order to provide base case conditions that may translate into an efficient photocatalytic method for a final water polishing step. Similarly, we aim to find experimental evidence that may indicate the important role that hydrogen-bonding interactions may play in their photooxidation at the catalyst surface. A better understanding of this important piece of the mechanistic aspects of SPOC photodegradation may lead to better treatability strategies for the abatement of these compounds in real waste- and graywater by the use of UV/TiO_2 photocatalysis.

CHAPTER 2

Effect of pH on the photocatalytic degradation of acetone and isopropanol in aqueous suspensions of titanium dioxide

2.1. Introduction

It is well documented that two types of hydroxyl groups exist on the surface of TiO_2 when the oxide is in contact with aqueous solution: the singly-coordinated or terminal OH group ($\equiv Ti\text{-}OH^{1/3-}$) and the doubly-coordinated or bridging OH group ($\equiv OH^{1/3+}$) [Boehm, 1971; Hiemstra et al., 1989a, 1989b, Hiemstra and Van Riemsdijk, 1991; Rodríguez et al., 1996].

According to the multisite proton adsorption modeling of the TiO_2/solution interface each hydroxyl group has its corresponding intrinsic proton dissociation constant and, therefore, the pH of the aqueous medium has an effect in the surface speciation and the resulting charging behavior of the oxide surface. The surface equilibria of the $\equiv Ti\text{-}OH^{1/3-}$ and $\equiv OH^{1/3+}$ hydroxyl groups and their corresponding pK_a values (for Degussa P25 TiO_2) [15] are given in Equations 2.1 and 2.2 as reported by Rodríguez et al. (1996).

$$\equiv Ti\text{-}OH_2^{2/3+} \leftrightarrow \equiv Ti\text{-}OH^{1/3-} + H^+ \qquad pK_{a1} = 5.38 \qquad (2.1)$$

$$\equiv OH^{1/3+} \leftrightarrow \equiv O^{2/3-} + H^+ \qquad pK_{a2} = 7.60 \qquad (2.2)$$

Rodríguez et al. (1996) were able to calculate the surface site distribution as a function of solution pH using experimental data obtained from acid/base titrations and

[15] Degussa P25 TiO_2 was used in this study and therefore the pK_a values calculated for this commercial brand are adopted in our analysis.

electrophoretic mobility of TiO_2 suspensions, and a fitting model based on a description of the electrical double layer. Their results suggested that since chemisorption of water on the TiO_2 surface imposes the constraint $K_{a1} > K_{a2}$ the OH-surface groups $\equiv Ti\text{-}OH^{1/3-}$ and $\equiv OH^{1/3+}$ (that is, the surface groups with the smallest residual charge numbers) prevail at pH values above and below the pH_{zpc} of TiO_2 (pH_{zpc} = 6.50, Rodríguez et al., 1996), respectively. The fractions of $\equiv Ti\text{-}OH_2^{2/3+}$ and $\equiv O^{2/3-}$ contributing to the net surface charge are smaller and they only become important under the effect of ionic strength.

The surface charge is not the only surface phenomenon that involves these reactive hydroxyl groups and that is affected by the pH of the aqueous solution. The production of hydroxyl radicals ($OH^{\bullet}$), which are strong oxidizing species capable of attacking many organic pollutants, are formed by trapping of photogenerated holes (h^+) in surface hydroxyl groups. Currently, there is no clear consensus on what surface site is involved in producing surface hydroxyl radicals. Hence the h^+ trapping reactions for either $\equiv Ti\text{-}OH^{1/3-}$ or $\equiv OH^{1/3+}$ at both acidic and basic pH have been suggested (see Equations 1.6 - 1.9) [Salvador, 2007]. However, independently of which surface hydroxyl group acts as hole trap, it is reasonable to suggest that holes react faster with negatively charged surface groups [Sun and Pignatello, 1995]. Therefore, surface hydroxyl radicals would be formed at a higher rate in neutral and, especially, at alkaline media [Riegel and Bolton, 1995].

To date, a large number of studies have focused on the effect of aqueous medium pH on the adsorption and TiO_2 photocatalytic decomposition of organic compounds that strongly interact with the oxide surface. This strong interaction occurs by formation of

chelate structures with the surface Ti^{4+} which leads to the displacement of the singly-coordinated OH group [Piscopo et al., 2001; Regazzoni et al., 1998; Rodríguez et al., 1996; Sun and Pignatello, 1995; Tunesi and Anderson, 1991; Vasudevan and Stone, 1996]. Generally these substrates are aromatic compounds possessing ligand donor groups (e.g., carboxylic, hydroxyl, or amino groups) and the stereochemical configuration to form rings in their chelate complexes. Correlations between the molecular form (protonated or deprotonated) present in solution and the parallel effect of pH on the TiO_2 surface phenomena have been successful in explaining results for these types of compounds [Piscopo et al., 2001; Tunesi and Anderson, 1991]. Specifically, when the functional group becomes charged with changes in solution pH, higher adsorption of the substrate is observed at the conditions where electrostatic interactions between the TiO_2 surface and adsorbate are favorable. Consequently, the higher the adsorption (chemisorption by displacement of surface OH groups) the higher the degradation rate once the sample is illuminated. For example, Piscopo et al. (2001) observed that the adsorption and degradation rate constant of *para*-hydroxybenzoic acid (4-HBZ) were at their maximum in the pH range 4-5. The adsorption occurred via formation of surface carboxylate species favored by the electrostatic attraction between the ion form of 4-HBZ ($pK_a = 4.48$) and the positively charged TiO_2 surface (reported pH_{zpc} was 6.3, Piscopo et al., 2001). At pH values higher than the pH_{zpc}, the degradation rate for 4-HBZ decreased with increasing pH due to the repulsive forces created by the change in the TiO_2 net surface charge to negative. A similar observation and analysis were made by Tunesi and Anderson (1991) for the photodecomposition rate of salicylic

acid (pK_a = 2.9) studied at pH 4.0, 7.5, and 9.5. The fastest degradation was obtained at pH 4.0, followed by a gradual decrease up to pH 9.5.

For these types of organic compounds, capable of inner sphere interactions (i.e., chemisorption) with the TiO_2 surface, the strong pH dependence of reaction rates is also attributed to the change in the reaction pathway that takes place under conditions of different acidity. It has been suggested, for example, that with changes in pH the route of degradation shifts from direct reaction with photoproduced holes at conditions where chemisorption to the TiO_2 surface occurs, to reaction with hydroxyl radicals (i.e., indirect transfer) at conditions where the interaction between the substrate and photocatalyst is weak due to electrostatic repulsion. Direct transfer mechanism is considered to be more efficient than the reaction with $OH^{\bullet}$ radicals, hence the strong observed trends with solution pH for this particular class of compounds [16]. Sun and Pignatello (1995) referred to this shift in reaction mechanism as a dual hole-radical mechanism controlling the photodegradation of the substrate.

Less attention has been paid to the photocatalytic degradation in aqueous phase of other important classes of water pollutants that, in contrast to the previous examples, do not posses any ionic functional group. According to our literature review, only a few studies have been dedicated to the effect of practical factors in the aqueous TiO_2 photooxidation of small polar organic compounds (SPOC) such as aliphatic alcohols and ketones [Abdullah et al., 1990; Chavadej et al., 2008; Chen et al., 1999; Cundall et al., 1976, Harvey et al., 1983, Kado et al., 2001; Sakaguchi et al., 2006]. In the case of aliphatic alcohols, the effect of solution pH on their photocatalytic degradation has been

[16] For titanium dioxide, it has not been established what mechanism is prominent over which pH region [Sun and Pignatello, 1995].

mostly studied on platinized TiO_2 (Pt/TiO_2) [Chavadej et al., 2008; Chen et al., 1999] rather than on native TiO_2 [Abdullah et al., 1990]. To the best of our knowledge, there is only one study by Abdullah et al. (1990) concerning the effect of pH on the photodecomposition of isopropanol and ethanol in aqueous solution using native TiO_2 (Degussa P25 type). These authors studied the rates of decomposition of these aliphatic alcohols by following their CO_2 production over time within the pH range of 2.0 - 5.5. Abdullah et al. (1990) observed that the maximum rate of isopropanol oxidation was above pH 3.4, while for ethanol a maximum in the rate of degradation occurred between pH 2.8 and 3.6 and then it decreased at higher pH values. Abdullah et al. (1990) considered their observations for ethanol as unexpected and explained that their values are most likely related to a pH-dependent effect on the decomposition of secondary oxidation products from the alcohol rather than a pH effect on the primary processes. In light of the above, it is clear that more studies on native TiO_2 are necessary to have a better understanding of the photodegradation processes of aliphatic alcohols and other SPOC under the effect of water parameters such as solution pH, especially if full advantage of other types of catalyst preparations (i.e., Pt/TiO_2) is to be obtained. In addition, these studies should investigate initial rates of decomposition of SPOC by following the consumption of the parent compound during the UV/TiO_2 treatment of the aqueous suspension to avoid the confusing effects of oxidation byproducts.

The less attention given to the aqueous TiO_2-photocatalytic decomposition of SPOC is probably due, first, to the fact that they are considered important air pollutants, hence they are mostly studied in gas-solid systems [Bickley et al., 1973; Bickley and Jayanty, 1974; Brinkley and Engel, 1998; Chang et al., 2004; Coronato et al., 2003a,

2003b; Cunningham and Hodnett, 1981; El-Maazawi et al., 2000; Hager and Bauer, 1999; Henderson, 2004; Kim et al., 1988; Kim and Barteau, 1990; Larson et al., 1995; Munuera and Stone, 1971; Nimlos et al., 1996; Ohko et al., 1997; Peral and Ollis, 1992; Rekoske and Barteau, 1997; Suda et al., 1987; Xu and Raftery, 2001a, 2001b; Xu et al., 2003], and second, small alcohols are mainly considered free $OH^{\bullet}$ radical scavengers that do not interfere with direct interfacial interactions of other species occurring in the TiO_2 in contact with their aqueous solution [Mrowetz and Selli, 2005; Sun and Pignatello, 1995; Tunesi and Anderson, 1991].

It is known that short aliphatic alcohols and ketones do not favorably compete with water for chemisorption to the TiO_2 surface [Bickley et al., 1973; Mandelbaum et al., 1999; Munuera and Stone, 1971]. Therefore, when these type of SPOC are added as probe molecules to aqueous TiO_2-photocatalytic systems containing chemisorbed organic species it is expected that they will not quench the degradation rates of the primary substrate degrading through direct interaction with photoproduced holes, as it has been reported by other authors [Sun and Pignatello, 1995; Tunesi and Anderson, 1991]. However, this lack of inhibition does not mean that SPOC such as isopropanol and acetone are unable to adsorb and degrade on the TiO_2 surface.

If small polar organic compounds such as acetone and isopropanol are not expected to strongly bind to the TiO_2 surface in contact with their aqueous solution, then their adsorption is more likely to occur on the layer of surface hydroxyl groups formed by water chemisorption through a weaker form of interaction (i.e., hydrogen-bonding). Hydrogen-bonding to the surface hydroxyl groups has already been observed for acetone and aliphatic alcohols in TiO_2/gas phase studies using pre-hydroxylated oxide samples

[Hollabaugh and Chessick, 1961; Munuera and Stone, 1971; Suda et al., 1987] and, therefore, it is reasonable to suggest that this outer sphere interaction would take place on the surface of the TiO_2 particles suspended in their aqueous solution. However, to the best of our knowledge, no study has been conducted to determine the possible key role that hydrogen-bonding capacities of these two compounds could play on their adsorption and subsequent degradation in TiO_2/aqueous systems.

In this chapter, the role played by pH and the surface phenomena in determining the photodegradation kinetics for two SPOC, acetone and isopropanol, is investigated. We hypothesize that the maximum in the rate of degradation for each of these compounds will occur at conditions where the surface speciation present at a given pH is optimal for both the hydrogen-bonding of the model substrate and the production of hydroxyl radicals. Since hydroxyl radical production is higher in neutral and, especially, at alkaline media the fastest degradation rates of our model compounds would occur within a neutral to alkaline pH range.

In order to evaluate our hypothesis the analysis of the kinetic data will be done on the basis of hydrogen-bonding capacities of our substrates [17] and the effect of pH on the surface hydroxyl group speciation according to a multisite (MUSIC) model of the TiO_2 surface, which have already been reported in the literature. This type of analysis has been lacking in the interpretation of photocatalytic results obtained for organic compounds that may adsorb to the TiO_2 surface through outer sphere interactions.

Although our model compounds are not strongly adsorbed species, it would be interesting to obtain insight on any possible role that surface phenomena may play on their TiO_2/aqueous photocatalytic degradation which would challenge the widespread

[17] Quantified in the form of empirical hydrogen-bonding parameters as reported by Abraham (1993).

conception that they do not compete for surface sites and merely degrade via free hydroxyl radicals in the bulk solution.

2.2. Experimental Section

2.2.1. Materials

In all experiments, titanium dioxide (TiO_2) Degussa P25 was used as the photocatalyst without modification (lot No. 2047, BET surface area = 50 ± 15 m^2g^{-1}, average particle size = 21 nm, Degussa Corporation). Isopropanol (ISP), ($(CH_3)_2CHOH$), and acetone (ACE), ($(CH_3)_2CO$), were purchased from Aldrich. These commercial materials were of 98% purity or higher, and used as received. NaOH (97% purity) and HNO_3 (90% purity) were obtained from Fisher Scientific and used for pH adjustment of the reaction suspensions. Nanopure water (18.1 MΩ·cm) from an Infinity ™ ultrapure purification system (model D8961, Barnstead) was used for preparation of all solutions.

2.2.2. Photooxidation apparatus

The photooxidation apparatus (Figure 2.1) consisted of a 450 W medium pressure mercury-vapor lamp (Ace Glass, Cat. 7825-34) positioned within a double-walled quartz immersion well (Ace Glass, Cat. 7874-35) with inlet and outlet water lines. The photochemical lamp was plugged to a 450 W power supply (Ace Glass, Cat. 7830-60). A water-flo power cut-off (Ace Glass, Cat. 2162-14) was used for safety in the event of a water or main power failure. The cooling water jacket was used to remove some of the lamp heat and maintained a temperature between 25 and 27°C inside the steel bench cabinet (measures: 89 cm high x 92 cm wide x 61.5 cm deep) where the photochemical

reaction equipment was operated. A cooling fan was located on top of the lamp housing for air movement.

The reaction solution (20 mL) was contained in a cylindrical cap-sealed quartz reaction vessel (Ace Glass, Cat. D116912, 25 mL capacity, 10 cm long x 22 mm O.D; screw cap with ¼" hole, thread GL25). The screw cap was fitted with a PTFE/silicone rubber septum (VWR, Cat. 66010-751). During the photocatalytic reaction the quartz reaction vessel was placed in a motor-driven rotating stirrer (Scientific Industries, Inc., Cat. 3-163-404) and directly exposed to the lamp. This experimental setup permitted simultaneous irradiation of several reaction vessels.

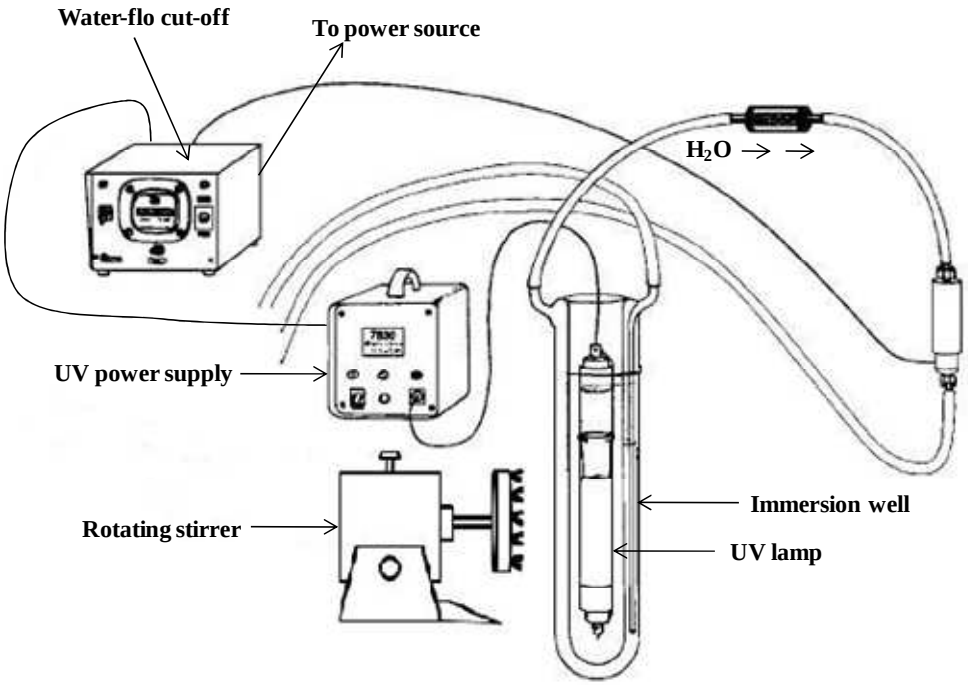

Figure 2.1. Experimental setup for photocatalytic reactor (partially reproduced from Ace Glass, catalog 0309 (2008), p.15).

A periodic check of the voltage and lamp current was performed by conducting parallel and serial tests with a digital multimeter. The calculated power output was used

to ensure consistent photointensity of the lamp over the course of our photocatalytic studies. If the output decreased 10% of the initial value the attenuated lamp was replaced.

2.2.3. Sample preparation and photocatalytic experiment

The reaction samples were prepared by suspending 2g/L of TiO_2 powder in 20 mL of freshly prepared aqueous solution of isopropanol or acetone. Preliminary experiments [18] where different quantities of TiO_2 (0.3 to 3.0 g/L) were used to degrade isopropanol and acetone (100 ppm) showed that the optimum catalyst concentration to be used is 2 g/L based on rate constant calculations [El-Morsi and Nanny, 2004]. Therefore, a TiO_2 concentration of 2 g/L was maintained in all further experiments. All solutions were prepared in duplicate.

Initial concentrations of our model compounds in the slurries ranged between $1.56x10^{-3}$ and $1.64x10^{-3}$ M. These values were selected in order to simulate typical concentrations of both compounds in wastewater (see below), yet high enough to give a good signal to noise ratio in the gas chromatograph experiments during the irradiation times used in our studies. Concentrations of our model compounds in wastewater treatment plants [Liu et al., 2004] and water recovery systems [Verostko et al., 2004] are reported as: acetone, (13368.1 – 6032.31) μg/L and 23700 μg/L, respectively; isopropanol, (1148.25 – 938.87) μg/L and 3297 μg/L, respectively.

The pH values of the suspensions were measured with a digital pH meter (Orion PerpHect, model 350, Fisher Scientific, Cat. 13-642-629) and a needle combination pH microelectrode (Microelectrodes, Inc., Cat. MI-414B). The pH was adjusted to the

[18] These experiments were performed in 2003 by Taha El-Morsi, Ph.D.

desired value by additions of NaOH or HNO_3 using a 10 μL microsyringe (Shimadzu, Cat. 221-34618-00). The suspensions were placed in the dark, shielded with aluminum foil and allowed to equilibrate overnight at 10°C.

After irradiation at regular time intervals, samples for analysis were withdrawn with a syringe (Perfektum Micro-mate interchangeable syringe, luer-lock tip, 2 mL, Fisher Scientific, Cat. 14-825-1A) and filtered through a 0.1 μm nylon membrane (Osmonics Inc., Fisher Scientific, Cat. R01SP01300) fitted in a 13mm-filter holder (Millipore, Fisher Scientific, Cat. XX3001200). The filtrate was transferred to two autosampler vials containing fixed 100 μL glass inserts (VWR, Cat. 66065-262) which were capped (open-top cap, 8-425 screw thread, with 8 mm PTFE/silicone septa, VWR, Cat. 66030-420), and stored in the dark at 10°C until gas chromatographic analysis (each vial was injected once).

Dissolved oxygen (DO) in the suspensions was not controlled, but monitoring of its concentration before and after irradiation of the samples showed that it was still present at the maximum irradiation time selected to sustain the photocatalysis reaction. DO was measured using a fiber optic oxygen sensor system equipped with a spectrofluorometer (Ocean Optics, Cat. USB4000-FL-450), a pulsed blue LED light source (Ocean Optics , Cat. USB-LS-450) and the OOISensors software (Ocean Optics). A 18-gauge needle probe containing the 300-micron fiber oxygen sensor (Ocean Optics, Cat. FOXY-18G-AF) and a RTD hypodermic temperature probe (Ocean Optics, Cat. USB-LS-450-TP16) were used for DO and temperature readings, respectively. Details on the calibration and operation of the fiber optic oxygen sensor system are given in Appendix A.

2.2.4. Gas Chromatographic Analysis

The degradation of isopropanol and acetone was followed by gas chromatography using a Shimadzu GC-17A gas chromatograph (GC) equipped with a fused silica capillary column (Supelcowax^{TM}-10, polyethylene glycol stationary phase, 30m length x 0.32mm i.d. x 1.0μm film thickness, Aldrich) and a FID detector (ultrahigh purity helium used as carrier gas). An oven temperature programming of 60ºC (2.0 min) to 80ºC @ 5ºC/min, injector and detector temperatures of 200ºC and 1 μL injection volume (split 15:1) were selected for the chromatographic analysis.

The concentration of isopropanol and acetone in the filtrates were calculated by seven point external standard calibration curves using freshly prepared standard solutions. Each standard was injected in duplicates (one injection per vial). R^2 values in the calibration curves for both compounds were between 0.9991 and 0.9999. Standard deviations were calculated by Equation 2.3 where x is the sample mean and N is the sample size.

$$\sigma = \sqrt{\frac{1}{N\text{-}1}\sum_{i=1}^{N}(x_i - x)^2} \qquad (2.3)$$

Acetone was the only reaction product of isopropanol photodegradation detected in the liquid phase by gas chromatography. A peak eluting at R_t= 0.8 minutes, corresponding to a product of acetone photodecomposition, was also observed in the chromatograms but it was not identified.

2.2.5. Determination of kinetic parameters

To determine the kinetics of the photocatalytic decomposition of a model compound its concentration versus time was measured during runs. In this study we assumed that the relationship between the reaction rate and the substrate concentration takes the simple form of the following differential rate equation:

$$R = -k[C]^n \qquad (2.4)$$

where R is the reaction rate, k is the rate constant, [C] is the concentration of substrate, and n is the order of the reaction with respect to C.

The photodegradation modeling of acetone and isopropanol was performed using a program written in Mathematica 5.2 [19] (Appendix B) where the experimental data was related to mechanistic models expressed as the integrated rate equations for a zero- and first-order reaction. A least-square analysis was used to determine the best fit and the model kinetic parameter (i.e., the rate constant).

Photooxidation rates were measured within the first two half-life periods and Van't Hoff plots of k versus time [Masel, 2001] showed that the rate constants were constant over the observed time period. k values for the Van't Hoff plots were calculated for first- and zero-order reactions according to Equations 2.5 and 2.6, respectively, where C_o is the initial concentration of substrate, and C is the concentration at the time t.

$$k_1 = -\frac{1}{t} \ln \frac{C_o}{C} \qquad (2.5)$$

$$k_o = \frac{1}{t} (C_o - C) \qquad (2.6)$$

[19] This program was written by Eduardo Martínez-Pedroza, Ph.D. in collaboration with the author.

2.3. Results and Discussion

2.3.1. Effect of pH upon the photocatalytic degradation of acetone and isopropanol

The influence of the solution pH on the photocatalytic degradation of isopropanol and acetone was examined separately for both compounds at three different pH values (4.10, 6.04, and 8.61). Figure 2.2 illustrates the results obtained in these experiments. Initial rates calculated by fitting the experimental data are given in Table 2.1. The analysis of the data indicates that acetone and isopropanol decompositions occur through mechanisms of first- and zero-order, respectively. Acetone exhibited the fastest degradation rate at pH 6.04 while for isopropanol it was observed at 8.61. However, it is evident for both model compounds that there is a lack of strong dependence of the degradation rates with changes in solution pH.

Table 2.1. Effect of pH on the initial rates of acetone (k_{ACE}) and isopropanol (k_{ISP}) degradation in UV-irradiated TiO_2 suspensions.

	Initial solution pH		
	pH 4.10	**pH 6.04**	**pH 8.61**
k_{ACE} (min^{-1})	$(1.05 \pm 0.07)x10^{-2}$	$(1.21 \pm 0.05)x10^{-2}$	$(1.04 \pm 0.06)x10^{-2}$
k_{ISP} (mol L^{-1} min^{-1})	$(6.22 \pm 0.09)x10^{-5}$	$(6.2 \pm 0.2)x10^{-5}$	$(7.5 \pm 0.3)x10^{-5}$

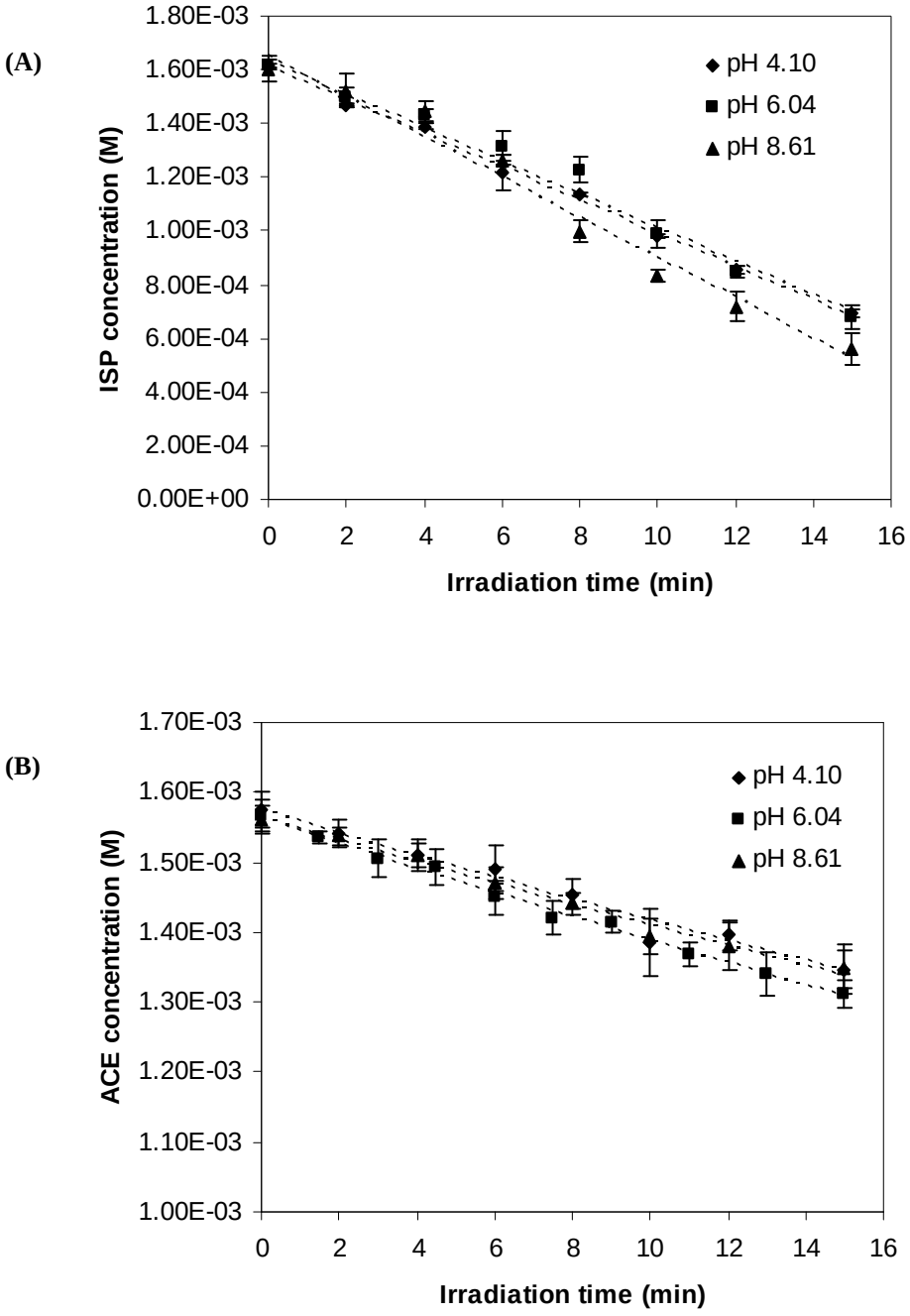

Figure 2.2. Substrate concentration against illumination time obtained from suspensions of TiO_2 at different initial pH (TiO_2, 2g/L; initial concentrations, (A) $[ISP]_o$ = (1.61-1.64)x10^{-3} M, (B) $[ACE]_o$ = (1.56-1.57)x10^{-3} M). The markers indicate experimental data. The dashed lines indicate the model fits.

The latter observation is not surprising considering that neither acetone nor isopropanol possesses ionic, ligand donor functional groups. This fact rules out electrostatic attractions and inner sphere coordination with the titanium ion as their sorptive interactions with the catalyst surface, which would have a marked dependence on pH. However, this is not an indication of the inability of our model compounds to adsorb to the TiO_2 surface.

Another reason that explains the observed weak dependence of degradation kinetics with solution pH is that acetone and isopropanol do not have a dual hole/hydroxyl radical mechanism of degradation operating in the range of experimental pH. We believe that hydroxyl radicals are the species responsible for the initial steps of their photodecomposition in all the range of pH used in this study since their adsorption to the TiO_2 surface very likely only involves an outer sphere interaction (i.e., hydrogen-bonding). If a shift from direct interaction with holes to a hydroxyl radical mechanism (where the former is considered a more efficient process) occurs with varying pH and varying adsorption behavior, then a greater change in degradation rates will be observed for our model compounds with changes in this aquatic parameter. For substrates that do not strongly adsorb to the surface the photodegradation mechanism occurs through reaction with hydroxyl radicals (protonated or deprotonated) produced on the catalyst surface [Monllor-Satoca et al., 2007; Salvador, 2007; Villareal et al., 2004]. Despite the weak dependence of degradation rates with pH, the observed differences are significant and can indicate the possible role of surface phenomena on the adsorption and degradation of our model compounds.

In order to give a simple explanation for the observed results the multisite protonated model proposed by Hiemstra et al. (1989a, 1989b, and 1991) was adopted. Therefore, it was assumed that the behavior of the TiO_2/solution interface for our particular system is dictated by the properties of the two distinctive surface hydroxyl groups formed upon dissociative water chemisorption (Equations 2.1 and 2.2). A simple interpretation of our experimental results on the basis of this current model of the surface behavior can serve as evidence that adsorption of our model compounds to the TiO_2 surface sites may occur through hydrogen-bonding to the surface hydroxyl groups.

If our hypothesis of hydrogen-bonding to the surface hydroxyl groups is correct, a substrate like isopropanol would have the capability to adsorb on TiO_2 in all the range of pH. By orienting the oxygen or hydrogen atom of its polarized hydroxyl group, isopropanol can approach surface sites with residual positive or negative charge. In addition, considering that the model alcohol has hydrogen donor ($\alpha^H = 0.33$; Abraham, 1993) and acceptor ($\beta^H = 0.56$; Abraham, 1993) capabilities several modes of adsorption can occur with the surface species bearing Brönsted acid/base properties (refer to Figure 1.5). On the other hand, acetone, which only possesses the ability to accept a proton through its carbonyl group ($\alpha^H = 0.04$, $\beta^H = 0.49$; Abraham, 1993), would be able to approach positively charged surface sites with acidic character because only the negative end of its dipole can be exposed to the charged surface (see Figure 1.5). Hence, acetone adsorption to the TiO_2 surface is more limited compared to isopropanol since it will mostly occur at $pH \leq pH_{zpc}$ where the surface groups with acidic character are present (refer to Figure 1.5).

The explanation of our data would not be complete without considering the pH dependence of the formation of the species responsible of the degradation of our model compounds. As it was already mentioned, surface hydroxyl radicals which can initiate the oxidation reactions in both acetone and isopropanol [Cundall et al., 1976; Cunningham and Srijaranai, 1988; Harvey et al., 1983; Mandelbaum et al., 1999; Sakaguchi et al., 2006; Stefan et al., 1996; Yamagata et al., 1988], would be formed at a higher rate in neutral and, especially, at alkaline media.

On the basis of the two aspects of our rationale, the faster reaction rates of isopropanol and acetone decomposition would be expected to occur in a pH range where optimum conditions for adsorption to the TiO_2 surface and optimum concentration of surface hydroxyl radicals coincide. This prediction is in complete agreement with the obtained results.

In the case of isopropanol, adsorption modes through hydrogen-bonding with surface sites may involve $\equiv Ti\text{-}OH^{1/3-}$ and $\equiv OH^{1/3+}$ groups. Since these surface sites are the most abundant sites at pH above and below the pH_{zpc} [Rodríguez et al., 1996], respectively, this substrate possesses fewer restrictions to adsorb to the surface at any of the pH values used in this study.

The above would also explain why zero-order kinetics is observed for the decomposition of isopropanol. The fact that the rate of degradation does not depend on isopropanol concentration (which ranges between (1.61-1.64) $x10^{-3}$ M) may be an indication that saturation coverage of the hydrogen-bonding active sites is attained. This can also be illustrated if the number of available acidic OH groups [20] ($Ns= \{\equiv OH^{1/3+}\} +$

[20] Using the same nomenclature of Rodríguez et al. (1996), the curly brakets denote surface concentration of the species.

$\{\equiv O^{2/3-}\}$ = 2.97 x10^{-6} mol m^{-2}) and the specific surface area (51.4 m^2g^{-1}) reported by Rodríguez et al. (1996) for Degussa P25 TiO_2 are used to obtain their total concentration in our photocatalytic reaction systems. From these values it can be calculated that under the conditions used in our studies there are 3.15 x10^{-4} moles of acidic OH groups per liter of solution compared to (1.61-1.64) x10^{-3} moles per liter of isopropanol. A similar concentration of basic OH groups (Ns= $\{\equiv Ti\text{-}OH^{1/3-}\}$ + $\{\equiv Ti\text{-}OH_2{}^{2/3+}\}$) can be assumed based on the determinations of Van Veen et al. (1985) (see Chapter 1). As a result of the above, the principal factor influencing isopropanol photooxidation could be the concentration of active species (i.e., hydroxyl radicals) that are formed under the given experimental conditions, as previously suggested by Cunningham and Srijaranai (1988) from an isotope-effect study. Therefore, the fastest degradation of isopropanol occurred at the most alkaline media (pH 8.61) where a higher concentration of surface hydroxyl radicals is expected.

On the other hand, adsorption of acetone is more restricted because it can only act as a hydrogen acceptor. Therefore, its mode(s) of adsorption onto the surface may only involve the acidic and positively charged $\equiv OH^{1/3+}$ and $\equiv Ti\text{-}OH_2{}^{2/3+}$ groups occurring at pH 4.10 and 6.04. However, the rate of degradation of acetone was found to be higher at pH 6.04 where the best compromise between a suitable surface site for adsorption and abundance of hydroxyl radicals is attained.

A first-order reaction for the photocatalytic conversion of acetone may be an indication that its adsorption to the surface is the most determining factor for its optimal degradation. A possible justification is that the nature of the degradation products resulting from $OH^{\bullet}$ radical attack might prevent the saturation coverage of the TiO_2

surface with our model compound. Formic acid and acetic acid are possible oxidation products of acetone [Stefan et al., 1996] that can form inner sphere complexes with Ti^{4+} ions which affects the surface density of hydrogen-bonding sites and the surface hydroxyl radical production. Formaldehyde, another plausible product [Stefan et al., 1996], would have a lesser effect as a surface site competitor since it is a weaker hydrogen acceptor (β^H = 0.33; Abraham, 1993) than the parent compound.

2.3.2. Direct photolysis studies

Acetone and isopropanol are weakly absorbing compounds in the UV range [21] at wavelengths below 350 and 250 nm, respectively [Xu et al., 2003]. Therefore, they may undergo decomposition through direct photolysis in their UV irradiated aqueous solutions. Since these wavelengths are emitted by the medium pressure mercury lamp (ACE glass, Inc) used in our studies, direct photolysis may be an alternative route for the decomposition of our compounds besides the TiO_2-mediated photooxidation in our heterogeneous photocatalytic systems. In order to determine the efficacy of this direct route compared to UV/TiO_2 photocatalysis, the occurrence of the former reaction (i.e., in the absence of TiO_2 catalyst) was investigated in solutions containing our model compounds at the same concentrations and initial pH conditions used in the heterogeneous photocatalytic experiments. Figure 2.3 shows a comparison of the direct photolysis of acetone and isopropanol while Figure 2.4 depicts a comparison of the efficacy of both methods for the treatment of our model compounds in water.

[21] Their molar absorption coefficients are ε_{260nm} = 15.4 $M^{-1}cm^{-1}$ [Feigenbrugel et al., 2005] and ε_{185nm} = 32 $M^{-1}cm^{-1}$ [Von Sonntag and Schuchmann, 1977], respectively.

In Figure 2.3 it can be observed that direct photolysis of both acetone and isopropanol shows similar S-shaped conversion time profiles. Therefore, the curves do not conform to simple zero- or first-order kinetics and the model parameters describing their direct degradation by UV light cannot be given.

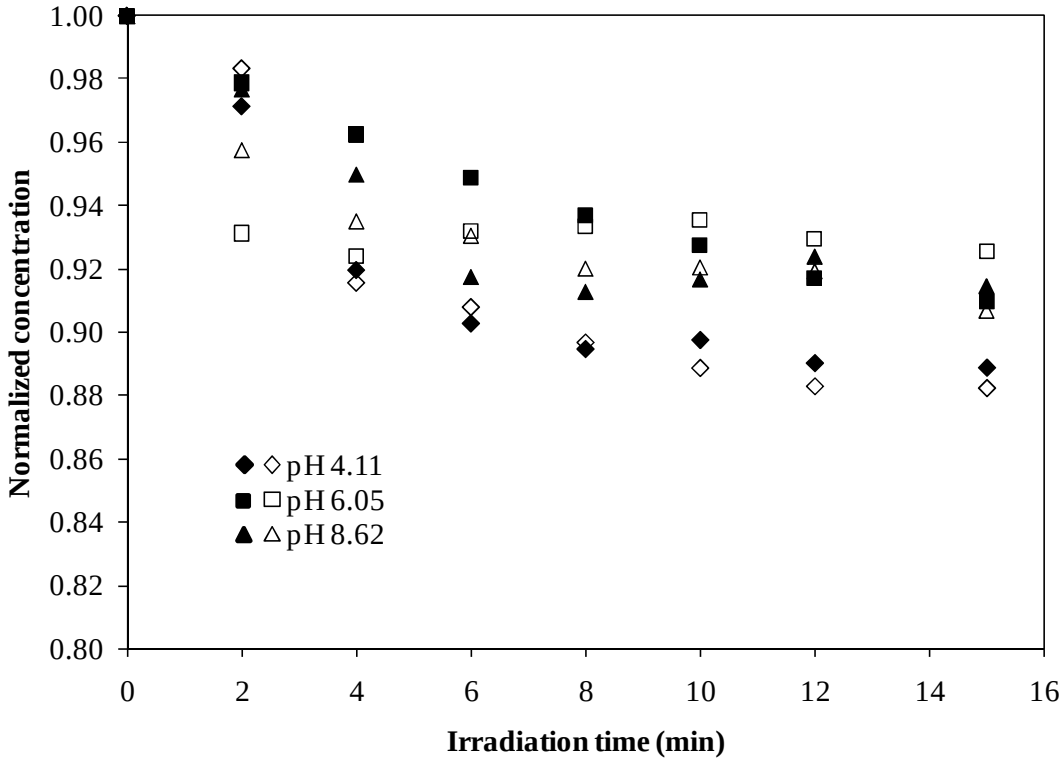

Figure 2.3. Direct UV photolysis of acetone (filled symbols) and isopropanol (open symbols) in water under different pH conditions. Average initial concentrations: $[ACE]_o = (1.55 \pm 0.06) \times 10^{-3}$ M, $[ISP]_o = (1.64 \pm 0.09) \times 10^{-3}$ M.

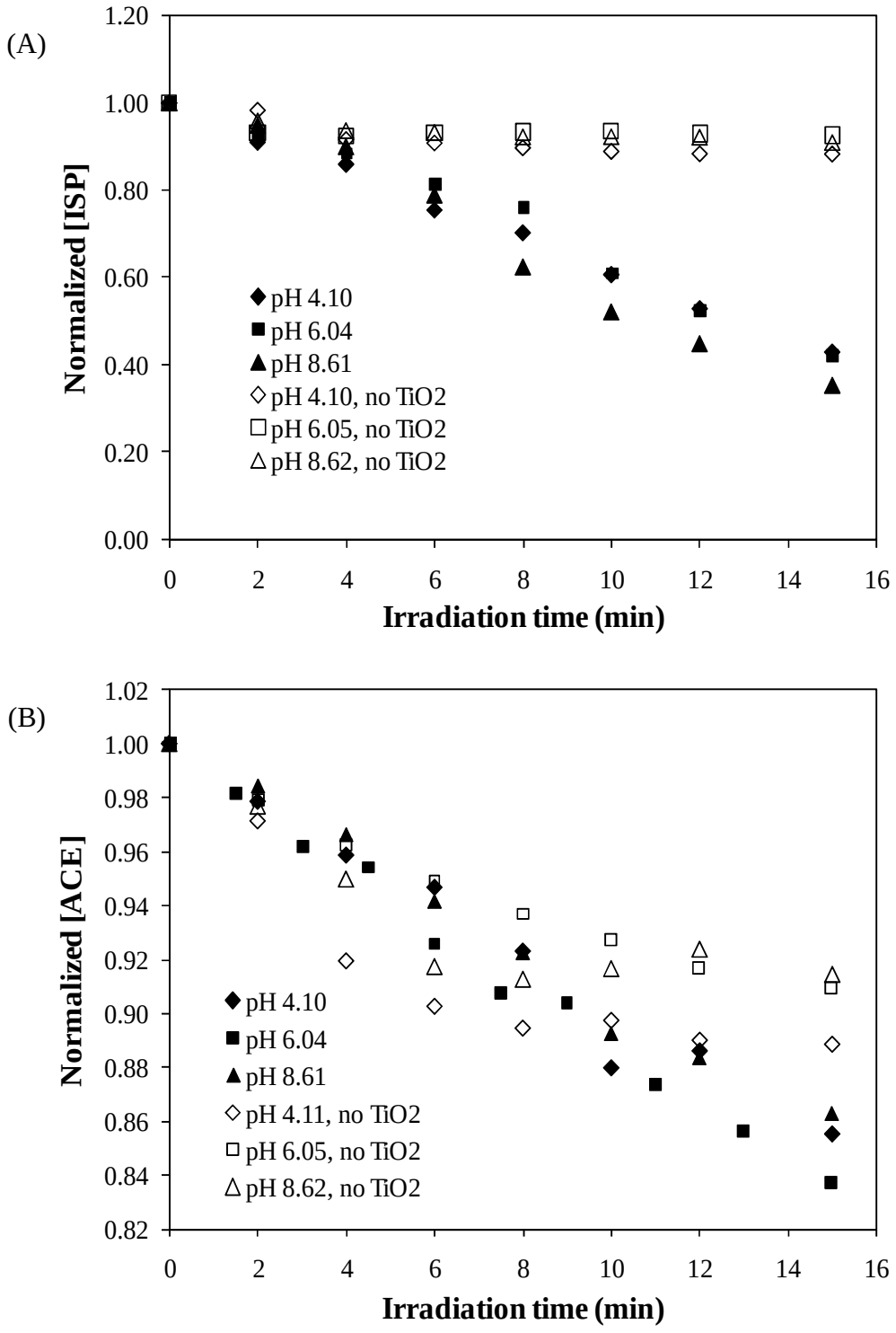

Figure 2.4. Effect of pH upon the direct photolysis (open symbols) and the UV/TiO_2 heterogeneous photodegradation (filled symbols) of (A) isopropanol and (B) acetone in aqueous solution. pH conditions are given in the legends.

The comparisons contained in Figure 2.4A show that under similar experimental conditions the photocatalytic reaction pathway is more effective than direct UV photolysis for the oxidation of isopropanol in aqueous solution at all the pH values tested in this study. Although acetone is the oxidation product of isopropanol under both treatment methods, its production is negligible through direct photolysis under the conditions used in our experiments. This is in agreement with the low yields of isopropanol UV photolysis reported in aqueous solution [Farkas and Hirshberg, 1937; Von Sonntag and Schuchmann, 1977]. Therefore, we can assume that in the TiO_2-containing photocatalytic systems direct photolysis is not an important pathway of isopropanol degradation.

For the case of acetone, a more careful examination of the conversion time profiles is necessary to reveal significant differences between the direct UV photolysis and the UV/TiO_2 degradation routes. Although the photocatalytic reaction pathway is not as effective for the degradation of acetone as it is for isopropanol in aqueous solution, Figure 2.4B shows that the direct photolysis route lags behind the former reaction in the later stages of the treatment. It is significant that at the initial pH of 8.62 and 4.11 the direct photochemical reaction levels off after 6 minutes while the photocatalytic reaction counterpart shows progressive acetone consumption through a first-order kinetic, as determined earlier in this chapter.

Several competitive processes may cause the level off of the direct photolysis curves of acetone. According to early studies, the photolysis of acetone in solution proceeds via the excited n-π^* triplet state with the formation of acetyl and methyl radicals

by α-cleavage (Equation 2.7 [22]) [Anpo and Kubokawa, 1977; Dalton and Turro, 1970; Pieck and Steacie, 1955; Porter et al., 1971, 1973].

$$(CH_3COCH_3)_{aq} + h\nu \leftrightarrow \underbrace{(CH_3CO^{\bullet} + CH_3^{\bullet})_{aq}}_{\text{solvent cage}} \rightarrow CH_3CO^{\bullet}{}_{free} + CH_3^{\bullet}{}_{free} \qquad (2.7)$$

However, the quantum yield of acetone decomposition in water is low (Φ_{270nm} = 0.061; Anpo and Kubokawa, 1977) due to recombination of the radicals because of the "cage" effect (Equation 2.3) or due to deactivation of the active molecules by several pathways: (i) collision [Pieck and Steacie, 1955], (ii) solvent-assisted photoenolization involving a six-membered intermediate species (Figure 2.5) [Porter et al., 1971, 1973] and, (iii) self-quenching by hydrogen abstraction from ground state acetone (Figure 2.6) [Porter et al., 1973]. In the last two mechanisms the enol form of acetone undergoes ketonization and the original compound is reformed. In dilute aqueous solutions, however, the self-quenching pathway is only a minor primary process compared to (ii) [Porter et al., 1973].

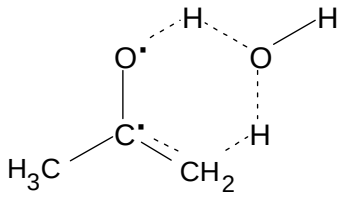

Figure 2.5. Proposed structure of intermediate for the water-assisted photoenolization mechanism of the triplet state of acetone (reproduced from Porter et al. (1971), p. 3153, Figure 4).

[22] The subscript "aq" means that the species are in the aqueous solution.

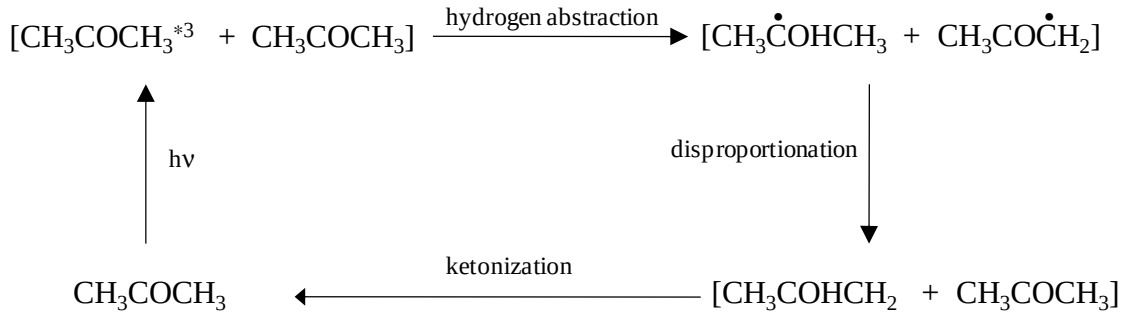

Figure 2.6. Hydrogen abstraction of excited triplet acetone from ground state acetone (reproduced from Anpo and Kubokawa (1977), p. 1915].

Our results in Figure 2.4 for the UV photolysis of acetone are in agreement with the reported competition between the fruitful pathway (right side of Equation 2.7) and the triplet state deactivation processes. The leveling off of the direct photolysis curves of acetone may indicate the offset to acetone UV photolysis caused by the deactivation processes that reform the ground state of the compound.

The observation of a slow degradation of acetone through the TiO_2-based photocatalytic reaction does not imply that the kinetics of this process is not controlled by the TiO_2 surface phenomena. Although a UV filter to block light below 350 nm was not used in our studies and we cannot mathematically account for an alternative decomposition pathway such as direct photolysis using our fitting program, there are reasons to believe that direct UV photolysis would be even less efficient to degrade acetone when the TiO_2 particles are present in the reactions solution.

First, TiO_2 absorbs at $\lambda \leq 388$ nm [De Lasa et al., 2005] and therefore the catalyst particles suspended in the aqueous media affect the fraction of light absorbed by acetone, which possesses a weak absorption band centered around 262 nm [Feigenbrugel et al., 2005] and is present at low concentration (mM level) in our suspensions. Second, it is

likely that the surface hydroxyl groups of TiO_2 participate in the deactivation of the triplet state of acetone. Using infrared and phosphorescence spectroscopy combined with isotopic labeling methods, Anpo (1987) indicated that the triplet state of acetone associated to the surface hydroxyl groups of porous Vycor glass (PVG) [23] underwent efficient radiationless deactivation through a similar photoenolization mechanism proposed in Figure 2.5. Therefore, it is possible that this additional mechanism of deactivation of the excited state of acetone takes place in the presence of TiO_2 catalyst, suppressing the direct photolysis degradation of acetone even more in the heterogeneous reaction systems.

In light of the above, we can conclude that the presence of TiO_2 may affect two important factors that determine the direct UV photolysis of acetone: the probability of the light absorption event and the probability that the excited state proceeds to a chemical reaction. Therefore, it is reasonable to suggest that with the addition of the catalyst the consumption of our model compound proceeds dominantly by the heterogeneous photocatalytic route. Hence, we believe that the differences observed in the heterogeneous photocatalytic rates at different pH conditions, which were discussed earlier in this chapter, are controlled by the presence of the TiO_2 catalyst.

It is worth mentioning that no attempt to identify the direct photolysis products of acetone was made, but methane, ethane, formaldehyde and acetic acid have been postulated in the literature [Dalton and Turro, 1970; Frankenburg and Noyes, 1953; Pieck and Steacie, 1955]. A compound eluting at 1.38-1.40 minutes was detected at all conditions used. The UV/TiO_2 photodecomposition product of acetone eluting at 0.8 min

[23] Major composition: SiO_2 = 96%, B_2O_3 = 3% [Anpo, 1987].

was not observed in the chromatograms obtained from the analysis of the UV direct photolysis of this model compound.

2.4. Conclusions

A simple interpretation on the grounds of the multisite model and the influence of pH on the surface behavior has been successful to explain the observed results for the effect of pH on the degradation of small polar organic compounds possessing hydrogen-bonding capabilities. This study could be the first in suggesting that substrates like small aliphatic alcohols and ketones may adsorb to the TiO_2 catalyst in contact with their aqueous solution through formation of hydrogen-bonds with the surface hydroxyl groups. In terms of the mechanistic aspects of the photocatalytic degradation of our model compounds, acetone and isopropanol, this is of great interest because the idea of these substrates being hydrogen-bonded to the layer of hydroxyl groups opens up the possibility that the reaction with the photogenerated hydroxyl radicals occurs at the surface of titanium dioxide. Therefore, our hydrogen-bonding hypothesis challenges the common assumption that our model compounds do not compete for surface sites and their oxidative pathways of degradation occur via homogeneous phase reaction with free hydroxyl radicals. Currently, with the emerging hypothesis that terminal bridging ions (O_s^{2-}) are the only hole traps and, therefore, the only source of $OH^{\bullet}$ radicals (Equation 2.5 and 2.5) [Salvador, 2007; Monllor-Satoca et al., 2007], the possibility of these reacting species desorbing into the finite thickness of a reaction volume in the proximity of the surface could be completely disregarded. If this emerging idea proves to be correct, then the hydrogen-bonding hypothesis presented in this study will help reconcile the apparent

contradiction of inexistent desorbing surface hydroxyl radicals attacking substrates that are not believed to interact with the surface.

In terms of practical applications, we have shown that factors like hydrogen donor or acceptor capacities and rate of hydroxyl radical production are of great importance at the moment of determining the optimal conditions for the degradation of substrates such as acetone and isopropanol. In order to develop a UV/TiO_2 process for the removal of these types of substrates (alone or in the presence of similar compounds bearing hydrogen-bonding capabilities) the above factors must be considered and the importance of their role on the rates of degradation must be assessed for the target compound. For example, a substrate that possesses both hydrogen donor and acceptor capabilities does not have restrictions to adsorb to the surface because hydrogen-bonding sites are present in all the range of pH. Therefore, its fastest degradation occurs at conditions where the rate of hydroxyl radical production is the most optimal (i.e., alkaline pH). On the contrary, if a given substrate does not possess the dual hydrogen donor and acceptor capacities, its adsorption to the surface is restricted to the conditions where suitable hydrogen-bonding surface sites exist. As a result, the adsorption to the surface is the most determining factor on its degradation.

CHAPTER 3

Effect of carbonate-bicarbonate alkalinity on the TiO_2-mediated photocatalytic degradation of acetone and isopropanol in aqueous solutions

3.1. Introduction

When hygiene and potable water quality standards are required Advanced Oxidation Processes (AOPs) such as UV/TiO_2 heterogeneous photocatalysis can be implemented in post-processor systems for the final polishing of the water feed.

Because this AOP is currently seen as a promising technology, there are many studies on the TiO_2 photocatalytic degradation of single contaminants that belong to various classes of organic compounds [Matthews, 1988; Sabin et al., 1992]. However, it is important to take into account the effect of various chemical compositions of the water feed if this technology is to be used in the final stages of the wastewater treatment. Among the relevant impurities that must be considered is the fraction of inorganic anions that are commonly present in wastewater and that may be highly resistant to previous treatment processes.

In addition, apart from being found in the influent water, inorganic anions may be present as reaction products in the degradation of organic compounds. On this respect, it is well known that in almost all cases, under appropriate conditions, TiO_2-mediated photocatalytic oxidation of aqueous aerated suspensions of organic compounds containing C, N, P, S, and X (X= halogen) atoms leads to their complete mineralization. Therefore, the inorganic forms of all these elements (carbon dioxide, nitrate, phosphate,

sulfate, and halides) are expected to be found in the treated water [Calza and Pelizzetti, 2001; Kormann et al., 1991; Low et al., 1991, Wang et al., 1999]. Although these anions may or may not affect water potability, their effect on the efficiency of the water treatment technology being in use must be assessed.

Among all the anions commonly present in wastewater, the effect of carbonate and bicarbonate anions on the performance of UV/TiO_2 photocatalysis is of great importance. This is not only due to the fact that these ions are omnipresent in water due to the carbon dioxide exchange with the atmosphere and its aqueous pH dependent equilibria, as described in Equations 3.1-3.4 [Oppenländer, 2003], but also because they are widely recognized as excellent scavengers of hydroxyl radicals [Behar et al., 1970; Buxton et al., 1988; Ross and Neta, 1979; Weeks and Rabani, 1966], the species responsible to initiate the organic substrate abatement in TiO_2 mediated photocatalysis (Equations 3.5 and 3.6).

$$CO_{2\,(gas)} \leftrightarrow CO_{2\,(aq)} \qquad (3.1)$$

$$CO_{2\,(aq)} \leftrightarrow H_2CO_{3\,(aq)} \qquad (3.2)$$

$$H_2CO_{3\,(aq)} \leftrightarrow HCO_3^-{}_{(aq)} \qquad pK_a = 6.28\ ^{24} \qquad (3.3)$$

$$HCO_3^-{}_{(aq)} \leftrightarrow CO_3^{2-}{}_{(aq)} \qquad pK_a = 10.36\ ^{25} \qquad (3.4)$$

$$OH^\bullet + HCO_3^- \rightarrow OH^- + HCO_3^\bullet \qquad k(OH^\bullet + HCO_3^-) = 8.5 \times 10^6\ M^{-1}s^{-1} \qquad (3.5)$$

$$OH^\bullet + CO_3^{2-} \rightarrow OH^- + CO_3^{-\bullet} \qquad k(OH^\bullet + CO_3^{2-}) = 3.9 \times 10^8\ M^{-1}s^{-1} \qquad (3.6)$$

The importance of this scavenging effect by carbonate species in UV/TiO_2 treatment can be evidenced considering that the rate constant for the reaction of hydroxyl

[24] pKa value obtained from Kumar and Mathur (2006).
[25] pKa value obtained from Chen and Hoffman (1972).

radicals with typical organic compounds ($k(OH^{\bullet}+M)$) ranges from 10^6 to 10^{10} $M^{-1}s^{-1}$ [Peyton et al., 1998], while the carbonate radical (formed in Equation 3.6) rate constants for typical aliphatic organic substances ($k(CO_3^{-\bullet}+M)$) lies in the range from 1 to 10^5 $M^{-1}s^{-1}$. Therefore, the presence of carbonate species in the aqueous media would have a dual adverse effect on UV/TiO_2 photocatalysis by lowering the concentration of hydroxyl radicals attacking the target organic substrate and by producing carbonate/bicarbonate radicals that are more selective and less reactive than the $OH^{\bullet}$ radical [Oppenländer, 2003].

Since UV/TiO_2 photocatalysis relies on the processes occurring on the surface of the catalyst, the possible inhibitory effect of carbonate-bicarbonate alkalinity by competition with the intended organic substrate for surface adsorption sites has to be also considered. Although there are reports on the extensive chemisorption of important anions such as sulfate and phosphate by displacing surface hydroxyl groups [26] and coordinating to surface titanium ions directly (Equation 3.7) [Abdullah et al., 1990; Chen et al., 1997, Chen et al., 2003] there is evidence in the literature to believe that this type of inner sphere interaction does not occur for carbonate species.

$$\equiv\text{Ti-OH} + A^- \rightarrow \equiv\text{Ti-A} + OH^- \qquad (3.7)$$

Infrared spectroscopic and X-ray diffraction studies conducted by Kumar and Mathur (2006) did not reveal any inner sphere interaction between the carbonate anion and TiO_2. Therefore, the authors proposed that CO_3^{2-} may be weakly hydrogen-bonded through its oxygen to a surface hydroxyl group, as shown in Figure 3.1. Their suggested

[26] Only the singly-coordinated hydroxyl group, $\equiv Ti\text{-}OH^{1/3-}$, is exchangeable for other anions [Boehm, 1971].

structure for this interaction involves the basic ≡Ti-$OH^{1/3-}$ surface group but no explanation was given for their rationale. A binding mode for the bicarbonate anion was not proposed by the authors since they were only interested in the pH range 10-12.5.

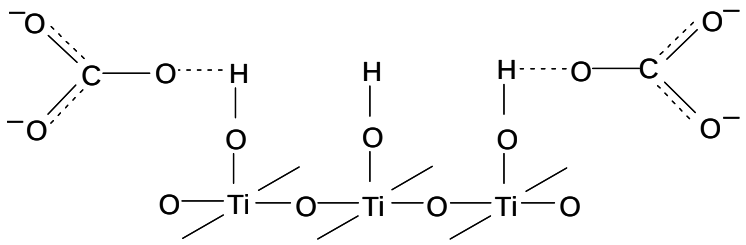

Figure 3.1. Hydrogen-bonding of carbonate anion to a surface hydroxyl group of TiO_2 (redraw from Kumar and Mathur (2006), p. 249, structure 1b).

Considering the surface multisite protonation model for TiO_2 [Hiemstra et al., 1989a,b, 1991] and a theoretical study on the structure and dynamics of hydrogen-bonding for carbonate species in aqueous solution [Kumar et al., 2009] we refined the proposed structure of Kumar and Mathur (2006). In the following paragraphs we suggest a different binding structure for the carbonate anion and propose a binding mode for the bicarbonate anion.

Theoretical calculations show that the hydrogen donor capacity through the hydroxyl group (-C-OH) is stronger than the hydrogen acceptor capacity through the carbonyl group (-C=O) in the bicarbonate anion [Kumar et al., 2009]. Therefore, one would expect a stronger hydrogen-bonding interaction between the hydroxyl group of the bicarbonate anion and a surface hydroxyl group with a basic character. According to the multisite model [Hiemstra et al., 1989a,b, 1991] the surface group with basic character is ≡Ti-$OH^{1/3-}$, which is more abundant at pH higher than the pH of zero charge point of

titanium dioxide (pH_{zpc} = 6.5 for Degussa P25 TiO_2, Rodríguez et al., 1996). However, this surface site carries a residual negative charge lessening the possibility of an interaction with the HCO_3^- anion [27]. Therefore, we conclude that the carbonyl group of the bicarbonate anion interacts with the acidic and positively charged $\equiv OH^{1/3+}$ surface site, which is more abundant at $pH \leq pH_{zpc}$. Nevertheless, this hydrogen-bond is weaker in nature since the hydrogen acceptor capacity is lower for the bicarbonate anion. For a similar reason, we propose that the same surface site is involved in the hydrogen-bonding of the carbonate anion (Figure 3.2).

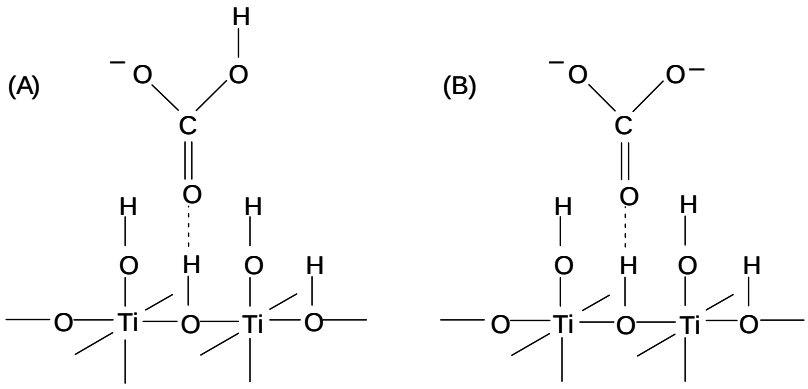

Figure 3.2. Suggested structures for the hydrogen-bonding of (a) bicarbonate and (b) carbonate anions to the TiO_2 surface (this work).

Our proposed structures for the modes of interaction of bicarbonate and carbonate anions with the $\equiv OH^{1/3+}$ surface group are in complete agreement with published results on the adsorption of these anions. Absorption studies showed that carbonate species are predominantly adsorbed onto TiO_2 particles (Degussa P25 type) in acidic and neutral solutions [Ku et al., 2004; Zhu et al., 2007]. In alkaline solutions the adsorption of carbonate is significantly decreased which is ascribed to electrostatic repulsion forces

[27] The same rationale applies to the CO_3^{2-} anion.

with the negatively charged TiO_2 surface. As we mentioned before, the $\equiv OH^{1/3+}$ surface site is more abundant when the pH of the aqueous solution is below or equal to the pH_{zpc} of TiO_2. We caution that although our proposed binding modes (Figure 3.2) would explain the predominant adsorption of carbonate species in the acidic and neutral pH range, more studies would be necessary to conclusively select one model over the other. However, since our model is plausible we will use our proposed binding modes to explain experimental results obtained in this work.

In the light of the above, it is possible that the inhibitory effect of carbonate and bicarbonate ions due to surface site competition would be important if the target organic substrate adsorbs to the metal oxide particles through outer sphere interactions such as hydrogen-bonding. However, the scavenging of hydroxyl radicals would be expected to be the most common inhibitory effect of carbonate-bicarbonate alkalinity on the action of the UV/TiO_2 treatment method.

In this research, we study the effect of carbonate-bicarbonate alkalinity on the TiO_2 photocatalytic degradation of acetone and isopropanol as a function of pH. To the best of our knowledge this effect has not been investigated. Only one study by Cundall et al. (1976) reported that the addition of $1.4x10^{-2}$ mol kg^{-1} of Na_2CO_3 (mostly present as CO_3^{2-} anion) to an aqueous solution of isopropanol (mole fraction = 0.414, TiO_2 = 10 g L^{-1}) greatly affected the rate of acetone photocatalytic formation. Their qualitative study showed that in the presence of Na_2CO_3 no acetone was detected in the first 30 minutes of irradiation and only evolved after prolonged reaction times, in contrast to the continuous acetone formation in the absence of the salt. The authors did not give an explanation to their findings.

In this investigation, we speculate that carbonate-bicarbonate alkalinity will have a detrimental effect on the photocatalytic oxidation of acetone and isopropanol by lessening their degradation rates in the reaction slurries. Based on the current knowledge on the effect of these anions in UV/TiO_2 photocatalysis, we hypothesize that the influence of carbonate-bicarbonate alkalinity on the photodegradation rates of our model compounds can be attributable to the effect of the competition for surface hydroxyl radicals between carbonate species (Equations 3.5 and 3.6) and our target compounds (Equations 3.7 and 3.8, k values from Buxton et al., 1988). Based on the values of the reaction rates for the scavenging reactions we expect that carbonate anions would be more detrimental in our photocatalytic systems than bicarbonate anions by decreasing to a higher extent the photooxidation of our target organic compounds. Since the carbonate and bicarbonate radicals formed in Equations 3.5 and 3.6 possess slower reactivity toward our model compounds (Equations 3.9 and 3.10, k values from Ross and Neta, 1979) compared to hydroxyl radicals, they will not contribute to a great extend to further organic substrate degradation. This will allow their $OH^{\bullet}$ scavenging effect to be readily evidenced in the kinetic parameters describing the photocatalytic oxidation of isopropanol and acetone in the presence of the anions.

$$OH^{\bullet} + (CH_3)_2CHOH \rightarrow H_2O + (CH_3)_2\dot{C}OH \qquad k(OH^{\bullet}+ISP) = 1.9 \times 10^9\ M^{-1}s^{-1} \qquad (3.7)$$

$$OH^{\bullet} + CH_3COCH_3 \rightarrow {}^{\bullet}CH_2COCH_3 + H_2O \qquad k(OH^{\bullet}+ACE) = 1.3 \times 10^8\ M^{-1}s^{-1} \qquad (3.8)$$

$$CO_3^{-\bullet} + (CH_3)_2CHOH \rightarrow HCO_3^{-} + (CH_3)_2\dot{C}OH \qquad k(CO_3^{-\bullet}+ISP) = 3.9 \times 10^4\ M^{-1}s^{-1} \qquad (3.9)$$

$$CO_3^{-\bullet} + CH_3COCH_3 \rightarrow \rightarrow \text{Products} \qquad k(CO_3^{-\bullet}+ACE) = 1.6 \times 10^2\ M^{-1}s^{-1} \qquad (3.10)$$

Considering that hydrogen-bonding interactions may play a role in the adsorption of carbonate species and our model compounds on the TiO_2 surface, the competition for

binding sites may be operative as well in our photocatalytic systems. However, since the kinetic analysis in our study do not quantify this effect, the interpretation of our results on the light of this possible competition will be based on the multisite model of the TiO_2 surface and the binding modes proposed in Figure 3.2, which derived from this surface model.

3.2. Experimental Section

3.2.1. Materials

Degussa P25 TiO_2 was used without purification. This catalyst has a BET surface of 50 ± 15 m^2g^{-1} and an average particle size of 21 nm as reported by the manufacturer. The chemicals isopropanol (ISP) and acetone (ACE) were purchased from Aldrich with a purity of 98% or higher. Anhydrous Na_2CO_3 (purity ≥ 99.5, Aldrich) was used as the source of carbonate species. NaOH (97% purity) and HNO_3 (90% purity) were obtained from Fisher Scientific and used for pH adjustment of the suspensions. All reagents were used as received. Nanopure water (18.1 mΩ·cm) from an Infinity ^{TM} ultrapure purification system (model D8961, Barnstead) was used for preparation of all solutions.

3.2.2. Photocatalytic oxidation experiments

The photocatalytic oxidation experiments were carried out using a 450 W medium pressure mercury-vapor lamp (Ace Glass, Cat. 7825-34) positioned within a double-walled quartz cooling water jacket (Ace Glass, Cat. 7874-35). A cylindrical cap-sealed quartz reaction vessel (Ace Glass, Cat. D116912) containing 20 mL of reaction solution was fitted in a motor-driven rotating stirrer (Scientific Industries, Inc., Cat. 3-163-404)

and directly exposed to the lamp. More details about the experimental photochemical apparatus were reported in Chapter 2.

A reaction mixture was prepared by introduction of TiO_2 (2g/L) into 20 mL of an aqueous mixture of carbonate and organic substrate (isopropanol or acetone) in the quartz reaction vessel. Concentrations of isopropanol and acetone ranged between (1.54-1.70) $x10^{-3}$ M. The pH of the suspensions were adjusted with addition of NaOH or HNO_3 to the values 6.35, 8.35, 10.36, and 12.0 in order to reflect different carbonate compositions (HCO_3^-/CO_3^{2-}) in our photocatalytic systems. Typical concentrations of bicarbonate ion in lakes and groundwater has been reported to be between 4-6 mM [Staehelin and Hoigne, 1985] and in NASA's Water Recovery System its concentration varies between 0.49-1.64 mM [Verostko et al., 2000]. Considering that the application of AOPs like UV/TiO_2 photocatalysis increases the content of carbonate-bicarbonate alkalinity during the treatment process, we use a high concentration of 0.01 M Na_2CO_3. All suspensions were prepared in duplicates, placed in the dark, shielded with aluminum foil and allowed to equilibrate overnight at 10°C.

After irradiation, samples for analysis were withdrawn with a syringe (Perfektum Micro-mate interchangeable syringe, Fisher Scientific) and filtered through a 0.1 μm nylon membrane (Osmonics Inc., Fisher Scientific) fitted in a 13mm-filter holder (Millipore, Fisher Scientific). The filtrate was transferred to autosampler vials containing fixed 100 μL glass inserts and stored in the dark at 10°C until gas chromatographic analysis (one injection per vial).

3.2.3. Gas chromatographic analysis

The degradation of isopropanol and acetone was followed by gas chromatography using a Shimadzu GC-17A gas chromatograph (GC) equipped with a fused silica capillary column (Supelcowax^{TM}-10, polyethylene glycol stationary phase, 30m length x 0.32mm i.d. x 1.0μm film thickness, Aldrich) and a FID detector (ultrahigh purity helium used as carrier gas). An oven temperature programming of 60ºC (2.0 min) to 80ºC @ 5ºC/min, injector and detector temperatures of 200ºC and 1 μL injection volume (split 15:1) were selected for the chromatographic analysis.

Identification and quantitation of isopropanol and acetone were performed by previously calibrating the GC with standards of varying concentrations of the selected compounds and analyzing the retention times and peak areas obtained in the chromatograms. Acetone was the only reaction product of isopropanol photodegradation detected in the liquid phase by gas chromatography. A peak eluting at R_t= 0.8 minutes, corresponding to a product of acetone photodecomposition, was also observed in the chromatograms but it was not identified.

3.2.4. Determination of kinetic parameters

The photodegradation modeling of acetone and isopropanol was performed using a program written by the authors in Mathematica 5.2 (Appendix B). The kinetic rates were followed in the region where the reaction was linear which occurred within the first two half-lives. All plots were analyzed in terms of formal kinetics. More details on the determination of kinetic parameters were given in Chapter 2.

3.3. Results and Discussion

3.3.1. Effect of bicarbonate alkalinity (HCO_3^-) on the photocatalytic degradation of isopropanol and acetone

In order to study the effect of bicarbonate ions in our photocatalytic systems, the initial degradation rate constants of isopropanol and acetone were examined in the presence of Na_2CO_3 at pH 6.35 (50% HCO_3^-) and pH 8.35 (100% HCO_3^-). Figure 3.3 illustrates the results obtained in these experiments. The kinetic parameters (reaction orders and initial rate constants) computed by fitting the experimental data are given in Table 3.1. The results obtained under the effect of pH alone (Chapter 2) will be used for comparison and they will be referred as kinetic parameters calculated in the absence of Na_2CO_3.

The first point to observe from our kinetic results is that in the absence of Na_2CO_3 the initial rate of photodegradation of isopropanol (k_{ISP}) depicts an increase from $6.2x10^{-5}$ M min^{-1} at pH 6.04 to $7.5x10^{-5}$ M min^{-1} at pH 8.61. The increase in bicarbonate concentration from 50% (pH 6.35) to 100% (pH 8.35) resulted in a comparable increase in k_{ISP} from $3.0x10^{-5}$ to $4.38x10^{-5}$ M min^{-1}, respectively. This observation suggests that the difference in initial rate constants obtained when the pH is increased from pH 6.35 to 8.35 in the presence of bicarbonate anions may be attributable to a pH effect on the rate of degradation of isopropanol, that is, the degradation of isopropanol is faster at conditions of alkaline (pH~8) where a suitable concentration of surface binding sites and hydroxyl radicals occurs simultaneously.

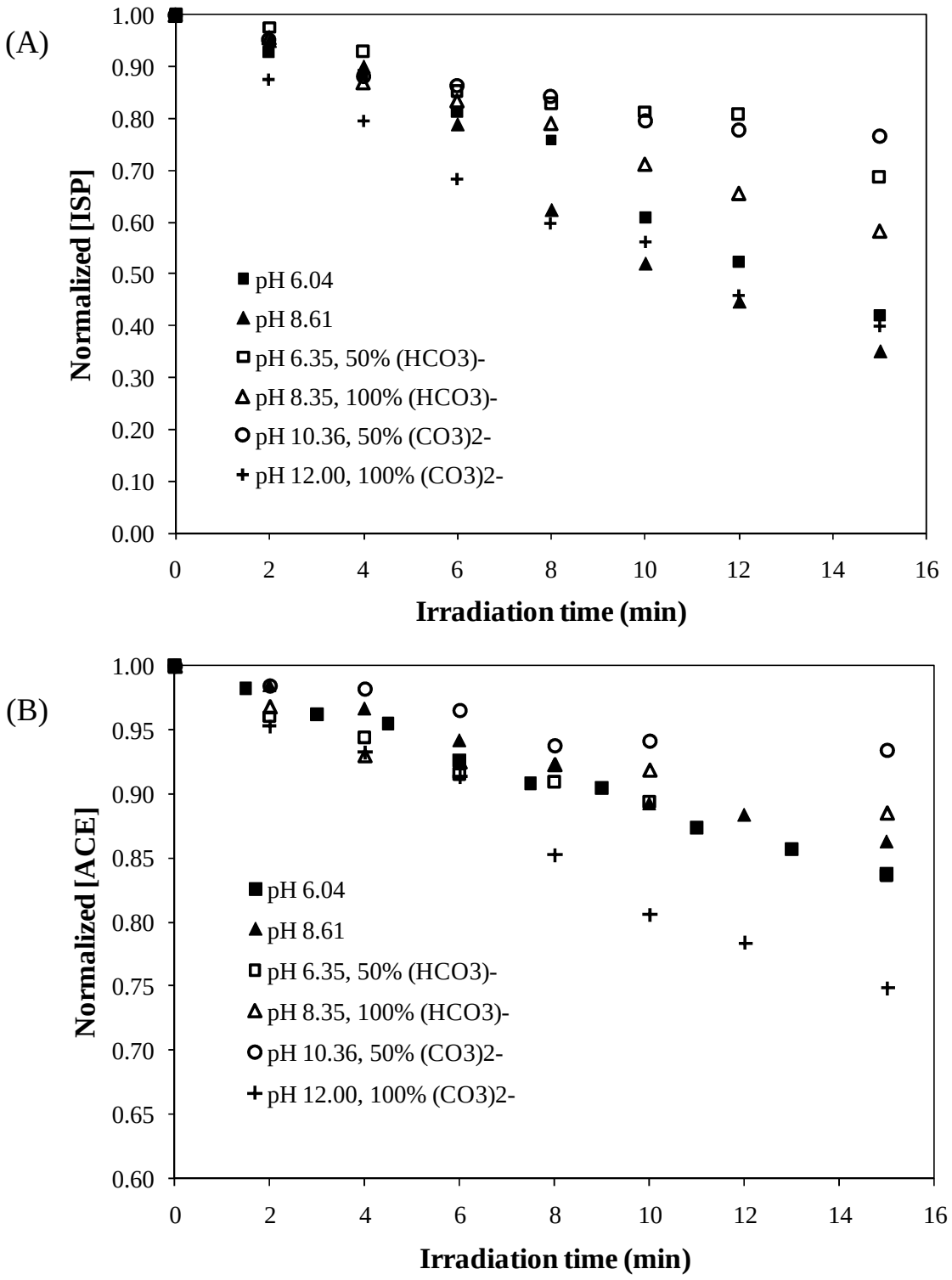

Figure 3.3. Photocatalytic degradation of (A) isopropanol [(1.54-1.62) x10^{-3} M] and (B) acetone [(1.58-1.70) x10^{-3} M] in TiO_2 (2g/L) aqueous slurries containing Na_2CO_3 (0.01 M) at different initial pH values. Filled symbols represent the degradation profiles obtained under the effect of pH alone (Chapter 2) and are given for comparison.

Table 3.1. Initial rate constants for the effect of pH and bicarbonate ions on the photocatalytic degradation of isopropanol [(1.54-1.56) $x10^{-3}$ M] and acetone [(1.69-1.70) $x10^{-3}$ M] in aqueous suspension of TiO_2 (2g/L).*

Initial pH (% carbonate species)	k_{ISP} (M min-1)	k_{ACE} (min^{-1})
6.35 (50% HCO_3^-)	$(3.0 \pm 0.1)\ x10^{-5}$	$(1.22 \pm 0.04)\ x10^{-2}$
8.35 (100% HCO_3^-)	$(4.38 \pm 0.09)\ x10^{-5}$	$(9.4 \pm 0.5)\ x10^{-3}$
6.04 (no HCO_3^-)	$(6.2 \pm 0.2)\ x10^{-5}$	$(1.21 \pm 0.05)\ x10^{-2}$
8.61 (no HCO_3^-)	$(7.5 \pm 0.3)\ x10^{-5}$	$(1.04 \pm 0.06)\ x10^{-2}$

* The effect of bicarbonate anions was studied by adding Na_2CO_3 to the slurries (0.01 M).

The results in Table 3.1 also show that at pH~6 and pH~8, k_{ISP} is around 2.07 and 1.71 times faster, respectively, than under the effect of 0.01 M Na_2CO_3 at similar pH conditions. This is in complete agreement with our hypothesis that the photocatalytic degradation of isopropanol is retarded under the addition of the bicarbonate anions to the slurries compared to conditions where the inorganic additive is absent. Therefore, although the k_{ISP} is faster on increasing the pH of the aqueous media from 6.35 to 8.35, the presence of bicarbonate anions significantly decreases the rate of degradation of isopropanol under the experimental conditions used.

To find a plausible explanation for the results presented above for isopropanol we can first consider the $OH^\bullet$ scavenging inhibition factor of bicarbonate anions. From Equations 3.5 and 3.7 we can see that bicarbonate anions react with hydroxyl radicals at a rate that is 3 orders of magnitude slower than the corresponding rate for isopropanol reacting with hydroxyl radicals. Let us consider a strictly homogeneous kinetic system and take into account the second order rate constant for the reaction of $OH^\bullet$ radicals with isopropanol ($k(OH^\bullet + ISP) = 1.9x10^9\ M^{-1}\ s^{-1}$, Buxton et al., 1988) and HCO_3^- ($k(OH^\bullet +$

HCO_3^-) = 8.5×10^6 M^{-1} s^{-1}, Buxton et al., 1988), and their respective concentrations as used in our experiments. From this, it could be estimated that approximately 98% and 97% of the hydroxyl radicals would react with isopropanol at the initial pH 6.35 and 8.35, respectively [28] (see Appendix C for details on calculations). Although this calculation does not account for differences in surface adsorption of isopropanol and bicarbonate, and therefore, assumes that their reaction with hydroxyl radicals only depends on their rates constants, it helps to put the effect of the scavenging reaction into perspective.

From the above analysis, it is observed that the $OH^\bullet$ scavenging reaction alone cannot explain the slowness in isopropanol initial rate constants observed in the presence of bicarbonate anions. Therefore is possible to suggest that this is also due to the hydrogen-bonding of bicarbonate anion to the TiO_2 surface. We previously suggested that bicarbonate may bind to the hydroxyl surface group $\equiv OH^{1/3+}$. In addition, according to our hydrogen-bonding hypothesis presented in Chapter 2, we proposed that isopropanol has the potential to bind to the most abundant surface hydroxyl groups in all the range of experimental pH, $\equiv OH^{1/3+}$ and $\equiv Ti\text{-}OH^{1/3-}$ (see also Figure 1.5). Therefore, there might be a possible competition between bicarbonate anion and isopropanol to hydrogen-bond to the $\equiv OH^{1/3+}$ surface group. The fact that the concentration of this surface site is higher at pH 6.35 than at pH 8.35 (pH_{zcp} of TiO_2 = 6.5, Rodríguez et al., 1996) would explain the slightly faster degradation of isopropanol at the slightly alkaline

[28] As stated by Larson and Zepp (1988), the calculated fraction of hydroxyl radicals ($f_{OH^\bullet,i}$) that reacts with a system component (i) represents the efficiency at the start of treatment. By no means, this value reflects the further decrease in efficiency that occurs as the target compound concentration decreases overtime. With this calculation we are also assuming that the surface hydroxyl radical possesses similar reactivities with the system components as the free hydroxyl radical in the solution bulk. In addition, this calculation does not take into account the effect of adsorption to the TiO_2 catalyst which may further affect the availability of surface hydroxyl radicals to the system component. Therefore, we caution that the second assumption, in particular, may give values of $f_{OH^\bullet,i}$ that are not completely valid for a given photocatalytic system. However, we may use $f_{OH^\bullet,i}$ values in order to put the initial $OH^\bullet$ radical scavenging into perspective.

pH in the presence of bicarbonate anions. Therefore, this view complements our previous suggestion that the increase in k_{ISP} obtained when the pH is raised from 6.35 to 8.35 in the presence of bicarbonate anions is due to a pH effect on the surface speciation and, consequently, on the rate of degradation of isopropanol. At pH 8.35 a decrease in the surface concentration of $\equiv OH^{1/3+}$ sites causes a lessening in the adsorption of bicarbonate anions, while the conditions are still given for the adsorption and reaction with hydroxyl radicals for isopropanol which has the ability to bind to other surface sites.

In light of the above, the inhibitory effect caused by bicarbonate anions on the degradation rate of isopropanol seems to be related not only to the $OH^{\bullet}$ scavenging effect but also to the competition for binding sites. The later may cause the decrease in the $f_{OH\bullet,ISP}$ values in our photocatalytic system compared to a strictly homogenous one leading to the slowness in the photocatalytic degradation of isopropanol, as it was observed. Due to the absorption of the anions, bicarbonate radicals would be formed on the surface of the catalyst which have extremely low reactivity toward the alcohol [29]. Although this conclusion explains the observed data, it is merely speculative. More studies would be necessary to test the validity of this competitive adsorption effect by bicarbonate anions.

The results for the photocatalytic degradation of acetone in the presence of bicarbonate alkalinity are more intriguing. In the absence of bicarbonate ions, the initial rate constant for acetone at pH 6.04 ($k_{ACE} = 1.21 \times 10^{-2}$ min^{-1}) showed a decrease when the pH of the aqueous medium increased up to pH 8.61 ($k_{ACE} = 1.04 \times 10^{-2}$ min^{-1}).

[29] Although we did not find a rate constant for the reaction of $HCO_3^{\bullet}$ with isopropanol in the revised literature, it has been reported that the bicarbonate radical has a decreased reactivity for hydrogen abstraction toward aliphatic alcohols as compared to carbonate radicals [Clifton and Huie, 1993]. Therefore, we assume the value of $k(HCO_3^{\bullet} + ISP)$ is much lower than 3.0×10^4 $M^{-1}s^{-1}$.

Interestingly, in the presence of bicarbonate alkalinity and under similar pH conditions, little (at pH 8.35, $k_{ACE} = 9.4 \times 10^{-3}$ min^{-1}) or no difference (at pH 6.35, $k_{ACE} = 1.22 \times 10^{-2}$ min^{-1}) was observed in the k_{ACE} values with respect to those given above. This indicates that, in a similar fashion to the case of isopropanol, the observed trend for the degradation of acetone corresponds to a pH effect (i.e., the fastest degradation of acetone occurs at pH ~6 [30]). However, the lack of effect of bicarbonate on the degradation of acetone is unexpected according to our hypothesis.

Similarly to the case of isopropanol, we will start the analysis of our data in terms of the $OH^{\bullet}$ scavenging effect of bicarbonate anions. If we calculate the $f_{OH\bullet,ACE}$ (as percentage) for the case of acetone, the values 82% and 72% are obtained for pH 6.35 and 8.35, respectively (see Appendix C for details on these calculations). Although, as we pointed out earlier, these values do not represent the actual situation in a photocatalytic system, they demonstrate that bicarbonate anions compete for hydroxyl radicals in a more efficient way with acetone than with isopropanol. Therefore, a decrease on the photocatalytic degradation of acetone under the presence of bicarbonate anions would be predicted.

In terms of competitive adsorption our observations are also unexpected. From the analysis presented in Chapter 2, we envisioned a more restricted adsorption of acetone to the catalyst surface that mainly involves the acidic $\equiv OH^{1/3+}$ and $\equiv Ti\text{-}OH_2^{2/3+}$ groups. According to the observed first-order kinetics, we speculated that there is a limited fraction of these surface sites reacting with acetone through hydrogen-bonding. Therefore, the adsorption of bicarbonate anion to the $\equiv OH^{1/3+}$ group (which has a major contribution to the surface speciation than the $\equiv Ti\text{-}OH_2^{2/3+}$, Rodríguez et al., 1996) results

[30] See more details on the effect of pH on the photocatalytic degradation of acetone in Chapter 2.

in a competition with acetone for binding sites. This in turns would cause an inhibiting effect on the degradation rate of the intended substrate, which was not observed.

In light of the previous analysis, our hypothesis to explain the unexpected results for acetone is to assume that our model compound has more affinity for the scarce surface group $\equiv Ti\text{-}OH_2^{2/3+}$ than for $\equiv OH^{1/3+}$. This would be consistent with our hypothesis of the limited adsorption of acetone, and it will explain its first-order kinetics for degradation and the reduced efficiency of the UV/TiO_2 process for the destruction of acetone in comparison to isopropanol. If acetone and the bicarbonate anion have both limited adsorption to the TiO_2 surface and they bind on different surface sites, then the probability for the attack of bicarbonate radicals on the adsorbed acetone molecules may be very low. Therefore, this hypothesis suggests that acetone continues to be degraded by a fraction of surface hydroxyl radicals which is not affected by the presence of adsorbed bicarbonate on TiO_2.

There are no reports on the affinity of acetone for a particular surface site on aqueous TiO_2 slurries to support our hypothesis. However, from TiO_2/gas phase studies, it has been suggested that the reactions of some small organic molecules on TiO_2 single crystals show a strong dependence on surface orientation [Brinkley and Engel, 1998]. Coronado et al. (2003a) also suggested that the photocatalytic oxidation of gaseous acetone on a prehydroxylated TiO_2 sample was comparatively slow with respect to aliphatic alcohols because it showed structural sensitivity (i.e., the TiO_2 crystal faces can have different reactivities depending on the availability of surface hydroxyl groups). In TiO_2/liquid systems, the determination of the actual TiO_2 crystal faces exposed to the aqueous solution is a difficult task. Therefore, for simplicity, the multisite model

assumes equilibrium crystal shape [Rodríguez et al., 1996]. However, keeping this drawback in mind, we do not discard that the photodegradation of acetone in aqueous solution is also affected by the crystallographic heterogeneity of the titanium dioxide and the associated phenomenon of different geometric arrangements of the surface hydroxyl groups. On the basis of these arguments, it is likely that acetone may have more affinity for a particular acid site over another, as suggested in our hypothesis.

Although the hypotheses and arguments given in our discussion for the effect of bicarbonate alkalinity on the photocatalytic degradation of acetone and isopropanol seem to explain the observed results, further studies will be necessary to ascertain their validity.

It is worth to point out that the most important contribution given by this study is that the TiO_2 surface does seem to control the photocatalytic destruction processes of our model compounds. For example, if the oxidation of acetone was to occur mainly by homogeneous reaction with free hydroxyl radicals (whose existence in photocatalytic systems is still in controversy), then the bicarbonate anions would have had a more detrimental effect on the photocatalytic reaction rates of our model compound. In such scenario, the free hydroxyl radicals would be also scavenged by the unadsorbed bicarbonate anions and the slowness of the reaction between $HCO_3^{\bullet}$ and acetone would have caused a decrease in the calculated degradation rates. Therefore, from our data, it seems reasonable to conclude that the $OH^{\bullet}$ scavenging reactions and the attack of radical species (either adsorbed $OH^{\bullet}$ or adsorbed $HCO_3^{\bullet}$) on the target substrates requires the initial adsorption on the surface of the system components (i.e., target organic compounds and bicarbonate anions).

3.3.2. Effect of carbonate alkalinity (CO_3^{2-}) on the photocatalytic degradation of isopropanol and acetone

The data obtained for the effect of carbonate alkalinity in our photocatalytic systems is summarized in Table 3.2 and Figure 3.3. Unlike our analysis for the effect of bicarbonate alkalinity, we do not compare with kinetic information for the degradation of our model compounds in the pH range 10.36 to 12.0 in the absence of Na_2CO_3 [31].

Table 3.2. Initial rate constants for the effect of carbonate ions on the photocatalytic degradation of isopropanol [1.62 x10^{-3} M] and acetone [(1.58-1.65) x10^{-3} M] in aqueous suspension of TiO_2 (2g/L) as a function of initial pH.*

Initial pH (% carbonate species)	**k_{ISP} (min^{-1})**	**k_{ACE} (min^{-1})**
10.36 (50% CO_3^{2-})	(2.09 ± 0.06) x10^{-2}	(5.5 ± 0.6) x10^{-3}
12.00 (100% CO_3^{2-})	(6.2 ± 0.2) x10^{-2}	(1.97 ± 0.04) x10^{-2}

* The effect of carbonate anions was studied by adding Na_2CO_3 to the slurries (0.01 M).

The most striking observation from Table 3.2 is the change in reaction order for the photocatalytic degradation of isopropanol to first-order kinetics under conditions of highly alkaline pH and in the presence of carbonate anions. This change in reaction mechanism does not allow a direct comparison of the degradation rate values for isopropanol under the effect of carbonate and bicarbonate anions. Despite this, it can be observed from Figure 3.3 that in the presence of 50% carbonate anion (pH 10.36) the degradation of isopropanol is slower than under the presence of bicarbonate anion (pH 6.35 and 8.35), according to our prediction. Interestingly, with further increase in pH and carbonate anion concentration the degradation rate of isopropanol undergoes a sudden

[31] High alkaline conditions had detrimental effects in our chromatographic column (SUPELCOWAX™ 10). Therefore, studies under conditions of highly basic pH were limited to the study of the effect of carbonate alkalinity on the photocatalytic degradation of our model compounds and their respective control solutions (without TiO_2).

increase from $2.09x10^{-2}$ min^{-1} (at pH 10.36, 50% CO_3^{2-}) to $6.2x10^{-2}$ min^{-1} ((at pH 12.0, 100% CO_3^{2-}).

The change in reaction order for the TiO_2-mediated photooxidation of isopropanol at the alkaline pH values of 10.36 and 12.0 can be explained by the decrease in the number of surface sites available for isopropanol binding at those experimental conditions. Considering the deprotonation constants (Equations 2.1 and 2.2) for the surface hydroxyl groups (pK_{a1} = 5.38 and pK_{a2} = 7.60, Rodríguez et al., 1996), at the highly alkaline pH of 10.36 and 12.0 the surface speciation mostly consists of $\equiv Ti\text{-}OH^{1/3-}$ and $\equiv O^{2/3-}$ sites. Being that isopropanol is a better hydrogen acceptor (β^H = 0.56; Abraham, 1993) than a hydrogen donor (α^H = 0.33; Abraham, 1993), it is likely that the fraction of effective binding sites for the alcohol is decreased at conditions of very high pH where the surface speciation is predominantly basic in character.

In addition, the slow degradation rate of isopropanol under the conditions of pH 10.36 and 50% carbonate anion can be explained as a result of a combined effect of these two water parameters. Although the amount of anions adsorbed on the surface may be limited by the number of $\equiv OH^{1/3+}$ sites present at pH 10.36, the carbonate anion is a better hydroxyl radical scavenger than bicarbonate anion by a factor of 46 ($k(OH^{\bullet}+CO_3^{2-})$ = 3.9 $x10^8$ $M^{-1}s^{-1}$ vs. $k(OH^{\bullet}+HCO_3^{-})$ = 8.5 $x10^6$ $M^{-1}s^{-1}$, Buxton et al., 1988) [32]. In addition, the rate constant for the reaction between carbonate radical and isopropanol is significantly slower ($k(CO_3^{-\bullet} + ISP)$ = 3.9 $x10^4$ $M^{-1}s^{-1}$, Ross and Neta, 1979) than the corresponding rate constant for the reaction with the hydroxyl radical ($k(OH^{\bullet} + ISP)$ = 1.9 $x10^9$ M^{-1} s^{-1},

[32] To put this into perspective, the fraction of hydroxyl radicals reacting with isopropanol ($f_{OH\bullet,ISP}$) in a perfectly homogeneous system is calculated in Appendix C. The calculations show that $f_{OH\bullet,ISP}$ is highly decreased in the presence of 50 % carbonate anions that on 100% of bicarbonate anions ($f_{OH\bullet,ISP}$ decreases from 0.97 at pH 8.35 to 0.61 at pH 10.36 in the presence of Na_2CO_3 under the conditions used in our experiments).

Buxton et al., 1988). Therefore, the small fraction of adsorbed carbonate anion on the TiO_2 surface may have a high negative impact on the photodegradation of isopropanol at pH 10.36 since the adsorption of the alcohol decreases under this pH condition, as explained earlier.

In our photocatalytic system, the sudden increase in the photooxidation of isopropanol at pH 12.0 in the presence of Na_2CO_3 is due to an important acid/base equilibrium of the hydroxyl radical (pK_a = 11.0, Buxton et al., 1988 [33]) that takes place at these conditions (Equation 3.11).

$$OH^{\bullet} \leftrightarrow O^{-\bullet} + H^{+} \qquad (3.11)$$

It is known that the oxide radical anion ($O^{-\bullet}$) does not react with the carbonate anion as efficiently ($k(O^{-\bullet}+CO_3^{2-}) = 2.7 \times 10^6\ M^{-1}s^{-1}$, Buxton et al., 1988) as the hydroxyl radical does ($k(OH^{\bullet}+CO_3^{2-}) = 3.9 \times 10^8\ M^{-1}s^{-1}$, Buxton et al., 1988). However, the absence of adsorbed anion at pH 12.0 due to electrostatic repulsion with the highly negative TiO_2 surface would preclude any reaction between these two species. Therefore, it is the efficiency of the reaction between the oxide radical anion and isopropanol ($k(O^{-\bullet}+ ISP) = 1.2 \times 10^9\ M^{-1}\ s^{-1}$, Buxton et al., 1988) which explains the observed results. Under these conditions (pH 12.0 and 100% CO_3^{2-}) the photocatalytic degradation of isopropanol has a comparable efficiency with that observed under the effect of pH 8.61 alone since the percentage of degraded isopropanol was 60% and 65%, respectively (in Chapter 2, pH 8.61 was found to give the best conditions for isopropanol

[33] Buxton et al. (1988) reported a pK_a value of 11.0 for the acid/base equilibrium

$$OH^{\bullet} \leftrightarrow O^{-\bullet} + H^{+}$$

in homogeneous phase. However, the pK_a for this equilibrium on the surface of TiO_2 (see Equation 1.8) has not been determined. Assuming a similarity between the $OH^{\bullet}$ radical in the bulk solution and the adsorbed $OH^{\bullet}$ radical this pK_a value will be adopted in our analysis.

photodegradation through hydroxyl radical attack). This might demonstrate the similarity in the reactivity of $OH^{\bullet}$ and $O^{-\bullet}$ radicals toward the model alcohol.

It is important to add that, according to the literature, the attack of $OH^{\bullet}$ [Asmus et al., 1973], $O^{-\bullet}$ [Buxton et al., 1988], and $CO_3^{-\bullet}$ [Clifton and Huie, 1993; Ross and Neta, 1979] radicals on isopropanol occur through hydrogen abstraction reactions. Correspondingly, in all of our chromatographic analysis acetone was the only oxidation product detected.

In terms of the degradation of acetone, the further increase in pH from 8.35 to 10.36, and the concomitant change in the nature of anion present in solution, caused a decrease in the degradation rate constant of acetone from 9.4×10^{-3} min^{-1} to 5.5×10^{-3} min^{-1}, as expected. In a similar fashion to isopropanol degradation, the efficiency of the photocatalytic degradation of acetone increased at pH 12.0 and 100% CO_3^{2-}. A k_{ACE} value of 1.97×10^{-2} min^{-1} was obtained at these conditions.

The results for acetone cannot be explained on the basis of a simple effect of pH, or even less on an anion adsorption effect. As we explained earlier, at highly alkaline pH the surface speciation mostly consists of $\equiv Ti\text{-}OH^{1/3-}$ and $\equiv O^{2/3-}$. According to our hydrogen-bonding hypothesis, acetone would not bind to these basic sites because our substrate only possesses hydrogen acceptor capabilities. Therefore, on the grounds of pH effect alone, the adsorption of acetone is not likely to occur at highly alkaline conditions.

In order to give a plausible explanation for the observed results, another water parameter must be considered. Therefore, the best possible explanation is that the addition of Na_2CO_3 to the TiO_2 slurries adds the effect of ionic strength on the photocatalytic process. Specifically, as the ionic strength increases the surface charge is

easily balanced by counterions in the nearby solution [Vasudevan and Stone, 1996]. This effect is expected to be higher in the presence of carbonate alkalinity since the ionic strength on the slurries is increased when the bivalent CO_3^{2-} anion is present (for example, it changes from ~0.017 M at pH 10.36 (50% CO_3^{2-}) to ~0.025 M at pH 12.0 (100% CO_3^{2-})). Therefore, our hypothesis is that by increasing the ionic strength the repulsion between the negative end of the dipole on the carbonyl oxygen of acetone and the negatively charged TiO_2 surface is diminished. This possibility would permit the reaction of unadsorbed acetone with the adsorbed $OH^{\bullet}$ and $CO_3^{-\bullet}$ radicals at pH 10.36 and with the adsorbed $O^{-\bullet}$ radicals at pH 12.0 within the thin interfacial layer vicinal to the surface. Additional research would be required to verify this hypothesis.

In light of the above and similarly to the case of isopropanol, the $OH^{\bullet}$ scavenging effect of CO_3^{2-} explains the observed decrease in k_{ACE} when the pH is raised from 8.35 to 10.36 [34]. The sudden increase in the initial rate of degradation of acetone at pH 12.0 is due to the preference of the oxide radical anion to attack acetone over the carbonate anion.

It is worth to mention that although we could not find a value for the rate constant ($k(O^{-\bullet}+ ACE)$) in the revised literature, it seems that the oxide radical anion may be just as or more efficient than the hydroxyl radical to degrade acetone. This remark is based on the observations that 25% of the initial concentration of acetone was degraded at

[34] In a perfectly homogeneous system the fraction of hydroxyl radicals reacting with acetone ($f_{OH^{\bullet},ACE}$) would be highly decreased in the presence of 50 % carbonate anions that on 100% of bicarbonate anions ($f_{OH^{\bullet},ACE}$ decreases from 0.72 at pH 8.35 to 0.10 at pH 10.36 in the presence of Na_2CO_3 under the conditions used in our experiment; see Appendix C for details on these calculations). However, as we already mentioned, this calculation does not account for the effect of surface binding. The limited adsorption of acetone and carbonate anions on the TiO_2 surface at pH 10.36 may decrease their respective $f_{OH^{\bullet},i}$ values with respect to those calculated for a homogeneous system.

conditions of pH 12.0 and 0.01 M Na_2CO_3, while 16% was degraded under the effect of pH 6.04 alone (in Chapter 2 this pH was found to render the best conditions for the degradation of acetone through hydroxyl radical attack). It has been previously noted that both $OH^{\bullet}$ and $O^{-\bullet}$ radicals react with aliphatic organic compounds through hydrogen abstraction reactions in aqueous solutions [Neta and Schuler, 1975], therefore relatively similar reactivities with acetone could be expected.

At this point is also important to add that the direct photolysis mechanism does not account for the values and trends observed for k_{ISP}, and k_{ACE} in the UV/TiO_2 photocatalytic system containing 0.01 M Na_2CO_3. The analysis of the control solutions (i.e., in the absence of TiO_2) containing the salt, shows that the degradation of isopropanol under the effect of UV light follows a first-order kinetics in all the range of experimental pH contrary to the observations in the UV/TiO_2 photocatalytic system. In addition, when the reaction orders allow direct comparison, the calculated rate constants for the direct photolysis (k_{DP}) of isopropanol are around one order of magnitude lower than those k_{ISP} values (in units of min^{-1}) in the presence of TiO_2. In the case of acetone, under identical conditions, the k_{DP} values were between $2.2 \times 10^{-3} - 3.3 \times 10^{-3}$ min^{-1}. These values were always significantly lower than the k_{ACE} values obtained in the heterogeneous photocatalytic experiment (the experimental data obtained from these control solutions is presented in Appendix D).

3.4. Conclusions

In this study we investigated the effect of carbonate-bicarbonate alkalinity (0.01 M Na_2CO_3) in the application of heterogeneous TiO_2 photocatalysis for the oxidation of

acetone and isopropanol (in the mM level) in water. The extent of inhibition on the rates of degradation varied according to the type of anions present in the photocatalytic system and their reactivity toward $OH^{\bullet}$ scavenging.

Although the carbonate anion adsorbs to a less extent on the TiO_2 surface than the bicarbonate anion, its higher ability for scavenging of hydroxyl radicals had a more detrimental effect on the photodegradation rates of our target compounds at the pH of 10.35. At the highly basic pH of 12.0, were the anions did not adsorb to the TiO_2 surface and the $OH^{\bullet}/O^{-\bullet}$ equilibrium was operating, the efficiency of the UV/TiO_2 process to degrade acetone and isopropanol was significantly enhanced with respect to any other pH in the presence of Na_2CO_3 since the attack of $O^{-\bullet}$ toward our model compounds was preferable over the reaction with the carbonate anions.

The results of this investigation provide the basis to determine the experimental conditions that can optimize the UV/TiO_2 treatment of water containing acetone and isopropanol when high levels of carbonate-bicarbonate alkalinity are present. The use of highly basic conditions of pH 12.0 obviously imposes limitations when dealing with large scale treatment systems. Therefore, the only practical improvement may be to decrease the hydroxyl radical scavenging by pH adjustment to $\leq$ 8.35 (in order to convert carbonate alkalinity to bicarbonate alkalinity), while optimal conditions for the adsorption of the intended substrate on the TiO_2 catalyst can still be attained. In addition, other pretreatment options before application of UV/TiO_2 photocatalysis should also be considered in order to reduce the alkalinity of the water at the beginning of the process.

CHAPTER 4

Effect of ionic strength on the TiO_2-mediated photocatalytic degradation of small polar organic compounds in aqueous solution

4.1. Introduction

Part of the current knowledge about the electrical properties of the titanium dioxide/aqueous interface has been obtained from potentiometric acid/base titrations of TiO_2 suspensions in the presence of indifferent electrolytes [Ahmed and Maksimov, 1969; Bérubé and Bruyn, 1968; Davis et al., 1978; Hiemstra and Van Riemsdijk, 1991; Kallay et al., 1986; Schindler and Gamsjäger, 1972]. The titration data is usually presented by plotting the relative ionic adsorption density of protons and hydroxyl ions ($\Gamma_{H+} - \Gamma_{OH-}$) [35] against pH of the solution.

When the so called adsorption isotherms of the potential determining ions (H^+ and OH^-) are obtained at varying concentrations of indifferent electrolytes (i.e., varying ionic strengths) they constitute a valuable experimental tool to study the oxide surface equilibria and confirm the importance of H^+ and OH^- in the establishment of the surface charge. It is precisely this uptake or release of potential determining ions what is now

[35] As described by Davis et al. (1978) and Rodríguez et al. (1996) the contribution to the surface charge density due to the adsorption of potential determining ions (i.e., ionization of surface hydroxyl groups) is expressed as:

$$\sigma_o = \sigma_o^+ - \sigma_o^- = F\,(\Gamma_{H+} - \Gamma_{OH-})$$

Where σ_o is the surface charge density (C/cm^2), Γ represents the surface concentration of potential determining ions (mol/cm^2) and F is the Faraday's constant. σ_o^+ and σ_o^- are defined as:

$$\sigma_o^+ = F\,(2/3\{\equiv Ti\text{-}OH_2^{2/3+}\} + 1/3\{\equiv OH^{1/3+}\})$$

$$\sigma_o^- = F\,(2/3\{\equiv O^{2/3-}\} + 1/3\{\equiv Ti\text{-}OH^{1/3-}\})$$

Using the nomenclature of Rodríguez et al. (1996), curly brakets represent surface concentrations of the hydroxyl groups.

known as the ionization of the surface hydroxyl groups (Equations 1.1 and 1.2) [36], which was explained in Chapter 1. The experimental details and the method of calculating the charge densities in metal oxide suspensions have been described elsewhere [Ahmed, 1966; Kallay et al., 1986] and it will not be given here.

Independently of the type of indifferent electrolyte chosen, the isotherms have common features related to the electrical properties of the colloid investigated. First, the series of titration curves obtained at varying ionic strengths intersect at a common point where the net surface charge is zero (i.e., pH_{zpc}). Second, when the ionic strength is increased, the adsorption of H^+ and OH^- is enhanced, causing an increase in the positive and negative surface charge above and below the pH_{zpc}, respectively. Adsorption isotherms can be found in the literature for TiO_2 in equilibrium with aqueous solutions of $NaNO_3$ [Bérubé and Bruyn, 1968], KNO_3 [Ahmed and Maksimov, 1969; Hiemstra and Van Riemsdijk, 1991], $LiNO_3$ [Davis et al., 1978], and KCl [Rodríguez et al. 1996]. A typical set of potentiometric titrations of TiO_2 in contact with supporting electrolyte are shown in Figure 4.1.

The experimental charging behavior of TiO_2 in the presence of indifferent electrolytes can be interpreted in terms of the MUSIC (multisite complexation) model and the physical representation of the double layer at the TiO_2/aqueous interface [Hiemstra and Van Rimesdijk, 1991]. According to the electrical double layer model (Figure 1.2), the indifferent electrolyte ions (i.e., those ions that are not specifically adsorbed by the mechanism of ligand exchange) and the potential determining ions (H^+

[36] For example, the adsorption of hydrogen ions can be described by the equation:

$$\equiv Ti\text{-}OH^{1/3-} + H^+ \leftrightarrow \equiv Ti\text{-}OH_2^{2/3+}$$

Whereas the uptake of hydroxyl ions can be presented as a deprotonation [Schindler and Gamsjäger, 1972]:

$$\equiv OH^{1/3+} \leftrightarrow \equiv O^{2/3-} + H^+$$

and OH^-) have a joint role in establishing the magnitude of the surface charge [Davis et al., 1978]. In this model, the electrolyte ions reside in a plane (σ_B) separating the Stern layer from the diffuse layer. From this distance, they counterbalance the surface charge by forming interfacial "ion-pairs" with the charged surface hydroxyl groups (located on the σ_o plane) [Hiemstra and Van Riemsdijk, 1991]. Due to this ion-pairing equilibrium, the Stern layer can be treated as an electrostatic condenser. Therefore, an increase in ionic strength causes an additional adsorption of potential determining ions, as observed in the titration curves of Figure 4.1 [Bérubé and Bruyn, 1968; Hiemstra and Van Riemsdijk, 1991].

Combining a model of the electric double layer with the multisite protonation model of the surface speciation, Rodríguez et al. (1996) successfully predicted the charging behavior of TiO_2 (Degussa P25) in the presence of KCl. According to their model calculations, the increase in electrolyte concentration affects the acid-base equilibria of the surface hydroxyl groups, increasing the contribution of $\equiv Ti\text{-}OH_2^{2/3+}$ (at $pH < pH_{zpc}$) and $\equiv O^{2/3-}$ (at $pH > pH_{zpc}$) to the surface speciation. The higher residual charge carried by these surface sites increases the net charge of the surface in the respective pH range, which is corroborated with experimental observations [Rodríguez et al., 1996].

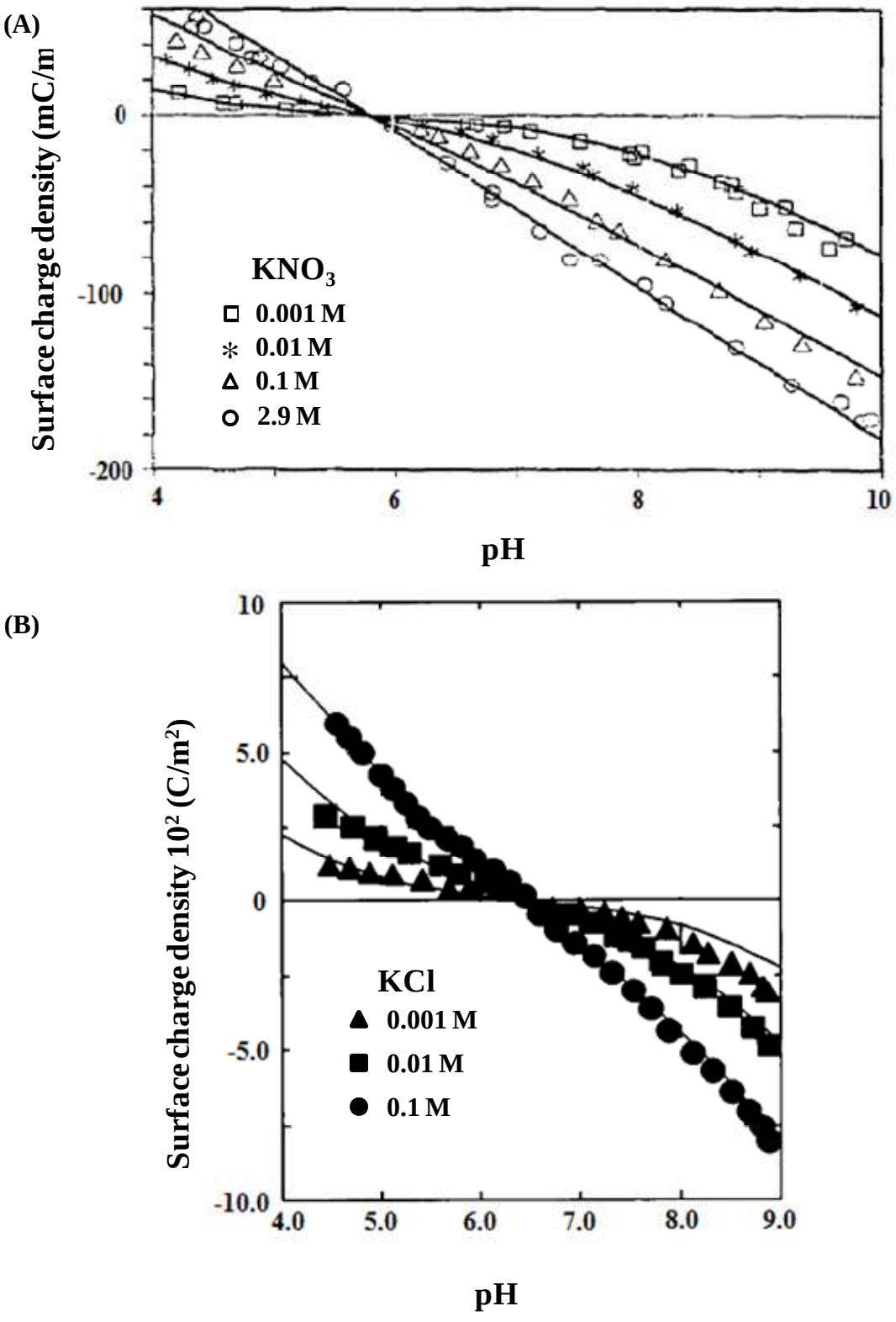

Figure 4.1. Surface charge density (σ_o) on (A) TiO_2 (rutile) in the presence of KNO_3 and (B) TiO_2 (Degussa P25) in the presence of KCl as a function of pH (reproduced from Hiemstra and Van Riemsdijk (1991), p. 20, Figure 6; and Rodríguez et al. (1996), p. 124, Figure 1).

The study of the effect of ionic strength in TiO_2 photocatalytic systems has been mostly related to adsorption studies of organic compounds. The influence of ionic strength on the charging behavior of TiO_2 has been shown to affect the adsorption of organic compounds possessing ligand donor groups that can form inner-sphere complexes with the catalyst [Rodríguez et al., 1996; Stone et al., 1993, Vasudevan and Stone, 1996]. For example, Rodríguez et al. (1996) studied the chemisorption of catechol (1,2-dihydroxybenzene) at the TiO_2/aqueous solution interface. In the absence of electrolyte, the authors observed that the formation of titanium-catecholate complexes produced an excess of negative surface charge as revealed by the shift of the isoelectronic point of the TiO_2 particles to lower pH values (the postulated surface complexation equilibria are given in Equation 4.1 and 4.2). The authors reported that in the presence of background electrolyte (0.1 M KCl) the screening effect caused by the ionic strength enhanced the chemisorption of catechol at pH values within the pH_{zpc} of TiO_2 and the pK_{a1} of cathecol (i.e., between 6.5 and 9.2) [Rodríguez et al., 1996].

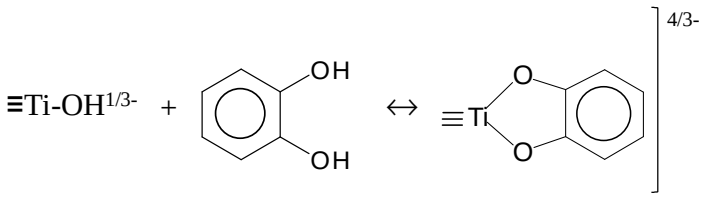

(4.1)

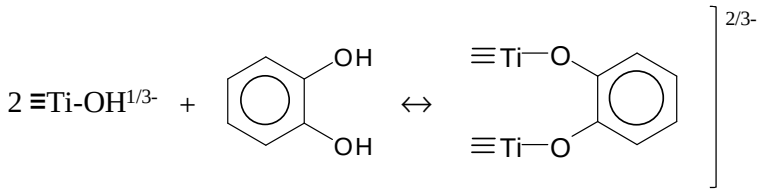

(4.2)

Fewer studies have been done with respect to the TiO_2-mediated photocatalytic reactions of organic substrates in the presence of indifferent electrolyte. For example, Brown and Darwent (1985) followed the kinetic salt effect for the electron transfer from

TiO_2 to methyl viologen (MV^{2+}). Since the reaction involved an ionic reagent the slope of a plot of the rate constant for the formation of $MV^{\bullet+}$ (as log k) against pH was dramatically affected with the increase in the ionic strength of the slurries. At low pH ($pH < pH_{zpc}$) the rate was accelerated by a high ionic strength. This was interpreted as a decrease of the electrostatic repulsion between methyl viologen and the positively charged TiO_2 particles due to the screening effect of the electrolyte. At conditions of electrostatic attraction ($pH > pH_{zpc}$) the opposite effect was observed. The plots intersected at a common point where the ionic strength had no effect in the rate of reduction of methyl viologen, and it was used to determine the pH_{zpc} of the colloid sample.

To the best of our knowledge, there are no systematic studies on the effect of indifferent electrolytes in the photocatalytic degradation of small polar organic compounds which do not specifically adsorb to the TiO_2 surface and do not possess any ionizable functional group. This lack of research is probably due to the major interest on the effect of the addition of salts containing strongly adsorbing anions in photocatalytic degradation rates of organic compounds [Abdullah et al., 1990; Calza and Pelizzetti, 2001; Chen et al., 1997; Chen et al., 2003; Hu et al., 2004; Minero et al., 2000; Söckmen and Özkan, 2002; Xing-hui et al., 2002]. When inorganic anions are specifically adsorbed to the TiO_2 surface (at $pH < pH_{zpc}$) and form inner sphere complexes (e.g., sulfate and phosphate) they clearly reduce the rates of degradation of target compounds by blocking surface sites and reacting with photoproduced oxidizing species (holes and hydroxyl radicals) [Abdullah et al., 1990; Araña et al., 2002; Chen et al., 1997; Chen et al., 2003; Hu et al., 2004].

According to our literature review, only one study by Abdullah et al. (1990) showed that the increasing concentration of $NaClO_4$ (up to 0.1 M) had no effect on the rate of oxidation of ethanol at pH 4.1. This was explained by the absence of any specific adsorption of perchlorate anion to the TiO_2 surface, which was also confirmed by other researchers [Bérubé and Bruyn, 1968; Bourikas et al., 2001; Kazarinov et al., 1981; Sanchez and Augustynski, 1979]. Although the study of Abdullah et al. (1990) was focused on the effect of inorganic anions and was not conducted at other pH conditions, the authors postulated that the reaction between a charged surface and an uncharged species such as ethanol should be unaffected by changes in ionic strength.

The conclusion of Abdullah et al. (1990) is merely based on the grounds of the effect of ionic strength on electrostatic interactions occurring in the TiO_2/aqueous interface. Their suggestion ignores the effect that the increasing concentration of indifferent electrolyte has in the distribution of surface hydroxyl groups which may participate in the adsorption of small polar organic compounds (e.g., ethanol) through other kind of outer-sphere interactions (i.e., hydrogen-bonding).

It is precisely the use of indifferent electrolytes what would permit to study the effect of ionic strength alone on the TiO_2 surface speciation and obtain further information on the possible role of hydrogen-bonding of small polar organic compounds to the surface hydroxyl groups in their photocatalytic degradation. The observations of Abdullah et al. (1990) at acidic pH do not preclude that the effect of increasing ionic strength in the oxidation reaction of small polar organic compounds on the TiO_2 surface may be evidenced at other pH values.

In the first two sections of this chapter the effect of ionic strength (as $NaClO_4$) in the photocatalytic oxidation of acetone and isopropanol in single and binary systems will be investigated in a wide range of pH.

Based on our hydrogen-bonding hypothesis presented in Chapter 2, we hypothesized that, at the pH values for the optimal degradation of our model compounds (i.e., at neutral and acid pH), increasing the indifferent electrolyte concentration will affect the photocatalytic degradation rate of the model compounds.

In the case of aqueous binary systems of acetone and isopropanol (1:1 ratio), we speculate that the photodegradation of isopropanol would be more predominant due to its dual hydrogen-donor and acceptor capabilities. However, some level of competition would be observed if the joint effect of pH and ionic strength enhances the adsorption of acetone to the surface as it will be determined in the study of the single compound.

The experimental data resulting from our studies will be evaluated on the grounds of the effect of ionic strength in the surface hydroxyl speciation as presented by Rodríguez el at. (1996) in their model calculations. Their results were mentioned earlier in this introduction. The reason behind the adoption of such model calculations is to obtain further evidence to determine the possible role played by hydrogen-bonding to the TiO_2 surface in the photocatalytic degradation of our model compounds, acetone and isopropanol.

In order to further test our hydrogen-bonding hypothesis, the last section of this chapter will be dedicated to the investigation of a third model compound, dimethylsulfoxide (DMSO), under similar experimental conditions used for acetone and isopropanol. This study may serve to determine how plausible is to construct a ranking

of competitiveness for TiO_2-mediated photocatalytic degradation of small polar organic compounds based upon their hydrogen-bonding abilities. According to the literature [Abraham, 1993], dimethylsulfoxide lacks hydrogen donor abilities but it is a better hydrogen acceptor than acetone and isopropanol [37]. Based merely on this property, we speculate that DMSO would be able to interact with surface hydroxyl groups (those with acidic character) more readily and, in consequence, degrade at faster rates than acetone. As it was speculated for isopropanol and acetone, we expect to observe an enhancement effect in the degradation rates of DMSO with increasing ionic strength.

As a last remark, in our study we selected sodium perchlorate as the indifferent electrolyte. This selection is based on experimental information that proves the absence of specific adsorption (i.e., chemisorption) of perchlorate ions to the TiO_2 surface [Bérubé and Bruyn, 1968; Bourikas et al., 2001; Kazarinov et al, 1981, Sanchez and Augustynski, 1979]. In addition, it has been reported that ClO_4^- does not react with hydroxyl radicals [Kormann et al., 1991]. Based on these two criteria, sodium perchlorate is a suitable indifferent electrolyte for the study of the ionic strength effect in photocatalytic systems.

4.2. Experimental Section

4.2.1. Materials

TiO_2 P25 (Degussa, lot No. 2047) was used in the form supplied in all the experiments. The manufacturer (Degussa Corporation) reported a specific surface area of 50 ± 15 m^2g^{-1} and an average particle size of 21 nm. Nanopure water (18.1 mΩ·cm) from

[37] A comparison of hydrogen-bonding empirical parameters among our model compounds is given later on in Table 4.4.

an Infinity ^{TM} ultrapure purification system (model D8961, Barnstead) was used for preparation of all solutions. Isopropanol (ISP), acetone (ACE) and dimethylsulfoxide (DMSO) were purchased from Aldrich with a purity of 98% or higher. Sodium perchlorate monohydrated ($NaClO_4 \cdot H_2O$, 98% purity, Aldrich) was used to maintain the ionic strength on the solutions at the desired value (0.01 and 0.1 M). NaOH (97% purity) and HNO_3 (90% purity) were obtained from Fisher Scientific and used for pH adjustment of the suspensions. All reagents were used as received except for DMSO. Nitrogen gas was bubbled through DMSO for 15-20 minutes before preparation of standards or reaction solutions. This precaution was taken in order to improve the quality of the chromatograms during its analysis.

4.2.2. Sample preparation

Suspensions of TiO_2 were obtained by adding 0.0413 g of the catalyst into 20 mL of aqueous model compound solution, containing a predetermined amount of $NaClO_4$ (0.0, 0.01, or 0.1 M). Average initial concentrations of model compounds were (1.62 ± 0.02) $x10^{-3}$ M for isopropanol, (1.56 ± 0.09) $x10^{-3}$ M for acetone, and (1.42 ± 0.08) $x10^{-3}$ M for dimethylsulfoxide. In the mixtures, the molar ratio between isopropanol and acetone was 1:1. All solutions were freshly prepared in duplicates.

The desired solution pH was adjusted by using NaOH or HNO_3. The pH values of the suspensions were measured with a digital pH meter (Orion PerpHect, model 350, Fisher Scientific, Cat. 13-642-629) and a needle combination pH microelectrode (Microelectrodes, Inc., Cat. MI-414B). The suspensions were placed in the dark, shielded with aluminum foil and allowed to equilibrate overnight at 10°C.

4.2.3. Photooxidation apparatus and photocatalytic oxidation experiments

After overnight equilibration, the sample contained in a screw capped quartz tube reaction vessel (Ace Glass, Cat. D116912), sealed with a PTFE/silicone rubber septum (VWR, Cat. 66010-751), was stirred for 0.5 h under dark conditions and immediately taken as the initial sample. The sample was then stirred whilst being irradiated with unfiltered radiation from a 450 W medium pressure mercury-vapor lamp (Ace Glass, Cat. 7825-34) fitted in a double-walled quartz immersion well (Ace Glass, Cat. 7874-35) with inlet and outlet water lines. More details on the photocatalytic oxidation apparatus and its schematic representation were given in Chapter 2.

After irradiation at the desired intervals, an aliquot of the reaction mixture was withdrawn with a syringe (Perfektum Micro-mate interchangeable syringe, Fisher Scientific). The catalyst was separated from the solution by filtration through a 0.1 μm nylon membrane (Osmonics Inc., Fisher Scientific, Cat. R01SP01300) fitted in a 13mm-filter holder (Millipore, Fisher Scientific, Cat. XX3001200). After filtration the sample was stored in two autosampler vials containing fixed 100 μL glass inserts (VWR, Cat. 66065-262), fitted with open-top caps and PTFE/silicone septa (VWR, Cat. 66030-420). The samples were stored in the dark at 10°C until gas chromatographic analysis (each vial was injected once).

Dissolved oxygen (DO) in the suspensions was not controlled but monitoring of its concentration with a fiber optic oxygen sensor system (Ocean Optics) showed that it was still present at the maximum irradiation time selected to sustain the photocatalytic reaction. The fiber optic oxygen sensor system consisted of four major components: a 18-gauge needle oxygen sensor probe (Ocean Optics, Cat. FOXY-18G-AF), a RTD

hypodermic temperature probe (Ocean Optics, Cat. USB-LS-450-TP16), a spectrofluorometer (Ocean Optics, Cat. USB4000-FL-450), and a pulsed blue LED light source (Ocean Optics, Cat. USB-LS-450). Details on the DO sensor components, its calibration and operation were given in Appendix A.

4.2.4. Gas chromatographic analysis

Samples of the reaction mixture were analyzed by a Shimadzu GC-17A gas chromatograph (GC) equipped with a flame ionization detector and a split/splitless injector. The GC separation was obtained on a fused silica capillary column (Supelcowax^{TM}-10, polyethylene glycol stationary phase, 30m length x 0.32mm i.d. x 1.0μm film thickness, Aldrich). For the analysis of DMSO the temperature of the injector and detector were maintained at 250°C and 300°C, respectively, and the GC oven was temperature programmed at 100ºC (1.0 min) @ 20ºC/min to 170°C (4.0 min), @ 40ºC/min to 230°C (2.0 min). Ultrahigh purity helium gas was used as the carrier gas.

The chromatographic conditions to determine the concentration of isopropanol and acetone in samples extracted from the reaction mixture were described in Chapter 2. The same chromatographic technique was used for the analysis of these compounds in their 1:1 molar ratio mixtures. 1 μL injection volume was selected for the chromatographic analysis.

Identification and quantitative evaluation of the model compounds were achieved by previously calibrating the gas chromatograph with freshly prepared standards of varying concentrations. Seven point standard calibration curves of peak area vs. known initial concentration were established for each component. Each standard was injected in

duplicates (one injection per vial). R^2 values in the calibration curves for all three model compounds were between 0.9988 and 0.9999.

4.2.5. Determination of kinetic parameters

The progress of the photocatalytic reaction for a model compound (isopropanol, acetone or dimethylsulfoxide) was monitored by following its concentration as a function of irradiation time. Initial rate method was used to study the kinetics of reaction and, therefore, the photooxidation rates were measured within the first two half time periods. The photodegradation modeling of acetone, isopropanol, and dimethylsulfoxide was performed using a program written in Mathematica 5.2 [38] (Appendix B). A least-square analysis of the experimental data was used to determine the best fit to the rate law of a zero- or first-order reaction. More details on the determination of the kinetic parameters were given in Chapter 2.

4.3. Results and Discussion

4.3.1. Effect of ionic strength on the photocatalytic degradation of acetone and isopropanol as individual compounds.

Figures 4.2 and 4.3 along with Tables 4.1 and 4.2 present the results of the study of the effect of ionic strength on the photocatalytic degradation of isopropanol and acetone in the presence of three different concentrations of $NaClO_4$, used as indifferent electrolyte. Due to the joint effect of ionic strength and pH on the development of TiO_2 surface charge and speciation, the experiments were performed in a wide range of pH (4.10, 6.04 and 8.61). The results obtained for the effect of pH alone ion our

[38] This program was written by Eduardo Martínez Pedroza, Ph.D. in collaboration with the author.

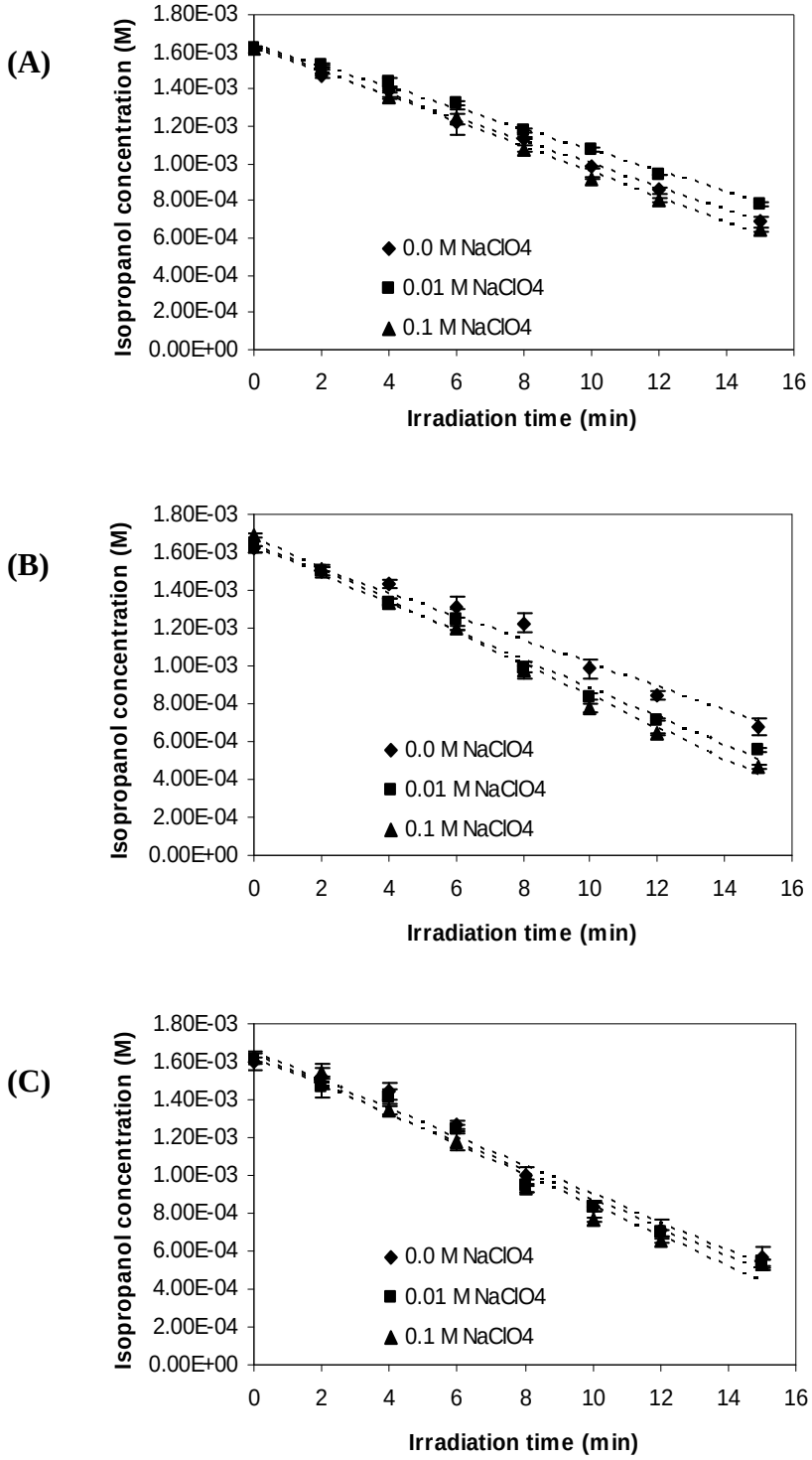

Figure 4.2. ISP concentration vs. time profile obtained from the UV/TiO_2-treatment of aqueous solutions of isopropanol at different ionic strengths (as $NaClO_4$). (A) pH 4.10, (B) 6.04, (C) 8.61. (TiO_2, 2 g/L; initial concentrations, $[ISP]_o$ = (1.60-1.69) $x10^{-3}$ M. The markers indicate experimental data. The dashed lines indicate the nonlinear least-square fit.

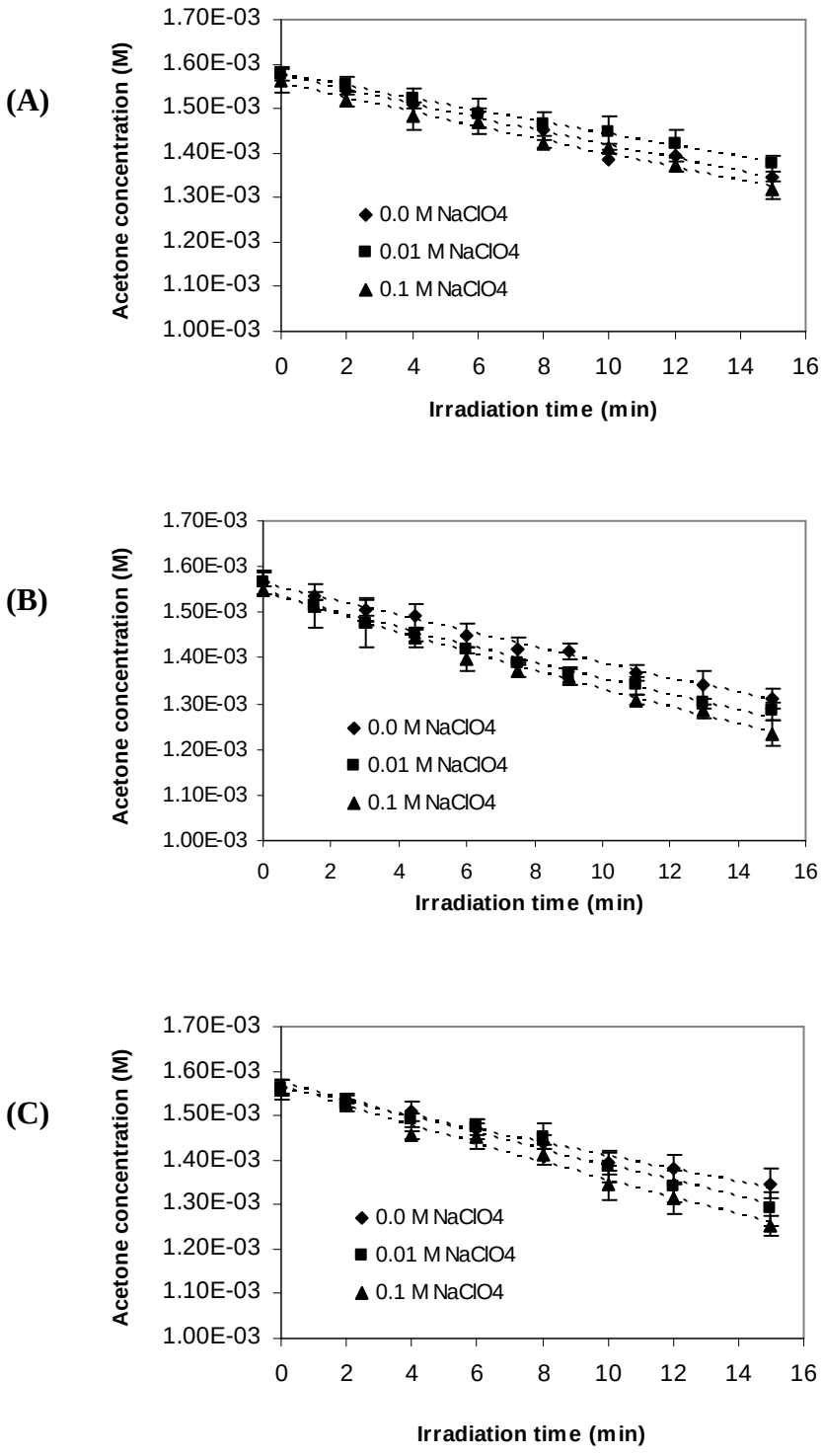

Figure 4.3. ACE concentration vs. time profile obtained from the UV/TiO_2-treatment of aqueous solutions of acetone at different ionic strengths ((as $NaClO_4$). (A) pH 4.10, (B) 6.04, (C) 8.61. (TiO_2, 2 g/L; initial concentrations, $[ACE]_o$ = (1.55-1.58) x10^{-3} M. The markers indicate experimental data. The dashed lines indicate the nonlinear least-square fit.

photocatalytic systems (Chapter 2) are given for comparison (they are presented as results for zero ionic strength).

Table 4.1. Effect of ionic strength and pH on the initial rates of isopropanol (k_{ISP}) degradation in UV-irradiated TiO_2 suspensions.

Ionic strength (as $NaClO_4$), M	**k_{ISP} (mol L^{-1} min^{-1})**		
	pH 4.10	**pH 6.04**	**pH 8.61**
0.0	$(6.22 \pm 0.09)x10^{-5}$	$(6.2 \pm 0.2)x10^{-5}$	$(7.5 \pm 0.3)x10^{-5}$
0.01	$(5.61 \pm 0.08)x10^{-5}$	$(7.5 \pm 0.2)x10^{-5}$	$(7.5 \pm 0.2)x10^{-5}$
0.1	$(6.75 \pm 0.09)x10^{-5}$	$(8.4 \pm 0.1)x10^{-5}$	$(8.0 \pm 0.2)x10^{-5}$

Table 4.2. Effect of ionic strength and pH on the initial rates of acetone (k_{ACE}) degradation in UV-irradiated TiO_2 suspensions.

Ionic strength (as $NaClO_4$), M	**k_{ACE} (min^{-1})**		
	pH 4.10	**pH 6.04**	**pH 8.61**
0.0	$(1.05 \pm 0.07)x10^{-2}$	$(1.21 \pm 0.05)x10^{-2}$	$(1.04 \pm 0.06)x10^{-2}$
0.01	$(0.90 \pm 0.06)x10^{-2}$	$(1.31 \pm 0.06)x10^{-2}$	$(1.26 \pm 0.07)x10^{-2}$
0.1	$(1.08 \pm 0.05)x10^{-2}$	$(1.51 \pm 0.02)x10^{-2}$	$(1.45 \pm 0.07)x10^{-2}$

Some features are noteworthy in the calculated kinetic parameters given in Table 4.1 and 4.2. Larger increments in the initial rates of degradation of isopropanol and acetone are observed at pH 6.04 and 8.61, respectively, in the presence of indifferent electrolyte. With respect to the conditions in the absence of $NaClO_4$, an increase of 21.0% and 35.5% was noticed in the degradation rate constants of isopropanol (k_{ISP}) at the pH of 6.04 as a result of increasing the ionic strength of the suspension to 0.01 and 0.1 M, respectively. At pH 8.61, the gradual increase in ionic strength of the suspension did not result in a gradual enhancement of the k_{ISP} values compared to the data obtained in the absence of $NaClO_4$. Only at 0.1 M ionic strength an increment of 6.67% in k_{ISP}

was observed. Meanwhile, the corresponding increments in the degradation rate constant of acetone (k_{ACE}) at pH 8.61 were 21.2% (at 0.01 M $NaClO_4$) and 39.4% (at 0.1 M $NaClO_4$). Compare to pH 8.61, the k_{ACE} values at the pH of 6.04 increased less readily at 0.01 M $NaClO_4$ (8.26% increment) but it showed a significant enhancement at 0.1 M $NaClO_4$ (24.8%).

It is noteworthy that the results obtained for both of our model compounds at pH 4.10 do not show the gradual enhancement in initial rates with increasing ionic strength. Interestingly, a decrease in reaction rates occurs for both compounds when the ionic strength is increased to 0.01 M at acidic pH. With further increase in electrolyte concentration up to 0.1 M an increment of only 8.52% was observed in k_{ISP} with respect to zero ionic strength. For the case of acetone, the k_{ACE} value remains the same at conditions of 0.0 and 0.1 M $NaClO_4$.

The observations outlined above support our hypothesis that under the right conditions of pH where both an efficient hydrogen-bonding to the surface and a suitable concentration of hydroxyl radicals are present for our model compounds, the effect of ionic strength in our photocatalytic systems would be observed. In Chapter 2, our findings showed that those favorable conditions occur at relatively neutral and basic pH (i.e., at pH 6.04 and 8.61). However, what is interesting is that despite the differences in the increments observed at pH 6.04 and 8.61, the degradation rates of isopropanol in the presence of indifferent electrolyte are fairly similar at these two pH values. Considering the intervals associated to the calculated uncertainty, the same observation is derived from the analysis of the degradation rate constants of acetone under identical experimental conditions.

Our proposed model for the hydrogen-bonding adsorption of acetone and isopropanol to the hydroxylated TiO_2 surface along with the model calculations of Rodríguez et al. (1996) that describe the effect of increasing ionic strength on the surface site speciation may explain the observations outlined above.

According to the multisite model calculations of Rodríguez et al. (1996) at the pH values of 4.10 and 6.04, the increase in ionic strength causes a major contribution of the positively charged site $\equiv Ti\text{-}OH_2^{2/3+}$ to the surface speciation. Due to its acidic character, this surface hydroxyl group may bind acetone and isopropanol, because both of our model compounds possess hydrogen acceptor capacities. It is possible that the higher positive residual charge carried by this binding site adds a strengthening component to the hydrogen-bonding interaction with our model compounds since there are dipoles associated to their hydroxyl and carbonyl functional groups. In view of this, a gradual increase in the degradation rates is expected with increasing ionic strength at conditions where the pH of the suspension is below the pH_{zpc} due to the enhancement in the adsorption of our model compounds.

Despite that a higher fraction of $\equiv Ti\text{-}OH_2^{2/3+}$ surface sites is created with increasing ionic strength at pH 4.10 than at pH 6.04, the effect of changing the distribution of surface speciation only influenced the degradation rates of our model compounds at pH 6.04. This is explained by the significantly lower rate of hydroxyl radical production at acidic pH in contrast to neutral conditions [Sun and Pignatello, 1995]. Without a proper concentration of oxidizing species to initiate the attack on our substrates an important component of the photocatalytic degradation is lacking and the expected increase in reaction rates is not observed at pH 4.10.

The effect of the increase in indifferent electrolyte concentration on the surface speciation is different at conditions of pH > pH_{zpc}. According to Rodríguez et al. (1996), at the alkaline pH of 8.60 used in our experiments as the ionic strength increases the fraction of the basic and negative $\equiv O^{2/3-}$ group becomes increasingly important. In terms of hydrogen-bonding adsorption of our model compounds, this change in surface site distribution may only affect the extent of adsorption of isopropanol since it is the only substrate possessing hydrogen donor capacities. Since the production of hydroxyl radicals is faster at alkaline conditions than at any other pH, an increase in degradation rate of isopropanol would be expected with increasing ionic strength at pH 8.60, which is not observed. As we outlined earlier, the degradation rate of isopropanol remained fairly constant and only a small increase of 6.67% was observed in k_{ISP} at 0.1 M $NaClO_4$ with respect to the value obtained at zero ionic strength.

The observations for isopropanol can find an explanation on the basis of the hydrogen-bonding ability of the alcohol. According to reported values of hydrogen-bonding empirical parameters, isopropanol is a better hydrogen acceptor ($\beta^H = 0.56$; Abraham, 1993) than a hydrogen donor ($\alpha^H = 0.33$; Abraham, 1993). Therefore, we speculate that the increase in the fraction of basic $\equiv O^{2/3-}$ sites on the surface does not have as great of an impact in the adsorption of isopropanol as it did the increase of the fraction of the acidic $\equiv Ti\text{-}OH_2^{2/3+}$ surface site at pH 6.04. In consequence, in terms of adsorption, there seems to be no significant enhancement for isopropanol with increasing ionic strength compared to the conditions in the absence of electrolyte at the alkaline pH.

For the case of acetone, the gradual increase in degradation rate with increasing ionic strength is unexpected considering the lack of interaction of this substrate with the

basic $\equiv O^{2/3-}$ surface site. Therefore, the only possible explanation for the observed trend is that due to the increasing concentration of indifferent electrolyte the electrostatic repulsion between the negative end of the carbonyl group in acetone and the negatively charged surface sites $\equiv Ti\text{-}OH^{1/3-}$ and $\equiv O^{2/3-}$ is lessened. This screening effect of ionic strength would permit the reaction of unadsorbed acetone with the adsorbed radicals ($OH^{\bullet}$ and $O^{-\bullet}$) within the thin interfacial double layer vicinal to the surface. This explanation is merely speculative and additional research is required to verify its validity.

It is worth mentioning that due to the increase in the fraction of $\equiv O^{2/3-}$ sites on the surface with increasing ionic strength at pH 8.61, a major concentration of $O^{-\bullet}$ radicals may be formed at those conditions [Salvador, 2007]. It has been previously noted that both $OH^{\bullet}$ and $O^{-\bullet}$ radicals react with aliphatic organic compounds through hydrogen abstraction reactions in aqueous solution [Neta and Schuler, 1975]. Therefore, the reactivities of these radicals toward our model compounds in the photocatalytic systems may be relatively similar. In fact, Buxton et al. (1988) reported that the rate constants for the reaction of $OH^{\bullet}$ and $O^{-\bullet}$ radicals with isopropanol in homogeneous aqueous phase are $k(OH^{\bullet} + ISP) = 1.9 \times 10^9\ M^{-1}s^{-1}$ and $k(O^{-\bullet} + ISP) = 1.2 \times 10^9\ M^{-1}s^{-1}$, respectively. In the revised literature only the value of $k(OH^{\bullet} + ACE)$ was found and is reported to be $1.3 \times 10^8\ M^{-1}s^{-1}$ [Buxton et al., 1988]. In light of this information, it is reasonable to speculate that any enhancement observed in the degradation rates of our model compounds at pH 8.61 with increasing ionic strength is mostly due to the effect that the indifferent electrolyte has in the mode of adsorption of our substrates (as explained before) and not on the relative ratio of surface radicals ($OH^{\bullet}/O^{-\bullet}$) formed on the surface [39].

[39] Buxton et al. (1988) reported a pK_a value of 11.0 for the acid/base equilibrium

In order to determine if the changes observed in the reaction rates of our model compounds are controlled by the photocatalytic process occurring on the surface of titanium dioxide, and not by the direct interaction of isopropanol and acetone with UV light, a series of experiments in the absence of catalyst (but keeping the rest of the conditions identical) were conducted. The calculated kinetic parameters corresponding to the experimental results of the control solutions are given in Tables 4.3 and 4.4.

In the absence of catalyst, for example, isopropanol degrades under a first-order reaction in all the range of experimental pH and ionic strength, contrary to the observations in the TiO_2/aqueous heterogeneous system. For both of our model compounds, the rates of degradation through the direct photolysis pathway show a tendency to decrease with the increasing concentration of indifferent electrolyte, which is in opposition to the trend observed when the degradation reaction is controlled by the TiO_2 surface.

The set of results obtained for acetone shows that this substrate undergoes direct photolysis through a first-order mechanism as it was observed in the photocatalytic systems. However, the corresponding calculated rates (k_{DP}) are one order of magnitude slower than those observed in the TiO_2 mediated photocatalytic process at conditions of relatively neutral and alkaline pH, where the major effect of ionic strength was observed.

$$OH^{\bullet} \leftrightarrow O^{-\bullet} + H^{+}$$

in homogeneous phase. However, the pK_a for this equilibrium on the surface of TiO_2 has not been determined. Assuming a similarity between the $OH^{\bullet}$ radical in the solution bulk and the adsorbed $OH^{\bullet}$ radical , less than 10% of the adsorbed hydroxyl radicals would be in the unprotonated form, $O^{-\bullet}$, at pH 8.61.

Table 4.3. Direct photolysis of isopropanol [$(1.63 \pm 0.08) \times 10^{-3}$ M] as a function of pH and ionic strength (as $NaClO_4$).

$NaClO_4$ concentration, (M)	$k_{DP, ISP}$ (min^{-1})		
	pH 4.10	**pH 6.05**	**pH 8.62**
0.0	$(1.1 \pm 0.1)\times10^{-2}$	$(7.1 \pm 0.7)\times10^{-3}$	$(8.2 \pm 0.5)\times10^{-3}$
0.01	$(1.00 \pm 0.08)\times10^{-2}$	$(5.7 \pm 0.7)\times10^{-3}$	$(8.7 \pm 0.6)\times10^{-3}$
0.1	$(1.1 \pm 0.2)\times10^{-2}$	$(3.3 \pm 0.3)\times10^{-3}$	$(7.5 \pm 0.5)\times10^{-3}$

Table 4.4. Direct photolysis of acetone [$(1.53 \pm 0.07) \times 10^{-3}$ M] as a function of pH and ionic strength (as $NaClO_4$).

$NaClO_4$ concentration, (M)	$k_{DP, ACE}$ (min^{-1})		
	pH 4.11	**pH 6.05**	**pH 8.62**
0.0	$(1.1 \pm 0.2)\times10^{-2}$	$(7.2 \pm 0.3)\times10^{-3}$	$(8.0 \pm 0.6)\times10^{-3}$
0.01	$(1.0 \pm 0.1)\times10^{-2}$	$(6.4 \pm 0.4)\times10^{-3}$	$(8.1 \pm 0.7)\times10^{-3}$
0.1	$(1.1 \pm 0.2)\times10^{-2}$	$(7.8 \pm 0.4)\times10^{-3}$	$(4.4 \pm 0.3)\times10^{-3}$

The results obtained from these control solutions of acetone and isopropanol show that the direct photolysis mechanism does not account for the values and trends observed in the fitting parameters obtained for the TiO_2 photocatalytic systems under the effect of indifferent electrolyte (as $NaClO_4$).

In light of these findings, it is reasonable to conclude that the changes observed in the fitted parameters for the photocatalytic systems are indeed controlled by the phenomena occurring at the catalyst surface under the effect of ionic strength. More evidence for direct photolysis not being important in our photocatalytic systems was given in Chapter 2.

4.3.2. Effect of ionic strength on the photocatalytic degradation of acetone and isopropanol in aqueous binary systems.

The influence of ionic strength on the photocatalytic degradation of our model compounds was examined in aqueous binary systems containing 1:1 ratios of acetone and isopropanol, under the same experimental conditions used in the single component systems. Figures 4.4 - 4.6 illustrate the results obtained in these experiments. Several common points can be noted in these figures. The first point to observe is that, according to our prediction, under all the experimental conditions the degradation of isopropanol was predominant over the degradation of acetone. Second, and probably the most striking observation, is the occurrence of inflection points in the degradation profiles of isopropanol which seem to simultaneously occur in the curves describing the change of acetone concentration in the TiO_2-containing irradiated mixtures. The figures also showed that the degradation of isopropanol in the mixtures seems to follow the same trends observed for the single component. That is, a faster decrease in isopropanol concentration over time occurs in the presence of indifferent electrolyte at the pH conditions used in these experiments. In terms of the acetone profiles, it is observed that acetone mainly accumulates in the mixtures up to the points where the inflections occur, after which a leveling off of acetone concentration (for example, at pH 6.04 in the presence of $NaClO_4$), or a sudden decrease followed by further formation is depicted (for example, as occurs at pH 4.09 and 8.61 in the presence of $NaClO_4$).

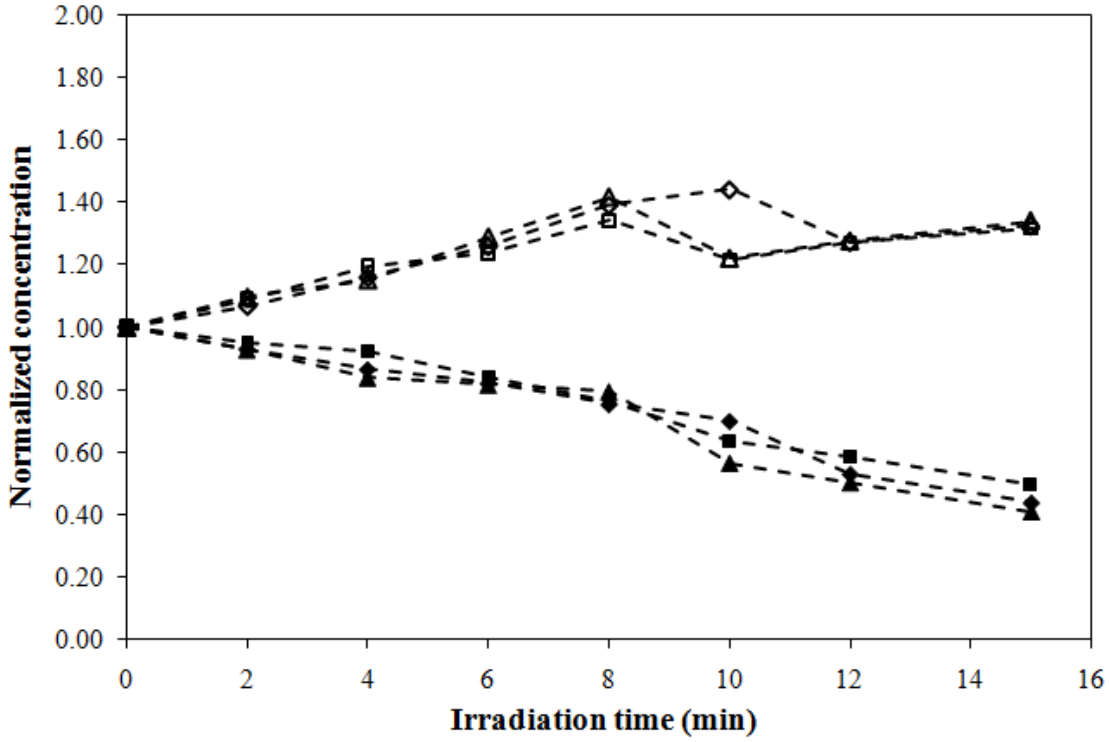

Figure 4.4. Normalized concentration vs. time profile obtained from the UV/TiO_2 treatment of 1:1 aqueous binary mixtures of isopropanol and acetone at pH 4.09 and different ionic strengths (as $NaClO_4$). Electrolyte concentration: 0.0 M (◆), 0.01 M (■), 0.1 M (▲). Open symbols represent results for acetone. Average initial concentrations: $[ISP]_o = (1.51 \pm 0.02)\ x10^{-3}$, $[ACE]_o = (1.58 \pm 0.01)\ x\ 10^{-3}$; $TiO_2 = 2$ g/L.

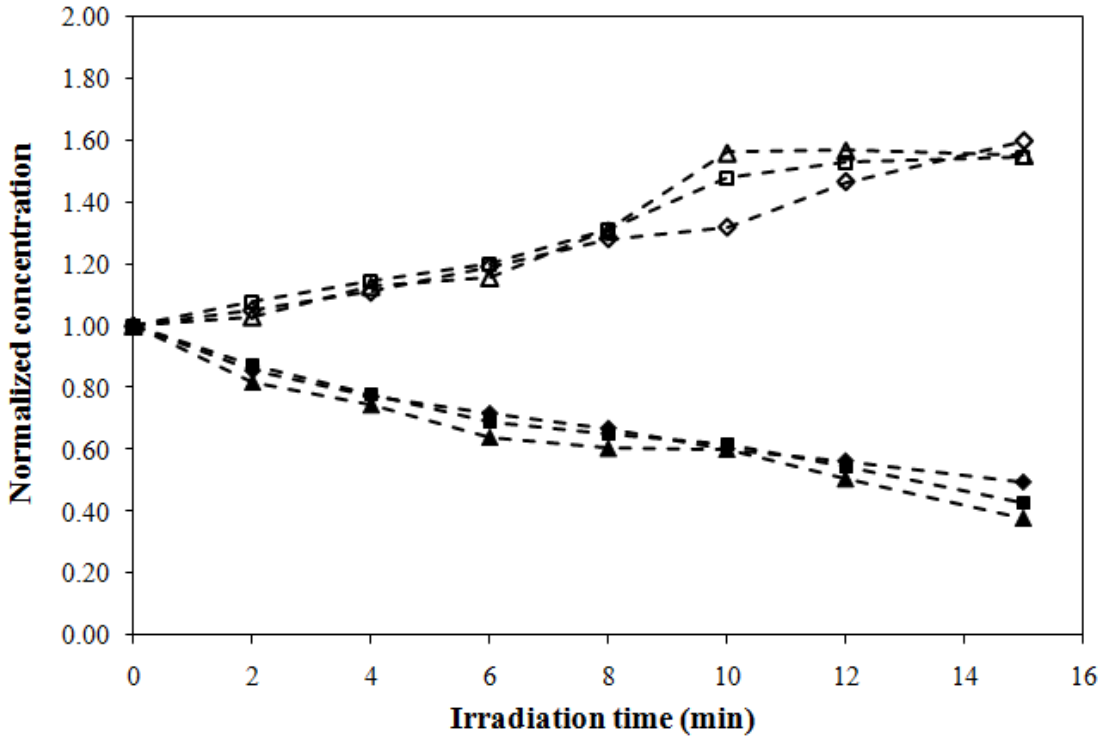

Figure 4.5. Normalized concentration vs. time profile obtained from the UV/TiO_2 treatment of 1:1 aqueous binary mixtures of isopropanol and acetone at pH 6.04 and different ionic strengths (as $NaClO_4$). Electrolyte concentration: 0.0 M (◆), 0.01 M (■), 0.1 M (▲). Open symbols represent results for acetone. Average initial concentrations: $[ISP]_o = (1.64 \pm 0.05) \times 10^{-3}$, $[ACE]_o = (1.68 \pm 0.04) \times 10^{-3}$; $TiO_2 = 2$ g/L.

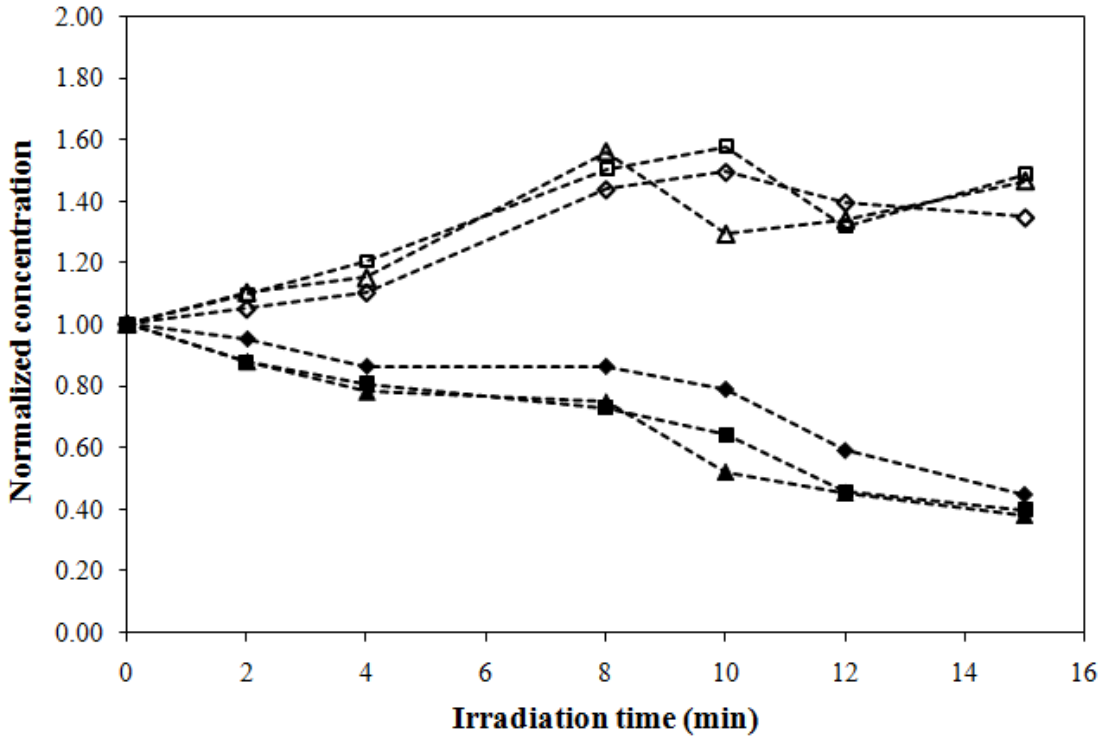

Figure 4.6. Normalized concentration vs. time profile obtained from the UV/TiO_2 treatment of 1:1 aqueous binary mixtures of isopropanol and acetone at pH 8.61 and different ionic strengths (as $NaClO_4$). Electrolyte concentration: 0.0 M (◆), 0.01 M (■), 0.1 M (▲). Open symbols represent results for acetone. Average initial concentrations: $[ISP]_o = (1.64 \pm 0.05)\ x10^{-3}$, $[ACE]_o = (1.68 \pm 0.04)\ x\ 10^{-3}$; $TiO_2 = 2$ g/L.

Since the inflection points seem to define a change in the decomposition behavior of our model compounds in the 1:1 aqueous binary mixtures, the ratios of the concentrations of isopropanol and acetone ([ISP]/[ACE]) were calculated at the times were they occurred in the corresponding curves. The calculation of these ratios illustrates that the inflection points are occurring almost consistently in the range of [ISP]/[ACE] = 0.44 – 0.57.

Further observations would be outlined if a kinetic analysis of the mixtures were performed. However, it is obvious that the mathematical model that was used in the analysis of individual component systems cannot fit the degradation of isopropanol in the mixtures.

Therefore, in order to have some level of quantitation for what is occurring under the current experimental conditions, we turned to the knowledge gained in the study of the degradation of individual compounds presented in Section 4.3.1. The kinetic parameters obtained from the single component systems and the initial concentrations of isopropanol employed in the mixtures were used to determine how much our kinetic model fails to estimate the degradation of isopropanol in the binary mixtures. For each point of the curves, we calculated the difference between the concentration of isopropanol predicted by the model (X_i) and the average experimental value (X_{exp}). The sum of the squares of these "residuals" [40] can be seen as the error of our model to predict the degradation behavior of isopropanol in the binary system. Therefore, in our

[40] Although from a strict statistic point of view these are not residuals, we adopt the term in our analysis. By definition, a residual is the difference between the fitted function and the data points [SPSS Inc.]. As we noted earlier, we are using a function that fits the degradation of the individual compound which does not necessarily correspond to the best fit for its degradation behavior in the binary system.

subsequent analysis, we will refer to the results of such calculation as the "error function". The results obtained from this analysis are given in Table 4.5.

From the values obtained for the error function at pH 4.09 and 6.04, it is evident that the prediction of the degradation of isopropanol in the mixture at each of these pH conditions incurs more error when the maximum concentration of electrolyte is used. Interestingly, at pH 8.61 the major error of the model occurred in the mixtures without electrolyte added.

Table 4.5. Calculated error function* values for the prediction of the degradation of isopropanol on its 1:1 aqueous binary mixtures with acetone in the presence of indifferent electrolyte ($NaClO_4$).

Ionic strength (as $NaClO_4$), M	Error function value		
	pH 4.09	pH 6.04	pH 8.61
0.0	6.92×10^{-8}	5.20×10^{-8}	5.08×10^{-7}
0.01	4.15×10^{-8}	1.06×10^{-7}	1.07×10^{-7}
0.1	8.25×10^{-8}	1.44×10^{-7}	1.29×10^{-7}

* See text for definition in our particular case.

It is possible to find an explanation for the results outlined above on the grounds of our hydrogen-bonding hypothesis for isopropanol and acetone, and the analysis on the effect of ionic strength on the degradation of the individual compounds. Our first observation, that is, isopropanol degrading predominantly in the mixtures, is to be expected. We already proposed (Chapter 2) that isopropanol is able to hydrogen-bond more readily to the surface than acetone, because this alcohol is both a hydrogen donor ($\alpha^H = 0.33$; Abraham, 1993) and a hydrogen acceptor ($\beta^H = 0.56$; Abraham, 1993) compound. These properties allow its interaction with both acidic and basic surface sites present in TiO_2 all the range of experimental pH. Since acetone lacks of hydrogen donor

abilities and possesses a hydrogen acceptor capacity much weaker than isopropanol (β^H = 0.49; Abraham, 1993), it will be out competed by the alcohol for degradation at the surface. However, it is plausible that the degradation of acetone only occurs when an appreciable concentration of isopropanol is already degraded in the mixtures.

This last supposition leads us to our next observation: the presence of inflection points in the concentration profiles of our model compounds obtained during 15 minutes of irradiation. We attribute the appearance of these changes to the starting point of a more favorable competition of acetone with isopropanol for binding sites and hydroxyl radicals on the TiO_2 surface. As we already noted, this effect can be seen as a leveling off of acetone concentration (e.g., as occurs at pH 6.04) or a decrease followed by further formation (e.g., as occurs at pH 4.09 and 8.61).

The leveling off of acetone concentration during the treatment process at conditions of pH 6.04 and in the presence of electrolyte suggests that the degradation of acetone occurs to a great extent to compete with its formation through the oxidation of the alcohol. At the pH of 4.09 and 8.61 (at all the ionic strength values used), although the competitive degradation of acetone clearly affects the photocatalytic oxidation of isopropanol, it does not completely offset this process and further acetone production is observed after the inflection point. In support of this view are our previous findings showing that the degradation of acetone as individual compound occurs at faster rates at relatively neutral pH, and it undergoes further enhancement with increasing ionic strength (the explanation of these findings was given in Section 4.3.1). Therefore, for the mixtures, it is reasonable to suggest that a better competition of acetone toward the predominant degradation of isopropanol on TiO_2 would occur at conditions were the

ketone (as individual compound) degraded with faster rates, as our results seem to demonstrate.

We must note, however, that this TiO_2-mediated competition is obviously conditioned to a proper ratio of isopropanol and acetone concentrations. We found that these ratios fall between 0.44 – 0.57 in our binary systems. These numbers may suggest that almost half of the initial concentration of isopropanol has to degrade in order to observe a change in the degradation profiles that may indicate the competition between the model compounds for degradation on the TiO_2 surface. However, more studies using a molar ratio 2:1 for acetone-isopropanol mixtures would be necessary to understand the chemical implications of this range.

Similarly, the values obtained for the error function can be interpreted on the basis of the knowledge gained from the single component systems under the effect of pH and ionic strength. Using this previous information it is possible to explain why at relative alkaline conditions (pH 8.61) the higher error in the prediction of isopropanol degradation occurs in the absence of electrolyte (Case I), while at pH 6.04 the larger value of the error function is obtained in the presence of 0.1 M $NaClO_4$ (Case II). In Case I, the alkaline pH created the best conditions for the adsorption of isopropanol on the surface and its subsequent reaction with hydroxyl radicals (as explained in Chapter 2). However, these conditions are not favorable for acetone degradation due to its restricted adsorption to a surface with a predominant basic character. As the degradation of isopropanol progresses, more acetone accumulates in the mixtures and the critical [ISP]/[ACE] ratio is reached. At this point, the accumulation of acetone degrading at a slow rate affects the photodegradation of isopropanol. This supposition can be

substantiated by observing Figure 4.7. This figure shows that the model predicts fairly well the degradation of isopropanol during the first minutes of irradiation, but then the values of the residuals greatly increase after the occurrence of the inflection point. This results in a larger contribution to the value of the error function. In addition, when the increasing concentration of electrolyte enhances the degradation of acetone at the relative alkaline pH, the value of the error function diminishes with respect to zero ionic strength.

In Case II, the picture is a little different. At relatively neutral pH the degradation of acetone alone is favored by the acidic character of the surface sites and the compound may react with hydroxyl radicals, which are still formed at an appreciable rate at neutral conditions [Sun and Pignatello, 1995]. Therefore, although isopropanol continues to degrade predominantly at pH 6.04 in the absence of $NaClO_4$, the presence of acetone constitutes a competition factor that was inexistent in the single component system. This may explain why early in the treatment the model fails to predict the degradation of isopropanol at pH 6.04 in contrast to 8.61, as shown in Figure 4.8A in the absence of electrolyte. However, the effect on the residuals is not as pronounced as it was at alkaline pH because acetone degrades more fairly at pH 6.04. With the addition of indifferent electrolyte, the value of the error function increases due to increasing concentration of acetone degradation on the surface, as confirmed by the level off of the acetone concentration profiles after the inflection points.

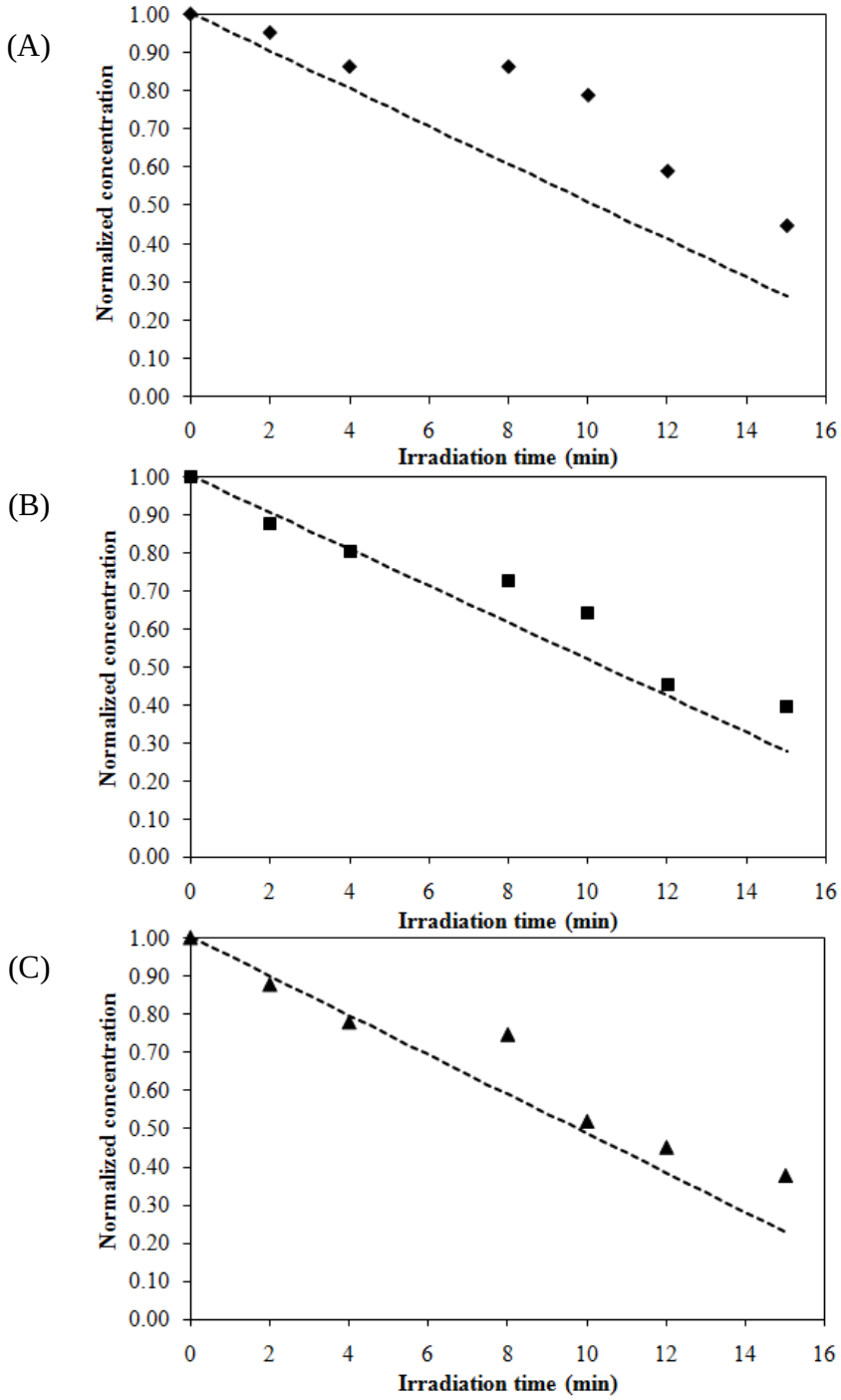

Figure 4.7. Comparison of isopropanol photodegradation in its 1:1 aqueous binary mixtures with acetone and the fitting model for its photooxidation as a single component at the initial pH 8.61 and in the presence of indifferent electrolyte (as $NaClO_4$). (A) 0.0 M $NaClO_4$, (B) 0.01 M $NaClO_4$, (C) 0.1 M $NaClO_4$. Conditions are identical to Figure 4.6. The markers indicate the experimental data. The dashed lines indicate the model for isopropanol degradation as a single component (kinetic parameters for this model were given in Table 4.1).

To summarize this subsection, our results suggest that in the 1:1 aqueous binary mixtures the presence of acetone influences the degradation of isopropanol on the TiO_2 catalyst at all conditions of pH and ionic strength, as evidenced by the appearance of inflection points in the concentration profiles. However, the magnitude of the error in the prediction of the photodegradation of isopropanol in the binary system largely depends on the capabilities of acetone to degrade at the particular conditions of the experiment. In a reaction medium where the conditions are given for a favorable degradation of acetone the error in the prediction of isopropanol degradation is not as large as in the case where acetone mainly accumulates and degrades slowly.

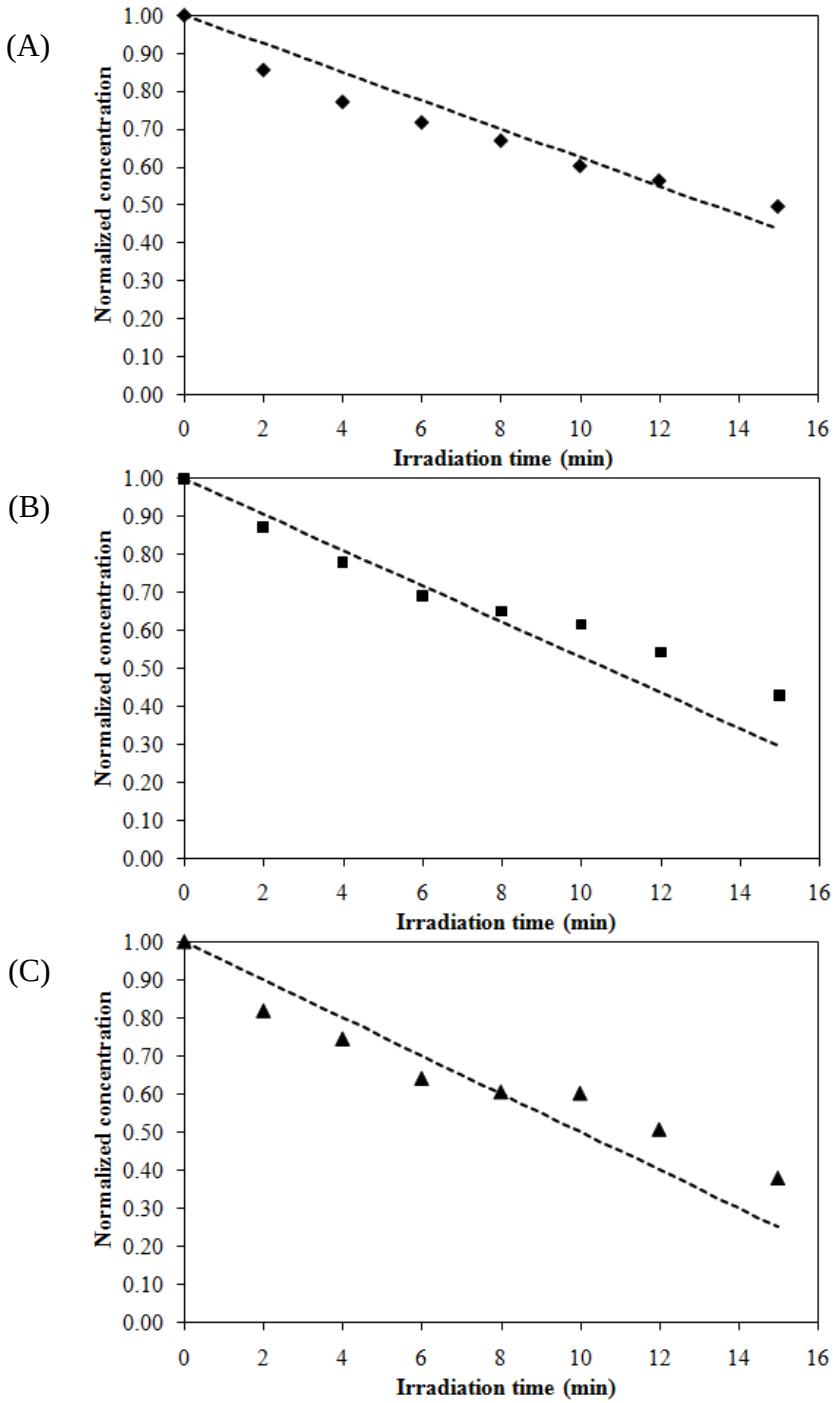

Figure 4.8. Comparison of isopropanol photodegradation in its 1:1 aqueous binary mixtures with acetone and the fitting model for its photooxidation as a single component at the initial pH 6.04 and in the presence of indifferent electrolyte (as $NaClO_4$). (A) 0.0 M $NaClO_4$, (B) 0.01 M $NaClO_4$, (C) 0.1 M $NaClO_4$. Conditions are identical to Figure 4.5. The markers indicate the experimental data. The dashed lines indicate the model for isopropanol degradation as a single component (kinetic parameters for this model were given in Table 4.1).

4.3.3. Effect of ionic strength on the photocatalytic degradation of dimethylsulfoxide in aqueous solutions.

As we mentioned earlier, we chose dimethylsulfoxide (DMSO) to test our hydrogen-bonding hypothesis using the same experimental approach employed for our previous model compounds. According to published values of hydrogen-bonding empirical parameters [Abraham, 1993], DMSO has a functional group that exhibits hydrogen acceptor capabilities that differ from those observed for isopropanol and acetone. This property is important in order to determine if a ranking of competitiveness for TiO_2-photodegradation of small polar organic compounds can be constructed based upon their hydrogen-bonding capacities. These properties are summarized and compared in Table 4.6. It is worth noting that to ensure that the differences in photodegradation rates among the studied model compounds are mostly due to their differences in adsorption abilities to the TiO_2 surface through hydrogen-bonding interactions, the third model compound must have a rate constant for the reaction with hydroxyl radicals comparable to those reported for isopropanol and acetone. DMSO meets this condition (see Table 4.6).

Table 4.6. Hydrogen-bonding empirical parameters and second order homogeneous rate constant for the reaction of hydroxyl radicals with small polar organic compounds used as model substrates.

Solute (M)	Hydrogen-bond acidity (α^H)[a]	Hydrogen-bond basicity (β^H)[a]	k($OH^\bullet$ + M) [b], $M^{-1}s^{-1}$
Acetone	0.04	0.49	1.3×10^8
Isopropanol	0.33	0.56	1.9×10^9
Dimethylsulfoxide	0.00	0.88	6.6×10^9

[a] Abraham, 1993; [b] Buxton et al., 1988.

Following the experimental approach used for isopropanol and acetone, in this section we investigated the effect of ionic strength (0.1 M $NaClO_4$) on the TiO_2-mediated photocatalytic degradation of dimethylsulfoxide. Slurries without electrolyte added were prepared in order to obtain a reference point to compare the results obtained in the presence of 0.1 M $NaClO_4$. Control solutions (without TiO_2) were also analyzed to determine if direct photolysis is an important path of degradation of DMSO under some of the experimental conditions used in the photocatalytic systems. The results of the photocatalytic studies are presented in Figure 4.9 for which the calculated kinetic parameters are given in Table 4.7. The results obtained from the control solutions are presented as insets.

Table 4.7. Effect of ionic strength and pH on the initial rates of dimethylsulfoxide (k_{DMSO}) degradation in UV-irradiated TiO_2 suspensions.

Ionic strength (as $NaClO_4$), M	**k_{DMSO} (min^{-1})**			
	pH 4.13	**pH 6.04**	**pH 8.61**	**pH 9.54**
0.0	$(5.5 \pm 0.1)x10^{-2}$	$(4.6 \pm 0.3)x10^{-2}$	$(3.8 \pm 0.2)x10^{-2}$	$(4.9 \pm 0.2)x10^{-2}$
0.1	$(4.24 \pm 0.04)x10^{-2}$	$(4.2 \pm 0.3)x10^{-2}$	$(3.6 \pm 0.1)x10^{-2}$	$(5.6 \pm 0.3)x10^{-2}$

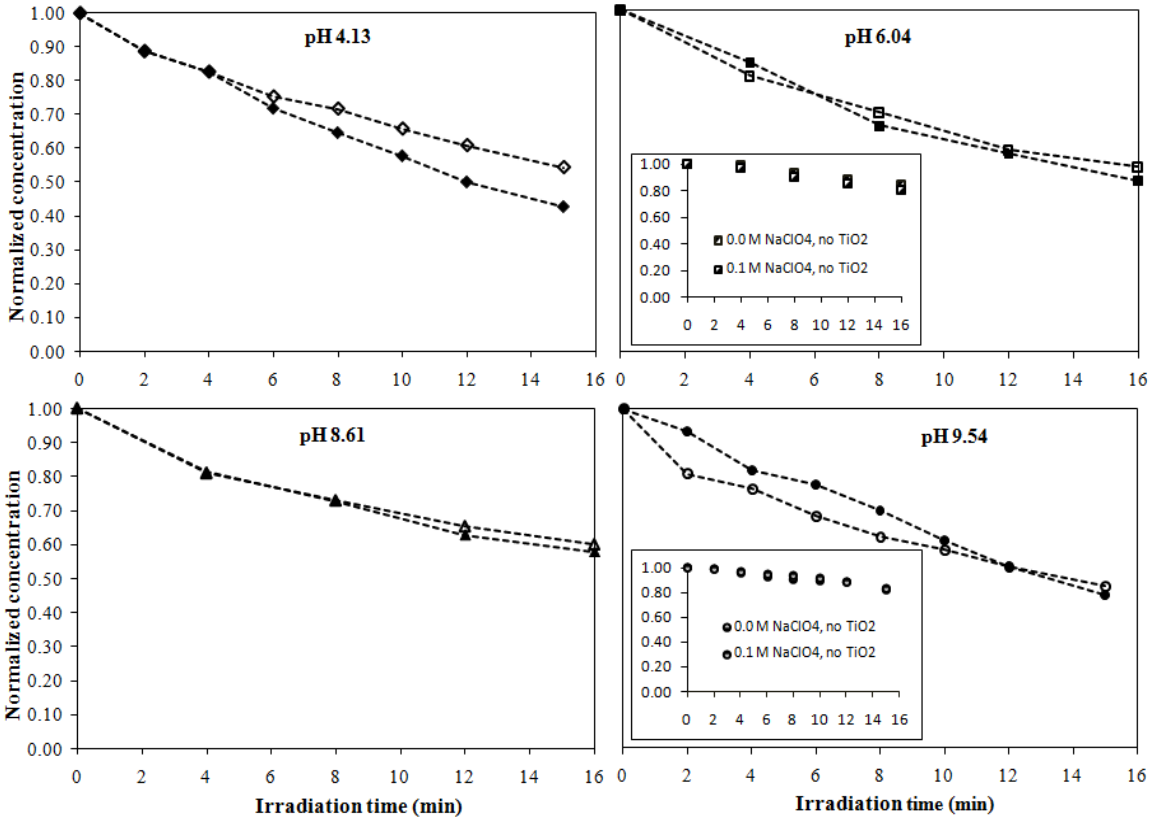

Figure 4.9. Changes in relative concentration of DMSO with irradiation time obtained from the UV/TiO_2 treatment of its slurries at different ionic strengths and pH conditions. Filled symbols correspond to 0.0 M $NaClO_4$, open symbols correspond to 0.1 M $NaClO_4$. pH conditions are given in the legends. Photocatalytic conditions: 2 g/L TiO_2, (1.42 ± 0.08) x10^{-3} M average DMSO concentration. Results from control solutions (without TiO_2) are given in the insets for comparison.

A comparison of the profiles and kinetic parameters obtained at the different pH conditions shows that the expected effect of ionic strength on the reaction rates of DMSO did not occur. At the initial pH of 4.13 the increase in ionic strength from zero to 0.1 M caused a decrease in the degradation rate of DMSO, while at pH 6.04 and 8.61 the degradation rates remain fairly similar disregarding of the increase in the ionic strength of the solutions. Only at the initial pH of 9.54 the expected trend is observed and the degradation rate of DMSO is faster in the presence of indifferent electrolyte. However, as Figure 4.9 shows, this trend is not occurring throughout the entire treatment.

It is evident that our hydrogen-bonding hypothesis and the multisite model cannot explain the trends outlined above and, therefore, we need to find a suitable explanation on the grounds of other factor that may have been unaccounted in order to explain the unexpected results.

To the best of our knowledge, there is only one report on the TiO_2 photocatalytic degradation of DMSO. In this study, Mori et al. (2006) found that the photocatalytic oxidative pathway of DMSO with hydroxyl radicals in aqueous phase produces methane sulfinic acid (MSI). We believe that although the study of initial rates of DMSO degradation may prevent a considerable accumulation of MSI in the slurries its dissociation ($pK_a = 2$; Mori et al., 2006) causes the confusing effect of pH and the concomitant problem of having a charged species in the reacting system. Therefore, we speculate that the observed change in degradation of DMSO with varying ionic strength at a given pH condition is influenced by the parallel adsorption and degradation of its photooxidation product on the TiO_2 surface.

From studies on the TiO_2-mediated photocatalytic degradation of charged species [Brown and Darwent, 1985] it is known that at pH conditions that cause the electrostatic repulsion between the ionic substrate and the charged TiO_2 surface, the rate of degradation of the former is accelerated by a high ionic strength due to a kinetic salt effect. Conversely, at pH conditions where electrostatic attraction occurs the opposite effect is observed. Applying this rationale to the adsorption and degradation of MSI at the TiO_2 surface it is possible to explain the results depicted in Figure 4.9 as follows.

At the initial acidic pH of 4.13, the TiO_2 surface is positively charged ($pH < pH_{zpc}$ of TiO_2) and electrostatic attractions favor the adsorption and degradation of the photooxidation product of DMSO, methane sulfinic acid. However, under the addition of $NaClO_4$, it is likely that the ionic strength of the solution slows down the photodegradation of the MSI^- anion, thus increasing the competition for active sites and inducing the slow decomposition of the starting reagent (DMSO). Conversely, at the initial alkaline pH of 9.54, the charged byproduct is not adsorbed due to electrostatic repulsion forces created with the negatively charged TiO_2 surface. Although the increase in ionic strength from zero to 0.1 M (as $NaClO_4$) may be lessening this repulsion, the degradation of the uncharged DMSO molecules is predominant due to reduction in the competition for active sites with its byproduct. Therefore, as a result of the combined effect of alkaline pH and ionic strength the degradation rate of DMSO increases with the addition of the indifferent electrolyte. This trend occurs up to a point (~ 12 min) where the confusing effect of pH favors the adsorption of MSI^- again, causing the reversed trend to start showing.

Although the expected influence of ionic strength on the degradation rate of DMSO occurs at pH 9.54, the results alone cannot support our hydrogen-bonding hypothesis. According to the multisite model [Rodríguez et al., 1996] a higher fraction of $\equiv O^{2/3-}$ surface sites is created on the surface of TiO_2 with an increase in ionic strength at alkaline conditions (pH > pH_{zpc} of TiO_2). In a similar fashion as acetone, it is possible that the screening effect of the electrolyte allows a better approach of the negative end of the sulfinyl group in DMSO to the negatively charged surface. In this way, DMSO reacts more readily with adsorbed radicals ($OH^{\bullet}$ and $O^{-\bullet}$) within the thin interfacial double layer vicinal to the TiO_2 surface and its rate of degradation is enhanced.

However, it is noteworthy that despite the negative impact that the charged byproduct MSI^- may have on DMSO degradation behavior, the degradation rates of DMSO are faster than those observed for acetone at any of the experimental conditions used in our experiments. This may be related to the better hydrogen acceptor capacity of the sulfinyl functional group in DMSO compared to the carbonyl group in acetone (see Table 4.4). From the results obtained with the control solutions (no TiO_2 present), it was demonstrated that those rates obtained from the study of the DMSO photocatalytic systems are controlled by the reaction with the TiO_2 surface since the direct photolysis pathway does not seem to have a comparable contribution to DMSO decomposition under similar experimental conditions (see insets in Figure 4.9).

It is important to mention at this point that another factor could be responsible for the unexpected results obtained for the degradation of DMSO under the joint effect of pH and ionic strength. It has been recognized in the past that DMSO is capable of acting as ambidentate ligand coordinating to specific metals via either oxygen or sulfur [Davies,

1981; Krishnan and Patel, 1964]. Due to the tendency of DMSO to complex with metal ions the possibility that dimethylsulfoxide participates in ligand exchange reactions with singly coordinated hydroxyl groups at the TiO_2 surface should also be considered.

On this respect, it is possible that O-bonding would be preferential in the chemisorption of DMSO on the TiO_2 surface since titanium has a strong affinity for oxygen [McMurry, 1974]. In support of this supposition is the report [Krishnan and Patel, 1974] on the preparation and characterization of titanyl complexes of the type $[TiO{\cdot}5DMSO][ClO_4]_2$. Infrared studies of these complexes implies O-bonding [Krishnan and Patel, 1974].

In light of the above, the observed trend in the degradation rate of DMSO with changes in pH from 4.13 to 8.61 can be consistent with the assumption of chemisorption to the TiO_2 surface through O-bonding with the titanium centers. The S=O bond in DMSO is polarized and, therefore, the oxygen atom carries a negative charge. With the decrease in positive charge on the TiO_2 surface as pH increases from 4.13 to 8.61, the affinity of DMSO for the TiO_2 surface diminishes thereby slowing down its photodegradation. Similarly, the noted ionic strength dependence on the degradation rate of DMSO at pH 4.13 may be viewed as a consequence of the screening effect of the indifferent electrolyte on the formation of the chemisorbed complex. However, the observed increase in degradation rate of DMSO when the solution pH varies from 8.61 to 9.54 is not consistent with this chemisorption model assumption.

Although to the best of our knowledge there are no systematic studies on the adsorption of DMSO on TiO_2 in contact with its aqueous solution, Mori et al. (2006) pointed out that adsorption of DMSO to the TiO_2 photocatalyst was not observed during

over 10 hours in the dark. In our photocatalytic systems the intended concentration of DMSO in the slurries was 1.5 $x10^{-3}$ M. After an equilibration period of 12 hours under the dark the gas chromatographic analysis of the initial concentration of DMSO in our photocatalytic systems was in average (1.42 ± 0.08) $x10^{-3}$ M.

Although more studies would be necessary to completely discard the chemisorption of DMSO to the TiO_2 surface, the results obtained in our experiments are more consistent with our initial supposition of the confusing effects of MSI on the degradation of the parent compound.

To summarize this section, our results for the third model compound, DMSO, are not enough to support or negate our hypothesis that hydrogen-bonding interactions with surface hydroxyl groups play an important role in the adsorption and degradation of small polar organic compounds in TiO_2/aqueous systems. Similarly, our results do not rule out the possibility of constructing a relative ranking of competitiveness for degradation of such compounds at the TiO_2 surface based on hydrogen-bonding capabilities. What our findings show is that in order to succeed in the construction of this ranking of degradation we must consider other factors that may obscure the surface phenomena related to hydrogen-bonding interactions of small polar organic compounds with surface hydroxyl sites. In the case of DMSO, the nature of its photodegradation product forbids the observation of the trends merely associated to the hydrogen-bonding of DMSO to the catalyst surface as result of changes in water parameters.

4.4. Conclusions

In this chapter we have obtained further evidence that supports our hypothesis that hydrogen-bonding interactions play an important role in the photocatalytic degradation of small polar organic compounds. Our experimental approach consisted in using the joint effect of pH and ionic strength on the TiO_2 surface speciation to determine if the degradation rates of small polar organic compounds were susceptible to changes in acid/base equilibria of the two types of surface hydroxyl groups.

Our results showed that there is a good correlation between the enhancement in the reaction rates of acetone and isopropanol and the increase in the acidic or basic character of the surface speciation as ionic strength of the slurries increased. Therefore, our findings cast doubt in the conception that the reaction between uncharged species and the TiO_2 surface are unaffected by changes in ionic strength of the aqueous solution.

The results obtained from the study of aqueous 1:1 binary mixtures of acetone and isopropanol also brought support to our hydrogen-bonding hypothesis. Isopropanol, the substrate bearing better hydrogen-bonding capacities, degraded predominantly in the binary system. However, at appropriate relative concentrations in the mixture ([ISP]/[ACE] = 0.44-0.57) the competition of acetone for surface sites was evidenced. It was observed in the mixtures that the experimental conditions where acetone competed more favorably against its further formation through the photooxidation of isopropanol coincided with those where acetone degraded faster as individual compound.

Finally, the study of a third model compound, DMSO, did not offer clear cut evidence to support or negate our hydrogen-bonding hypothesis due to the confusing effects caused by its charged byproduct in the photocatalytic reaction system. These

results do not rule out, however, the possibility that a relative ranking of competitiveness for degradation at the TiO_2 surface of small polar organic compounds can be constructed on the basis of their hydrogen-bonding capabilities. In order to succeed in this task, using the experimental approach employed in this study, factors that obscure the observation of trends associated to the effect of water parameters on the hydrogen-bonding of model compounds with the surface hydroxyl groups must be avoided.

For example, due to the nature of hydrogen-bonding interactions, other forms of association to the TiO_2 surface (i.e., electrostatic and inner sphere interactions) in the photocatalytic reaction medium must be completely absent or reduced to a minimum. This will not always be easy to attain since several compounds that are suitable candidates on the basis of their hydrogen-bonding capabilities (i.e., amides, amines, and carboxylic acids) possess proton related speciation and/or produce inorganic anions or ionizable organic intermediates during UV/TiO_2 treatment. Therefore, the construction of a ranking of degradation at the TiO_2 surface on the basis of hydrogen-bonding abilities of small polar organic compounds may be limited to functionalities such as alcohols, ketones, and aldehydes.

CHAPTER 5

Recommendations for future work

- Further test our hypothesis that the initial rates of isopropanol and acetone oxidation are proportional to the extent of their adsorption through hydrogen-bonding with hydroxyl groups on the TiO_2 surface by adopting Langmuir-Hinshelwood (L-H) kinetics. According to the L-H model, the observed variation in the initial rate of loss of organic (-r), with initial organic concentration (C_o) is described by the kinetic equation [Matthews, 1988]:

$$-r_o = -\frac{dC}{dt} = \frac{k_{LH} K_{LH} C_o}{1 + K_{LH} C_o} \qquad (5.1)$$

Where k_{LH} and K_{LH} are the apparent reaction rate and adsorption constants under illumination for the organic solute, respectively. K_{LH} is also known as the photoadsorption equilibrium constant. In order to estimate the parameters in Equation 5.1, a series of concentration-time runs can be made using different initial conditions of C_o, pH, and ionic strength (as $NaClO_4$) for each of our model compounds. The data sets for each solute can be treated by the method of least-squares assuming that the data is described by Equation 5.1. The calculated parameters, k_{LH} and K_{LH}, obtained for each set of experimental conditions can be evaluated on the grounds of the multisite model of the TiO_2 surface. K_{LH} values would give an estimation of the effects that changes in surface speciation have on the adsorption of our model compounds.

- Since bicarbonate and carbonate anions may compete with our model compounds for adsorption to the TiO_2 surface through hydrogen-bonding with the hydroxyl groups, the quantitation of this adsorption competition in our photocatalytic systems can be determined by adopting the extended form of the L-H equation for the initial rate of degradation of the organic substrate given in Equation 5.2 [Chen et al., 1997].

$$-r_o = -\frac{dC}{dt} = \frac{k_{deg} K_{LH} C_o}{1 + K_{LH} C_o + K_i C_i} \qquad (5.2)$$

Where k_{deg} is the rate constant, K_{LH} is the adsorption constant of the reactant of concentration C_o and K_i is the adsorption constant of an added anion of concentration C_i. Equation 5.2 can be written in the linear form [Chen et al., 1997]:

$$-r_o = -\frac{1}{k_{deg} K_{LH} C_o}\left[1 + K_{LH} C_o + K_i C_i\right] \qquad (5.3)$$

According to Equation 5.3, the values of the adsorption constants K_i for carbonate and bicarbonate anions can be determined from plots of $1/r_o$ vs. C_i at constant C_o (values of adsorption constants of our model compounds obtained in the previous proposed experimental work can be used and optimized until best fits are obtained).

- Study the photocatalytic degradation of isopropanol in the presence of inert electrolytes other than $NaClO_4$ in order to investigate the effect of different cations and anions. According to the electric double layer model, the distance (d) between the σ_o and σ_B planes (Figure 1.2) depends on the nature of the counterions and therefore one would expect a characteristic capacitance (C) value for the Stern layer for each case [Bourikas et al., 2001; Davis et al., 1978]. With changes in the C value, the concentration of highly charged surface groups (i.e.; $\equiv Ti\text{-}OH_2^{2/3+}$ and $\equiv O^{2/3-}$

groups at pH values below and above the pH_{zpc} of TiO_2, respectively) varies and may affect the adsorption and degradation of the model alcohol. Reported intrinsic equilibrium constants for the counterion association with the surface hydroxyl groups (i.e., equilibrium constants for the ion-pairs) could be used to determined suitable cations and anions to test this hypothesis.

- Study the TiO_2-mediated photocatalytic degradation of isopropanol and acetone in their binary mixtures containing a molar ratio [ISP]/[ACE] = 0.5 under the effect of ionic strength. In Chapter 4, our experimental data showed that this ratio seems to be critical for the competition of acetone with isopropanol for the binding sites on the TiO_2 surface. This study may give more insight on the chemical implications of these relative concentrations in reference to our hydrogen-bonding hypothesis.

- Study the effect of TiO_2 surface fluorination (F-TiO_2) on the photocatalytic degradation of isopropanol and acetone in order to investigate how the modification in TiO_2 surface hydroxyl groups and their related phenomena affect their decomposition. This study would give more insight on our proposed model of hydrogen-bonding between our model compounds and the surface hydroxyl groups, since in the acidic pH region the dominant surface species $\equiv Ti\text{-}OH_2^{2/3+}$ is replaced by the fluoride anion due to a complexation reaction (~ 99% completion at pH 3-4) [Mrowetz and Selli, 2005; Park and Choi, 2004]. This decrease in Brönsted acidity on the F-TiO_2 at acidic pH and the concomitant reduction of positive charge on the surface due to the fluoride adsorption are accompanied by an enhancement in

hydroxyl radical production, as determined by spin trapping techniques (valence band holes do not react with adsorbed F^-) [Morwetz and Selli, 2005]. These fluoride-induced modifications make the surface properties of F-TiO_2 very different from those on native TiO_2 in acidic aqueous medium. Therefore, it will be interesting to determine if the degradation of our model compounds is affected by these changes in surface speciation, in accord to our hydrogen-bonding hypothesis.

LITERATURE CITED

Abdullah, M.; Low, G. K.-C.; Matthews, R. W. Effect of common inorganic anions on rates of photocatalytic oxidation of organic carbon over illuminated titanium dioxide. *J. Phys. Chem*. **1990**, 94, 6820-6825.

Abraham, M. H. Scales of solute hydrogen-bonding: their construction and application to physicochemical and biochemical processes. *Chem. Soc. Rev.* **1993**, 22, 73-83.

Ace Glass, Inc. Spectral energy distribution of radiated mercury lines in Ace-Hanovia medium pressure quartz mercury vapor arc lamps. 9 pages, 2008.

Ace Glass, Inc. Photochemical equipment. Catalog 0309. 15 pages, 2008.

Ahmed, S. M. Studies of the dissociation of oxide surfaces at the liquid-solid interface. *Can. J. Chem.* **1966**, 44 (14), 1663-1670; **1966**, 44 (22), 2769-2769 (erratum).

Ahmed, S. M.; Maksimov, D. Studies of the double layer on cassiterite and rutile. *J. Colloid Interface Sci.* **1969**, 29 (1), 97-104.

Anpo, M. The effect of surface hydroxyl groups upon the deactivation of excited triplet acetone adsorbed on porous Vycor glass. *Chem. Lett.* **1987**, 1221-1224.

Anpo, M.; Kubokawa, Y. Reactivity of excited triplet alkyl ketones in solution. I. Quenching and hydrogen abstraction of triplet acetone. *Bull. Chem. Soc. Jpn.* **1977**, 50 (8), 1913-1916.

Anpo, M.; Shima, T.; Kubokawa, Y. ESR and photoluminescence evidence for the photocatalytic formation of hydroxyl radicals on small TiO_2 particles. *Chem. Lett.* **1985**, 14 (12), 1799-1802.

Araña, J.; Herrera Melián, J. A.; Doña Rodríguez, J. M.; Gonzálex Díaz, O.; Viera, A.; Pérez Peña, J.; Marrero Sosa, P. M.; Espino Jiménez, V. TiO_2-photocatalysis as a tertiary treatment of naturally treated wastewater. *Catal. Today* **2002**, 76, 279-289.

Asmus, K.-D.; Möckel, H.; Henglein, A. Pulse radiolytic study of the site of $OH^{\bullet}$ radical attack on aliphatic alcohols in aqueous solution. *J. Phys. Chem*. **1973**, 77 (10), 1218-1221.

Bahnemann, D.; Henglein, A.; Lilie, J.; Spanhel, L. Flash photolysis observation of the adsorption spectra of trapped positive holes and electrons in colloidal TiO_2. *J. Phys. Chem.* **1984a**, 88 (4), 709-711.

Bahnemann, D.; Henglein, A.; Spanhel, L. Detection of the intermediates of colloidal TiO_2-catalyzed photoreactions. *Faraday Discuss. Chem. Soc.* **1984b**, 78, 151-163.

Behar, D.; Czapski, G.; Duchovny, I. Carbonate radical in flash photolysis and pulse radiolysis of aqueous carbonate solutions. *J. Phys. Chem*. **1970**, 74, 2206-2210.

Bérubé, Y. G.; Bruyn, P. L. Adsorption at the rutile-solution interface. II. Model of the electrical double layer. *J. Colloid Interface Sci.* **1968**, 28, 92-105.

Bickley, R. I.; Jayanty, R. K. M. Photo-adsorption and photo-catalysis on titanium dioxide surfaces. Photo-adsorption of oxygen and photocatalytic oxidation of isopropanol. *Faraday Discuss. Chem. Soc.* **1974**, 58, 194-204.

Bickley, R. I.; Munuera, G.; Stone, F. S. Photoadsorption and photocatalysis at rutile surfaces. II. Photocatalytic oxidation of isopropanol. *J. Catal.* **1973**, 31, 398-407.

Boddy, P. J. The structure of the semiconductor-electrolite interface. *J. Electroanal. Chem*. **1965**, 10, 199-244.

Boehm, H. P. Acidic and basic properties of hydroxylated metal surfaces. *Discuss. Faraday Soc.* **1971**, 52, 264-275.

Boonstra, A. H.; Mutsaers, C. A. H. A. Relation between the photoadsorption of oxygen and the number of hydroxyl groups on a titanium dioxide surface. *J. Phys. Chem.* **1975**, 79 (16), 1694-1698.

Bourikas, K.; Hiemstra, T.; Van Riemsdijk, W. H. Ion pair formation and primary charging behavior of titanium oxide (anatase and rutile). *Langmuir* **2001**, 17, 749-756.

Brinkley, D.; Engel, T. Photocatalytic dehydrogenation of 2-propanol on TiO_2 (110). *J. Phys. Chem. B* **1998**, 102, 7596-7605.

Brown, G. T.; Darwent, J. R. Zeta potential and interfacial electron transfer in colloidal TiO_2. *J. Chem. Soc.; Chem. Commun*. **1985**, 2, 98-100.

Buxton, G. V.; Greenstock, C. L.; Helman, W. P.; Ross, A. B. Critical review of rate constants for reactions of hydrated electrons, hydrogen atoms and hydroxyl radicals ($OH^{\bullet}/O^{-\bullet}$) in aqueous solution. *J. Phys. Chem. Ref. Data* **1988**, 17 (2), 513-886.

Calza, P.; Pelizzetti, E. Photocatalytic transformation of organic compounds in the presence of inorganic ions. *Pure Appl. Chem.* **2001**, 73 (12), 1839-1848.

Chang, C. -P.; Chen, J. -N.; Lu, M. -C. Characteristics of photocatalytic oxidation of gaseous 2-propanol using thin-film TiO_2 photocatalyst. *J. Chem. Technol. Biotechnol.* **2004**, 79, 1293-1300.

Chavadej, S.; Phuaphromyod, P.; Gulari, E.; Rangsunvigit, P.; Screethawong, T. Photocatalytic degradation of 2-propanol by using Pt/TiO_2 prepared by microemulsion technique. *Chem. Engin. J.* **2008**, 137, 489-495.

Chen, S.; Hoffman, M. Acid-base properties of the $CO_3^{-\bullet}$ radical in aqueous solution. *Chem. Commun.* **1972**, 991-992.

Chen, J.; Ollis, D. F.; Rulkens, W. H.; Bruning, H. Photocatalyzed oxidation of alcohols and organochlorides in the presence of native TiO_2 and metalized TiO_2 suspensions. Part (I): Photocatalytic activity and pH influence. *Wat. Res.* **1999**, 33 (3), 661-668.

Chen, H. Y.; Zahraa, O.; Bouchy, M. Inhibition of the adsorption and photocatalytic degradation of an organic contaminant in an aqueous suspension of TiO_2 by inorganic ions. *J. Photochem. Photobiol., A* **1997**, 108, 37-44.

Chen, F.; Zhao, J.; Hidaka, H. Adsorption factor and photocatalytic degradation of dye constituent aromatics on the surface of TiO_2 in the presence of phosphate anions. *Res. Chem. Intermed.* **2003**, 29 (7-9), 733-748.

Clifton, C. L.; Huie, R. E. Rate constants for some hydrogen abstraction reactions of the carbonate radical. *Int. J. Chem. Kinet.* **1993**, 25 (3), 199-203.

Coronado, J. M.; Kataoka, S.; Tejedor-Tejedor, I.; Anderson, M. A. Dynamic phenomena during the photocatalytic oxidation of ethanol and acetone over nanocrystalline TiO_2: simultaneous FTIR analysis of gas and surface species. *J. Catal.* **2003a**, 219, 219-230.

Coronado, J. M.; Zorn, M. E.; Tejedor-Tejedor, I.; Anderson, M. A. Photocatalytic oxidation of ketones in the gas phase over TiO_2 thin films: a kinetic study on the influence of water vapor. *Appl. Catal. B* **2003b**, 43, 329-344.

Cundall, R. B.; Rudham, R.; Salim, M. S. Photocatalytic oxidation of propan-2-ol in the liquid phase by rutile. *J. Chem. Soc., Faraday Trans. 1*, **1976**, 72, 1642-1651.

Cunningham, J.; Hodnett, B. Kinetic studies of secondary alcohol photo-oxidation on ZnO and TiO_2 at 348 K studied by gas-chromatographic analysis. *J. Chem. Soc., Faraday Trans. 1*, **1981**, 77, 2777-2801.

Cunningham, J.; Srijaranai, S. Isotope-effect evidence for hydroxyl radical involvement in alcohol photooxidation sensitized by TiO_2 in aqueous suspension. *J. Photochem. Photobiol. A* **1988**, 43, 329-335.

Dalton, J. C.; Turro, N. J. Photoreactivity of n,π* excited states of alkyl ketones. *Ann. Rev. Phys. Chem.* **1970**, 21, 499-560.

Danielli, J. F.; Rosenberg, M. D.; Cadenhead, D. A. Electric double layer on the semiconductor-electrolite interface. *Progr. Surface Membrane Sci*. **1973**, 7, 57-93.

Davies, J. A. "The coordination chemistry of sulfoxides with transition metals" in *Advances in Inorganic Chemistry and Radiochemistry*, vol. 24, pp. 115-197, New York: Academic Press, 1981.

Davis, J. A.; James, R. O.; Leckie, J. O. Surface ionization and complexation at the oxide/water interface. I. Computation of electrical double layer properties in simple electrolytes. *J. Colloid Interface Sci.* **1978**, 63 (3), 480-499.

Dawson, P. T. Transition between localized and condensed layers in the adsorption of water vapor onto titania. *J. Phys. Chem.* **1967**, 71 (4), 838-844.

Degussa Website. https://www1.sivento.com/wps/portal/p3/aerosil/productsearch (accessed on March 4, 2004).

De Lasa, H.; Serrano, B.; Salaices, M. "Establishing photocatalytic kinetic rate equations: basic principles and parameters". Chapt. 1 in *Photocatalytic Reaction Engineering*, New York, USA: Springer Science, 2005.

El-Maazawi, M.; Finken, A. N.; Nair, A. B.; Grassian, V. H. Adsorption and photocatalytic oxidation of acetone on TiO_2: an *in situ* transmission FT-IR study. *J. Catal.* **2000**, 191, 138-146.

El-Morsi, T.; Nanny, M. A. "Photooxidation of isopropanol and acetone using TiO_2 suspension and UV light". 227th American Chemical Society Meeting, Anaheim, CA, USA, March 28-April 1, 2004.

Farkas, L.; Hirshberg, Y. The photochemical decomposition of aliphatic alcohols in aqueous solution. *J. Am. Chem. Soc.* **1937**, 59 (11), 2450-2453.

Feigenbrugel, V.; Loew, C.; Le Calvé, S.; Mirabel, P. Near-UV molar absorptivities of acetone, alachlor, metolachlor, diazinon and dichlorvos in aqueous solution. *J. Photochem. Photobiol., A* **2005**, 174, 76-81.

Fox, M. A.; Dulay, M. T. Heterogeneous photocatalysis. *Chem. Rev*. **1993**, 93, 341-357.

Frankenburg, P. E.; Noyes, W. A. Photochemical studies. XLVII. Liquid acetone-oxygen and liquid acetone-heptane-oxygen. *J. Am. Chem. Soc.* **1953**, 75, 2847-2850.

Gerischer, H.; Heller, A. The role of oxygen in photooxidation of organic molecules on semiconductor particles. *J. Phys. Chem*. **1991**, 95, 5261-5267.

Gonzalez-Elipe, A. R.; Munuera, G.; Soria, J. Photo-adsorption and photo-desorption of oxygen on highly hydroxylated TiO_2 surfaces, Part 2. – Study of radical intermediates by EPR. *J. Chem. Soc. Faraday Trans. 1* **1979**, 75, 748-761.

Griffiths, D. M.; Rochester, C. H. Infrared study of the adsorption of water on to the surface of rutile. *J. Chem. Soc. Faraday Trans. 1* **1977**, 73, 1510-1529.

Hager, S.; Bauer, R. Heterogeneous photocatalytic oxidation of organics for air purification by near UV irradiated titanium dioxide. *Chemosphere* **1999**, 38 (7), 1549-1559.

Harada, M.; Honda, M.; Yamashita, H.; Anpo, M. Preparation of titanium photocatalysts loaded on activated carbon and their photocatalytic reactivity for the degradation of 2-propanol diluted in water. *Res. Chem. Intermed*. **1999**, 25 (8), 757-768.

Harvey, P. R.; Rudham, R.; Ward, S. Photocatalytic oxidation of liquid propan-2-ol by titanium dioxide. *J. Chem. Soc., Faraday Trans. 1*, **1983**, 79, 1381-1390.

Henderson, M. A. Structural sensitivity in the dissociation of water on TiO_2 single-crystal surfaces. *Langmuir* **1996**, 12, 5093-5098.

Henderson, M. A. Acetone chemistry on oxidized and reduced TiO_2 (110). *J. Phys. Chem. B* **2004**, 108, 18932-18941.

Henglein, A. Mechanism of reactions on colloidal microelectrodes and size quantization effects. *Top. Curr. Chem.* **1988**, 143, 113-180.

Herrmann, J. M.; Pichat, P. Heterogeneous photocatalysis. Oxidation of halide ions by oxygen in ultraviolet irradiated aqueous suspension of titanium dioxide. *J. Chem. Soc. Faraday Trans. 1* **1980**, 76, 1138-1146.

Hiemstra, T.; De Wit, J. C. M.; Van Riemsdijk, W. H. Multisite proton adsorption modeling at the solid/solution interface of (hydr)oxides: a new approach. II. Application to various important (hydr)oxides. *J. Colloid Interface Sci.* **1989a**, 133 (1), 105-117.

Hiemstra, T. Van Riemsdijk, W. H. Physical chemical interpretation of primary charging behavior of metal (hydr)oxides. *Colloids Surf.* **1991**, 59, 7-25.

Hiemstra, T.; Van Riemsdijk, W. H.; Bolt, G. H. Multisite proton adsorption modeling at the solid/solution interface of (hydr)oxides: a new approach. I. Model description and evaluation of intrinsic reaction constants. *J. Colloid Interface Sci.* **1989b**, 133 (1), 91-104.

Hollabaugh, C. M.; Chessick, J. J. Adsorption of water and polar paraffinic compounds onto rutile. *J. Phys. Chem.* **1961**, 65, 109-114.

Howe, R. F.; Grätzel. EPR observations of trapped electrons in colloidal TiO_2. *J. Phys. Chem*. **1985**, 89 (21), 4495-4499.

Howe, R. F.; Grätzel, M. EPR study of hydrated anatase under UV irradiation. *J. Phys. Chem*. **1987**, 91 (14), 3906-3909.

Hu, C.; Yuchao, T.; Lanyu, L.; Zhengping, H.; Yizhong, W.; Hongxiao, T. Effects of inorganic anions on photoactivity of various photocatalysts under different conditions. *J. Chem. Technol. Biotechnol.* **2004**, 79 (3), 247-252.

Ilan, Y.; Rabani, J.; Henglein, A. Pulse radiolytic investigations of peroxy radicals produced from 2-propanol and methanol. *J. Phys. Chem*. **1976**, 80 (14), 1558-1562.

Izumi, I.; Dunn, W.; Wilbourn, K. O.; Fan, F. R. F.; Bard, A. J. Heterogeneous photocatalytic oxidation of hydrocarbons on platinized titanium dioxide powders. *J. Phys. Chem*. **1980**, 84 (24), 3207-3210.

Jackson, P.; Parfitt, G. D. Infra-red study of the surface properties of rutile. Water and surface hydroxyl species. *Trans. Faraday Soc.* **1971**, 67, 2469-2483.

Jaeger, C. D.; Bard, A. J. Spin trapping and electron spin resonance detection of radical intermediates in the photodecomposition of water at TiO_2 particulate systems. *J. Phys. Chem.* **1979**, 83 (24), 3146-3152.

Jones, P.; Hockey, J. A. Infra-red studies of rutile surfaces. Part 1. *Trans. Faraday Soc.* **1971a**, 67, 2669-2678.

Jones, P.; Hockey, J. A. Infra-red studies of rutile surfaces. Part 2.- Hydroxylation, hydration and structure of rutile surfaces. *Trans. Faraday Soc.* **1971b**, 67, 2679-2685.

Jones, P.; Hockey, J. A. Infra-red studies of rutile surfaces. Part 3.- Adsorption of water and dehydroxylation of rutile. *J. Chem. Soc., Faraday Trans. 1* **1972**, 68, 907-913.

Jurinak, J. J. Interaction of water with iron and titanium oxide surfaces: Goethite, hematite, and anatase. *J. Colloid Sci.***1964**, 19 (5), 477-487.

Kado, Y.; Atobe, M.; Nonaka, T. Ultrasonic effects on electroorganic processes – Part 20. Photocatalytic oxidation of aliphatic alcohols in aqueous suspension of TiO_2 powder. *Ultrason. Sonochem.* **2001**, 8, 69-74.

Kallay, N.; Babíc, D.; Matijevíc, E. Adsorption at solid/solution interfaces. II. Surface charge and potential of spherical colloidal titania. *Colloids Surf.* **1986**, 19, 375-386.

Kazarinov, V. E.; Andeev, V. N.; Mayarov, A. P. Investigation of the adsorption properties of the TiO_2 electrode by the radioactive tracer method. *J. Electroanal. Chem*. **1981**, 130, 277-285.

Kim, K. S.; Barteau, M. A. Reactions of aliphatic alcohols on the {011}-facetted TiO_2 (001) surface. *J. Mol. Catal.* **1990**, 63, 103-117.

Kim, K. S.; Barteau, M. A.; Farneth, W. E. Adsorption and decomposition of aliphatic alcohols on TiO_2. *Langmuir* **1988**, 4, 533-543.

Kormann, C.; Bahnemann, D. W.; Hoffman, M. R. Photolysis of chloroform and other organic molecules in aqueous TiO_2 suspensions. *Environ. Sci. Technol*. **1991**, 25 (3), 494-500.

Kozlov, D.; Bavykin, D.; Savinov, E. Effect of the acidity of TiO_2 surface on its photocatalytic activity in acetone gas-phase oxidation. *Catal. Letters* **2003**, 86 (4), 169-172.

Krishnan, V.; Patel, C. C. Dimethyl sulphoxide complexes of titanyl zirconyl and thorium perchlorates. *J. Inorg. Nucl. Chem.* **1964**, 26, 2201-2206.

Ku, Y.; Lee, W.-H.; Wang, W.-Y. Photocatalytic reduction of carbonate in aqueous solution by UV/TiO_2 processes. *J. Mol. Catal. A: Chem.* **2004**, 212, 191-196.

Kumar, P. P.; Kalinichev, A. G.; Kirkpatrick, J. R. Hydrogen-bonding structure and dynamics of aqueous carbonate species from Car-Parrinello molecular dynamics simulation. *J. Phys. Chem. B* **2009**, 113 (3), 794-802.

Kumar, A.; Mathur, N. Photocatalytic degradation of aniline at the interface of TiO_2 suspensions containing carbonate ions. *J. Colloid Interface Sci.* **2006**, 300, 244-252.

Larson, S. A.; Widegren, J. A.; Falconer, J. L. Transient studies of 2-propanol photocatalytic oxidation on titania. *J. Catal.* **1995**, 157, 611-625.

Larson, R. A.; Zepp, R. G. Reactivity of the carbonate radical with aniline derivatives. *Environ. Toxicol. Chem.* **1988**, 7, 265-274.

Lawless, D.; Serpone, N.; Meisel, D. Role of $OH^{\bullet}$ radicals and trapped holes in photocatalysis. A pulse radiolysis study. *J. Phys. Chem.* **1991**, 95, 5166-5170.

Lewis, K. E.; Parfitt, G. D. Infra-red study of the surface of rutile. *Trans. Faraday Soc.* **1966**, 62, 204-214.

Liu, H.-W.; Wu, C.-H.; Lo, J.-G. "Volatile organic compounds in wastewater during treatment" in *The Handbook of Environmental Chemistry*, vol. 5, pp. 29-70, Berlin: Springer-Verlag, 2004.

Low, G. K.-C.; McEvoy, S. R.; Matthews, R. W. Formation of nitrate and ammonium ions in titanium dioxide mediated photocatalytic degradation of organic compounds containing nitrogen atoms. *Environ. Sci. Technol.* **1991**, 25 (3), 460-467.

Mandelbaum, P. A.; Regazzoni, A. E.; Blesa, M. A.; Bilmes, S. A. Photo-electro-oxidation of alcohols on titanium dioxide thin film electrodes. *J. Phys. Chem. B* **1999**, 103, 5505-5511.

Mao, Y.; Schoeneich, C.; Asmus, K. D. Identification of organic acids and other intermediates in oxidative degradation of chlorinated ethanes on titania surfaces en route to mineralization: a combined photocatalytic and radiation chemical study. *J. Phys. Chem*. **1991**, 95 (24), 10080-10089.

Masel, R. I. "Analysis of rate data" Chap. 3 in *Chemical kinetics and catalysis.* New York, USA: John Wiley & Sons, Inc., 2001.

Matthews, R. W. Kinetics of photocatalytic oxidation of organic solutes over titanium dioxide. *J. Catal.* **1988**, 111, 264-272.

McMurry, J. E. Organic chemistry of low-valent titanium. *Acc. Chem. Res.* **1974**, 7 (9), 281-286.

Micic, O. I.; Zhang, Y.; and Cromack, K. R. Trapped holes on titania colloids studied by electron paramagnetic resonance. *J. Phys. Chem.* **1993**, 97 (28), 7277-7283.

Minero, C.; Mariella, G.; Maurino, V.; Pelizzetti, E. Photocatalytic transformation of organic compounds in the presence of inorganic anions. 1. Hydroxyl mediated and direct electron-transfer reactions of phenol on a titanium dioxide-fluoride system. *Langmuir* **2000**, 16, 2632-2641.

Miyake, M.; Yoneyama, H.; Tamura, H. Two step oxidation reactions of alcohols on an illuminated rutile electrode. *Chem. Lett.* **1976**, 5 (6), 635-640.

Monllor-Satoca, D.; Gómez, R.; González-Hidalgo, M.; Salvador, P. The "direct-indirect" model: an alternative kinetic approach in heterogeneous photocatalysis based on the degree of interaction of dissolved pollutant species with the semiconductor surface. *Catal. Today* **2007**, 129, 247-255.

Mori, M.; Tanaka, K.; Taoda, H.; Ikedo, M.; Itabashi, H. Ion-exclusion/adsorption chromatography of dimethylsulfoxide and its derivatives for the evaluation to quality-test of TiO_2-photocatalyst in water. *Talanta* **2006**, 70, 169-173.

Morrison, S. R. Surface phenomena associated with the semiconductor/electrolyte interface. *Prog. Surf. Sci*. **1971**, 1, 105-154.

Mrowetz, M.; Selli, E. Enhanced photocatalytic formation of hydroxyl radicals on fluorinated TiO_2. *Phys. Chem. Chem. Phys.* **2005**, 7, 1100-1102.

Munuera, G.; Rives-Arnau, V.; Saucedo, A. Photo-adsorption and photo-desorption of oxygen on highly hydroxylated TiO_2 surfaces, Part 1. – Role of hydroxyl groups in photo-adsorption. *J. Chem. Soc. Faraday Trans. 1* **1979**, 75, 736-747.

Munuera, G.; Stone, F. S. Adsorption of water and organic vapours on hydroxylated rutile. *Discuss. Faraday Soc.* **1971**, 52, 205-214.

Neta, P.; Schuler, R. H. Rate constants for the reaction of $O^{-\bullet}$ radicals with organic substrates in aqueous solution. *J. Phys. Chem.* **1975**, 79 (1), 1-6.

Nimlos, M. R.; Wolfrum, E. J.; Brewer, M. L.; Fennell, J. A.; Bintner, G. Gas-phase heterogeneous photocatalytic oxidation of ethanol: pathways and kinetic modeling. *Environ. Sci. Technol.* **1996**, 30, 3102-3110.

Ohko, Y.; Hashimoto, K.; Fujishima, A. Kinetics of photocatalytic reactions under extremely low-intensity UV illumination on titanium dioxide thin films. *J. Phys. Chem. A* **1997**, 101, 8057-8062.

Okamoto, K.-I.; Yamamoto, Y.; Tanaka, H.; Tanaka, M.; Itaya, A. Heterogeneous photocatalytic decomposition of phenol over TiO_2 powder. *Bull. Chem. Soc. Jpn.* **1985**, 58 (7), 2015-2022.

Öppenlander, T. *Photochemical purification of water and air. Advanced oxidation processes (AOPs): principles, reaction mechanisms, reactor concepts.* Weinheim: WILEY-VCH Verlag, 2003.

Parfitt, G. D. The surface of titanium dioxide. *Prog. Surf. Membr. Sci.* **1976**, 11, 181-226.

Park, H.; Choi, W. Effects of TiO_2 surface fluorination on photocatalytic reactions and photoelectrochemical behaviours. *J. Phys. Chem. B* **2004**, 108, 4086-4093.

Peral, J.; Ollis, D. F. Heterogeneous photocatalytic oxidation of gas-phase organics for air purification: acetone, 1-butanol, butyraldehyde, formaldehyde, and *m*-xylene oxidation. *J. Catal.* **1992**, 136, 554-565.

Peyton, G. R.; Bell, O. J.; Girin, E.; LeFaivre, M. H.; Sanders, J. *Effect of bicarbonate alkalinity on performance of advanced oxidation processes*. Denver: American Water Works Association, 1998.

Pieck, R.; Steacie, E. W. R. The photolysis of acetone in the liquid phase: the gaseous products. *Can. J. Chem.* **1955**, 33 (8), 1304-1315.

Piscopo, A.; Robert, D.; Weber, J. V. Influence of pH and chloride anion on the photocatalytic degradation of organic compounds. Part I. Effect on the benzamide and *para*-hydroxybenzoic acid in TiO_2 aqueous solution. *Appl. Catal., B* **2001**, 35 (2), 117-124.

Porter, G.; Dogra, S. K.; Loutfy, R. O.; Sugamori, S. E.; Yip, R. W. Triplet state of acetone in solution. Deactivation and hydrogen abstraction. *J. Chem. Soc., Faraday Trans. 1* **1973**, 69, 1462-1474.

Porter, G.; Yip, R. W.; Dunston, J. M.; Cessna, A. J.; Sugamori, S. E. Detection and lifetime of the triplet state of acetone in solution. *Trans. Faraday Soc.* **1971**, 67, 3149-3154.

Primet, M.; Pichat, P.; Mathieu, M. V. Infrared study of the surface of titanium dioxides. I. Hydroxyl groups. *J. Phys. Chem.* **1971**, 75 (9), 1216–1220.

Rajh, T.; Saponjic, Z. V.; Micic, O. I. Reactions of hydrous titanium oxide colloids with strong oxidizing agents. *Langmuir* **1992**, 8 (5), 1265-1270.

Regazzoni, A. E.; Mandelbaum, P.; Matsuyoshi, M.; Schiller, S.; Bilmes, S. A.; Blesa, M. A. Adsorption and photooxidation of salicylic acid on titanium dioxide: a surface complexation description. *Langmuir* **1998**, 14 (4), 868-874.

Rekoske, J. E.; Barteau, M. A. Kinetics and selectivity of 2-propanol conversion on oxidized anatase TiO_2. *J. Catal.* **1997**, 165, 57-72.

Riegel, G.; Bolton, J. R. Photocatalytic efficiency variability in TiO_2 particles. *J. Phys. Chem.* **1995**, 99, 4215-4224.

Rochester, C. H. Infrared studies of adsorbed species on rutile at the solid-vapour and solid-liquid interfaces. *Colloid Surf.* **1986**, 21, 205-217.

Rodríguez, R.; Blesa, M. A.; Regazzoni, A. E. Surface complexation at the TiO_2 (anatase)/aqueous solution interface: chemisorption of catechol. *J. Colloid Interface Sci.* **1996**, 177 (1), 122-131.

Ross, A. B.; Neta, P. Rate constants for reactions of inorganic radicals in aqueous solution. National Standard Reference Data System (NSRDS). NSRDSNBS 65, U.S. Department of Commerce. U.S. Government Printing Office, Washington, D.C: 1979. Available at: http:www.nist.gov/srd/nsrds/NSRDS-NBS-65.pdf , accessed on January 15, 2009.

Sabin, F.; Türk, T.; Vogler, A. Photo-oxidation of organic compounds in the presence of titanium dioxide: determination of the efficiency. *J. Photochem. Photobiol. A* **1992**, 63, 99-106.

Sakaguchi, N.; Matsuo, S.; Kurisaki, T.; Matsuo, T.; Wakita, H. Effect of dissolved oxygen and lanthanide ions in solution on TiO_2 photocatalytic oxidation of 2-propanol. *Res. Chem. Intermed.* **2006**, 32 (2), 95-101.

Sakata, T.; Kawai, T.; Hashimato, K. Heterogeneous photocatalytic reactions of organic acids and water. New reactions paths besides the photo-Kolbe reaction. *J. Phys. Chem.* **1984**, 88 (11), 2344-2350.

Salvador, P. On the nature of photogenerated radical species active in the oxidative degradation of dissolved pollutants with TiO_2 aqueous suspensions: a revision in the light of the electronic structure of adsorbed water. *J. Phys. Chem. C* **2007**, 111, 17038-17043.

Sanchez, J.; Augustynski, J. X-ray photoelectron spectroscopic study of the interaction of various anions with the oxide-covered titanium metal. *J. Electroanal. Chem.* **1979**, 103, 423-426.

Schindler, P. W.; Gamsjäger, H. Acid-base reactions of the TiO_2 (anatase) – water interface and the point of zero charge of TiO_2 suspensions. *Kolloid – Z. U. Z. Polymere* **1972**, 250, 759-763.

Sökmen, M.; Özkan, A. Decolourising textile wastewater with modified titania: the effect of inorganic anions on the photocatalysis. *J. Photochem. Photobiol., A* **2002**, 147, 77-81.

SPSS Inc. SigmaPlot 8.0 user's guide, http://www.physiol.ox.ac.uk/Computing/Online_Documentation/sigmaplot/spw8user.pdf/ (accessed February 24, 2009).

Staehelin, J.; Hoigne, J. Decomposition of ozone in water in the presence of organic solutes acting as promoters and inhibitors of radical chain reactions. *Environ. Sci. Technol.* **1985**, 19 (12), 1206-1213.

Stefan, M.; Hoy, A. R.; Bolton, J. R. Kinetics and mechanism of the degradation and mineralization of acetone in dilute aqueous solution sensitized by the UV photolysis of hydrogen peroxide. *Environ. Sci. Technol.* **1996**, 30, 2389-2390.

Stone, A. T.; Torrents, A.; Smolen, J.; Vasudevan, D.; Hadley, J. Adsorption of organic compounds possessing ligand donor groups at the oxide/water interface. *Environ. Sci. Technol.* **1993**, 27 (6), 895-909.

Suda, Y.; Morimoto, T. Molecularly adsorbed H_2O on the bare surface of TiO_2 (rutile). *Langmuir* **1987a**, 3, 786-788.

Suda, Y.; Morimoto, T.; Nagao, M. Adsorption of alcohols on titanium dioxide (rutile) surface. *Langmuir* **1987b**, 3, 99-104.

Sun, Y.; Pignatello, J. J. Evidence for a surface dual hole-radical mechanism in the TiO_2 photocatalytic oxidation of 2,4-dichlorophenoxyacetic acid. *Environ. Sci. Technol.* **1995**, 29, 2065-2072.

Tunesi, S.; Anderson, M. Influence of chemisorption on the photodecomposition of salicylic acid and related compounds using suspended TiO_2 ceramic membranes. *J. Phys. Chem.* **1991**, 95 (8), 3399-3405.

Turchi, C. S.; Ollis, D. F. Photocatalytic degradation of organic water contaminants: mechanisms involving hydroxyl radical attack. *J. Catal.* **1990**, 122, 178-192.

Van Veen, J. A. R.; Veltmaat, F. T. G.; Jonkers, G. A method for the quantitative determination of the basic, acidic, and total surface hydroxyl content of TiO_2. *J. Chem. Soc., Chem. Commun.* **1985**, 23, 1656-1658.

Vasudevan, D.; Stone, A. T. Adsorption of catechols, 2-aminophenols, and 1,2-phenylenediamines at the metal (hydro)oxide/water interface: effect of ring substituents on the adsorption onto TiO_2. *Environ. Sci. Technol.* **1996**, 30 (5), 1604-1613.

Verostko, C. E.; Carrier, C.; Finger, B. W. “Ersatz wastewater formulations for testing water recovery systems”. International Conference in Environmental Systems, Colorado Springs, CO, USA, July 2004.

Verostko, C. E.; Finger, B. W.; Duffield, B. E. “Design of a post-processor for a water recovery system”. International Conference on Environmental Systems, Toulouse, France, July 2000.

Villacres, R.; Ikeda, S.; Torimoto, T.; Ohtani, B. Development of a novel photocatalytic reaction system for oxidative decomposition of volatile organic compounds in water with enhanced aeration. *J. Photochem. Photobiol., A* **2003**, 160, 121-126.

Villareal, T. L.; Gómez, R.; González, M.; Salvador, P. A kinetic model for distinguishing between direct and indirect interfacial hole transfer in the heterogeneous photooxidation of dissolved organics on TiO_2 nanoparticle suspensions. *J. Phys. Chem. B.* **2004**, 108, 20278-20290.

Von Sonntag, C.; Schuchmann, H. -P. Photolysis of saturated alcohols, ethers, and amines. *Adv. Photochem.* **1977**, 10, 59-145.

Wang, K.; Hsieh, Y.; Chou, M.; Chang, C. Photocatalytic degradation of 2-chloro and 2-nitrophenol by titanium dioxide suspension in aqueous solution. *Appl. Catal., B* **1999**, 21 (1), 1-8.

Weeks, J. L.; Rabani, J. The pulse radiolysis of deaerated aqueous carbonate solutions. I. Transient optical spectrum and mechanism. II. pK for $OH^{\bullet}$ radicals. *J. Phys. Chem.* **1966**, 70, 2100-2106.

Xing-hui, X., Jian-lin, X., Ying, Y. Effects of common inorganic anions on the rates of photocatalytic degradation of sodium dodecylbenzene sulfonate over illuminated titanium dioxide. *J. Environ. Sci.* **2002**, 14 (2), 188-194.

Xu, W.; Raftery, D. *In situ* solid-state nuclear magnetic resonance studies of acetone photocatalytic oxidation on titanium oxide surfaces. *J. Catal.* **2001a**, 204, 110-117.

Xu, W.; Raftery, D. Photocatalytic oxidation of 2-propanol on TiO_2 powder and TiO_2 monolayer catalysis studied by solid-state NMR. *J. Phys. Chem. B* **2001b**, 105, 4343-4349.

Xu, W.; Raftery, D.; Francisco, J. S. Effect of irradiation sources and oxygen concentration on the photocatalytic oxidation of 2-propanol and acetone studied by in situ FTIR. *J. Phys. Chem. B* **2003**, 107, 4537-4544.

Yamagata, S.; Nakabayashi, S.; Sancier, K. M.; Fujishima, A. Photocatalytic oxidation of alcohols on TiO_2. *Bull. Chem. Soc. Jpn.* **1988**, 61, 3429-3434.

Yamashita, H.; Honda, M.; Harada, M.; Ichihashi, Y.; Anpo, M. Preparation of titanium oxide photocatalyst anchored on porous silica glass by a metal ion-implantation method and their photocatalytic reactivities for the degradation of 2-propanol diluted in water. *J. Phys. Chem. B* **1998**, 102, 10707-10711.

Yates, D. J. C. Infrared studies of the surface hydroxyl groups on titanium dioxide, and of the chemisorption of carbon monoxide and carbon dioxide. *J. Phys. Chem.* **1961**, 65 (5), 746–753.

Yates, D. E.; Levine, S.; Healy, T. W. Site-binding model of the electrical double layer at the oxide/water interface. *J. Chem. Soc. Faraday Trans. 1* **1974**, 70, 1807-1881.

Zhu, X. D.; Nanny, M. A.; Butler, E. C. Effect of inorganic anions on the titanium dioxide-based photocatalytic oxidation of aqueous ammonia and nitrite. *J. Photochem. Photobiol., A* **2007**, 185, 289-294.

APPENDIX A

Oxygen sensor system [41]

FOXY Oxygen Sensor System components

The FOXY Fiber Optic Sensor spectrophotometric system for oxygen sensing consists of these key components:

1. A fiber optic fluorescence probe in which the active material is a fluorescent ruthenium organic complex immobilized in a sub-micron thin-glass film. The FOXY-18G-AF consist of a 300 μm optical fiber housed in a 18-gauge stainless steel needle probe (1.27 mm diameter, 90 mm length tip) for penetrating vial septa.
2. A bifurcated optical fiber assembly with splice bushing that connects the fluorescence probe to the spectrometer and the LED.
3. A fiber optic spectrometer configured for fluorescence. The USB4000-FL-450 spectrometer has the advantage of plugging directly into the USB port of a computer.
4. An excitation source. The LS-450 Blue LED pulsed light source excites at 475 nm and is integrated with the spectrometer.
5. A platinum 100 ohm resistance temperature device (USB-LS-450-TP16) to monitor the temperature of the sensing environment. This 16-guage needle type RTD connects to the USB-LS-450 light source via a circular 4-pin connector.
6. The Oxygen Sensor Operating Software (OOISensors).

[41] Ocean Optics. Software, Manuals & Technical Resources. Dunedin, FL, USA. April 2006, Volume 4. CD-ROM.

How the FOXY Oxygen Sensor System works

The FOXY fiber optic oxygen sensor uses a fluorescence method to measure the partial pressure of dissolved or gaseous oxygen:

1. The pulsed blue LED sends light (at ~475 nm) to one leg of a bifurcated optical fiber.
2. The optical fiber carries the light to the FOXY probe. The distal end of the probe tip consists of a ruthenium complex trapped in a thin layer of a sol-gel matrix. This immobilizes the ruthenium complex and protects it from water.
3. The light from the LED excites the ruthenium complex at the probe tip.
4. The excited ruthenium complex fluoresces, emitting energy at ~600 nm.
5. If the excited ruthenium complex encounters an oxygen molecule the excess energy is transferred to the oxygen molecule in a non-radiative transfer, decreasing or quenching the fluorescence signal. The degree of quenching correlates to the level of oxygen concentration or to oxygen partial pressure in the film, which is in dynamic equilibrium with oxygen in the sample.
6. The fluorescence is collected by the probe and carried through the optical fiber to the spectrometer via the other leg of the bifurcated optical fiber. The fluorescence intensity is measured and related to the oxygen concentration through a second order polynomial algorithm:

$$\frac{I_o}{I} = 1 + K_1[O] + K_2[O]^2$$

Where I_o is the intensity of fluorescence at zero pressure of oxygen, I is the intensity of fluorescence at a pressure *p* of oxygen, K_1 is the first coefficient, and K_2 is the second coefficient.

Oxygen Sensor System operation: Calibration of the oxygen sensor with factory calibration and DO measurements.

Perform the steps below to calibrate the oxygen sensor for temperature compensation using the factory calibration file (0-45°C, 0-40 mg/L DO, Ocean Optics, Cat. FOXY-CAL). This file must be saved from the floppy disk into the computer before proceeding.

1. Double click on OOIBase 32 to open it. Check if the detector is acquiring data, which is shown as a continuous red baseline.
2. Open OOISensors software.
3. Select **Continuous** in the scan control and turn the switch **on** in the main display window. Position the cursor in the 600 nm peak. The FOXY and temperature probes must be in the 0% oxygen standard (i.e., nitrogen gas)
4. Set the integration time for the calibration procedure. For the USB4000 spectrometer use an integration time such that the fluorescence peak does not exceed 50000 counts. Set the integration time to powers of two to ensure a constant number of LED pulses during the integration time.
5. Select **Calibrate | Oxygen, Multiple temperature** from the menu bar. The **Multiple Temperature Calibration** screen appears.
6. Select **File | Open Calibration Table** from the menu bar. The name of the file of the in-house calibration for the FOXY system corresponds to the serial number of the probe that you are calibrating (file name: G132, file path: My Computer/Local disk C/Program files/Ocean optics). Once the file is opened, the **Calibration Table** on the screen should be populated with oxygen concentration amounts and temperatures.

7. Select the green **Curve Fit** button. Graphs displaying the curves appear in the bottom of the dialog box.
8. Click the green **Update Channel Calibration** button to save information from this calibration procedure.
9. Select **File | Close** from the menu bar to return to the main display window.
10. Select **Calibrate | Oxygen, Single Temperature** from the menu bar.
11. Click on the **Calibration Type** drop-down menu and select **Single Point**.
12. Click on the **Curve Fitting** drop-down menu and select **Second Order Polynomial**.
13. Enter the known oxygen concentration of your standard under **Concentration**.
14. Change the switch in the **Temp Compensation** section of the **Single Temperature Calibration** screen to **Yes**. The reading from the temperature probe will appear. If not, select **Action | Sample Temperature** from the menu bar in the **Single Temperature Calibration** screen.
15. Leave the oxygen probe in the standard for at least 5 minutes. This guarantees equilibrium.
16. Place the cursor in the **Intensity** box.
17. Click the green **Scan Standard** button or select **Spectrometer | Scan Standard** from the menu bar. Enable the optional **Continuous** function, located to the right of the **Scan Standard** button, to allow continuous intensity values of the standard. To use this function check the **Continuous** box.
18. Once you click the green Scan Standard button, a red Scanning button appears. Watch the values in the Intensity column. When there appears to be no changes in this value, select the read Scanning button to accept the intensity value.

19. To finalize the calibration, click the green **Curve Fit** button. A graph displaying the results of your calibration procedure appears in the bottom of the screen.
20. Save the calibration table for future use. Select **File | Save Calibration Table** from the menu bar.
21. Select **File | Close** from the menu bar to return to the main display window.
22. To start taking DO measurements of your sample insert the FOXY and temperature probes in your vial. The readings will appear in the main display window.

APPENDIX B

A fitting program for the calculation of initial degradation rates

The photodegradation modeling of small polar organic compounds used in our study was performed using a program written in Mathematica 5.2 [42] where the experimental data was related to mechanistic models expressed as the integrated rate equations for a zero- and first-order reaction of the differential equation 2.4. A least-square analysis was used to determine the best fit and the rate constant. Estimates of the uncertainty in the fitted rate constants were done based on the latest approach recommended by the International Committee for Weights and Measures (CIPM) as described by Husain and An-Nahdi (2000) [43]. According to this approach, the uncertainty $u_c(y)$ of a measurement result (or estimate) $y = f(x_1, x_2, \ldots, x_N)$ of the measurand $Y = f(X_1, X_2, \ldots, X_N)$ is the positive square root of the estimated variance $u_c^2(y)$ obtained from the following equation:

$$u_c^2(y) = \sum_{i=1}^{N} (\partial f/\partial x_i)^2 u^2(x_i) + 2 \sum_{i=1}^{N-1} \sum_{j=i+1}^{N} (\partial f/\partial x_i)\,(\partial f/\partial x_j)\, u(x_i, x_j)$$

where $u(x_i)$ is the standard uncertainty associated with the input estimate x_i, and $u(x_i,x_j)$ is the estimated covariance associated with x_i and x_j. This equation is solved by a matrix method.

[42] This program was written by Eduardo Martínez-Pedroza, Ph.D. in collaboration with the author.
[43] Husain, R.; An-Nahdi, K. A. Uncertainty calculations in a measurement standards laboratory. *Proc. Natl, Sci. Counc.* **2000**, 24, 210-215.

INPUT DATA SPECIFICATION

expTIME	List of experimental times
c_n	List of concentrations determined from replicates for each experimental time

VARIABLES

expTIME	List of experimental times
numberT	Number of experimental times
expC	List of average experimental concentrations
stdC	List of standard deviations for the experimental concentrations
A0	Initial concentration
bestk1	Best rate constant value for first-order reaction model
fitting1	Fitting evaluation for bestk1
bestk0	Best rate constant value for zero-order reaction model
fitting0	Fitting evaluation for bestk0

STANDARD PACKAGES

<<Graphics`MultipleListPlot`	This loads the MultipleListPlot package which provides a way to plot several lists of data on the same graph.
<<Statistics`MultiDescriptiveStatistics`	This loads the MultidescriptiveStatistics. The functions in this package compute descriptive statistics of data arranged in a (n x p) data matrix.

TEST CASE

To exemplify program operation, we analyze the photodegradation data of isopropanol under the effect of pH 4.10. The program code is given below.

TEST RUN

Experimental data

```
expTIME= {0,2,4,6,8,10,12,15};

c1={0.001613881, 0.001626577, 0.001607470, 0.001614996};
c2={0.001474046, 0.001478118, 0.001461148, 0.001469138};
c3={0.001393964, 0.001395667, 0.001379502, 0.001433246};
c4={0.001283007, 0.001273236, 0.001161319, 0.001164540};
c5={0.001139239, 0.001128400, 0.001140911, 0.001137969};
c6={0.000970930, 0.000974630, 0.000983719, 0.000988148};
```

c7={0.000852649, 0.000848282, 0.000878894, 0.000845495};
c8={0.000682760, 0.000683766, 0.000704979, 0.000713077};

numberT=Length[expTIME];
expCData={c1, c2, c3, c4, c5, c6, c7, c8} ;

Statistic analysis

<<Graphics`MultipleListPlot`
<<Statistics`MultiDescriptiveStatistics`

Transpose[expCData] //MatrixForm
Output =

0.00161388	0.00147405	0.00139396	0.00128301	0.00113924	0.00097093	0.000852649	0.00068276
0.00162658	0.00147812	0.00139567	0.00127324	0.0011284	0.00097463	0.000848282	0.000683766
0.00160747	0.00146115	0.0013795	0.00116132	0.00114091	0.000983719	0.000878894	0.000704979
0.001615	0.00146914	0.00143325	0.00116454	0.00113797	0.000988148	0.000845495	0.000713077

expC=Mean[Transpose[expCData]]
output = {0.00161573, 0.00147061, 0.00140059, 0.00122053, 0.00113663, 0.000979357, 0.00085633, 0.000696146}

stdC=StandardDeviation[Transpose[expCData]]
output = {$7.95493\text{x}10^{-6}$, $7.30005\text{x}10^{-6}$, $2.29438\text{x}10^{-5}$, $6.66386\text{x}10^{-5}$, $5.61723\text{x}10^{-6}$, $7.95126\text{x}10^{-6}$, $1.53281\text{x}10^{-5}$, $1.52439\text{x}10^{-5}$}

CovMatrix=Table[Covariance[expCData[[i]], expCData[[j]]], {i, numberT},{j, numberT}];
CovMatrix//MatrixForm
Output =

6.32809×10^{-11}	5.14409×10^{-11}	3.63564×10^{-11}	3.28787×10^{-10}	-4.34796×10^{-11}	-2.60583×10^{-11}	-8.63054×10^{-11}	-6.49744×10^{-11}
5.14409×10^{-11}	5.32908×10^{-11}	3.05787×10^{-11}	4.17686×10^{-10}	-3.1768×10^{-11}	-3.9553×10^{-11}	-9.02079×10^{-11}	-8.24812×10^{-11}
3.63564×10^{-11}	3.05787×10^{-11}	5.26419×10^{-10}	-4.17737×10^{-10}	-7.77409×10^{-12}	9.14005×10^{-11}	-2.55216×10^{-10}	1.7209×10^{-10}
3.28787×10^{-10}	4.17686×10^{-10}	-4.17737×10^{-10}	4.44071×10^{-9}	-1.9974×10^{-10}	-5.08707×10^{-10}	-4.6118×10^{-10}	-9.86598×10^{-10}
-4.34796×10^{-11}	-3.1768×10^{-11}	-7.77409×10^{-12}	-1.9974×10^{-10}	3.15532×10^{-11}	1.57873×10^{-11}	4.62399×10^{-11}	4.24827×10^{-11}
-2.60583×10^{-11}	-3.9553×10^{-11}	9.14005×10^{-11}	-5.08707×10^{-10}	1.57873×10^{-11}	6.32225×10^{-11}	2.40788×10^{-11}	1.19565×10^{-10}
-8.63054×10^{-11}	-9.02079×10^{-11}	-2.55216×10^{-10}	-4.6118×10^{-10}	4.62399×10^{-11}	2.40788×10^{-11}	2.3495×10^{-10}	5.49228×10^{-11}
-6.49744×10^{-11}	-8.24812×10^{-11}	1.7209×10^{-10}	-9.86598×10^{-10}	4.24827×10^{-11}	1.19565×10^{-10}	5.49228×10^{-11}	2.32377×10^{-10}

Rate Constant Calculation for first-order reaction (n=1)

mink1=0;
maxk1=1;
maxA0=expC[[1]]+stdC[[1]];
minA0=expC[[1]]-stdC[[1]];

modelC [t_, k_, A0_] := $A0e^{-kt}$

```
errorfunction[k_]:=Sum[
   (expC[[i]] - modelC[ expTIME[[i]], k, expC[[1]] ]  )^2 , {i, 1, numberT} ]

calculation=NMinimize[{errorfunction[k],  mink1 ≤  k ∧ k ≤ maxk1 }, {k},
AccuracyGoal → Infinity, PrecisionGoal → Infinity, MaxIterations → 500]
output = {1.49662x10^-8, {k → 0.0500537}}

fitting1=calculation[[1]]
output = 1.49662x10^-8

bestk1=k/.calculation[[2]]
 output = 0.0500537

ExpData=Table[{expTIME[[i]],expC[[i]]},{i,1,numberT}];

ModelData1=Table[{expTIME[[i]], modelC[expTIME[[i]],bestk1,
expC[[1]]]},{i,1,numberT}];
```

Uncertainty of Rate Constant Calculation for first-order reaction (n=1)

```
KErrorfunction[k_, A_]:=Sum[(A[[t]]-modelC[expTIME[[t]], k,  A[[1]] ])^2  ,{t, 1,
numberT} ]

KFunction1[A_]:=k/.NMinimize[{KErrorfunction[k,A],  mink1 ≤  k ∧ k≤ maxk1 }, {k},
AccuracyGoal→Infinity, PrecisionGoal→Infinity ,  MaxIterations→500][[2]]

bestk=KFunction1[expC]
output = 0.0500537

EE=IdentityMatrix[numberT];

GradKFunction=Table[(KFunction1[expC+  0.00000000001 EE[[i]] ]-
bestk)/0.00000000001,{i, 1, numberT}]

%//MatrixForm
Output =
```

$$\begin{pmatrix} 68.538 \\ -10.8239 \\ -10.5432 \\ -14.2352 \\ -17.1301 \\ -19.346 \\ -20.9927 \\ -42.2052 \end{pmatrix}$$

uncertainty1=Sqrt[Abs[GradKFunction.CovMatrix.GradKFunction]]
output = 0.000596741

Rate Constant Calculation for zero-order reaction (n=0)

mink1=0;
maxk1=1;
maxA0=expC[[1]]+stdC[[1]];
minA0=expC[[1]]-stdC[[1]];
modelC[t_, k_, A0_]:= A0-k t

errorfunction[k_]:=Sum[(expC[[i]] - modelC[expTIME[[i]],k, expC[[1]]])^2 , {i, 1, numberT}]

calculation=Minimize[{errorfunction[k], mink1≤ k ∧ k≤maxk1 }, {k}]
output = $2.94435x10^{-9}$, {k → 0.0000621819}}

fitting0=calculation[[1]]
output = $2.94435x10^{-9}$

bestk0=k/.calculation[[2]]
output = 0.0000621819

ExpData=Table[{expTIME[[i]],expC[[i]]},{i,1,numberT}];

ModelData0=Table[{expTIME[[i]], modelC[expTIME[[i]],bestk0, expC[[1]]]},{i,1,numberT}];

Uncertainty of Rate Constant Calculation for zero-order reaction (n=0)

bestk0=KFunction1[expC]
output = 0.0000621819

GradKFunction=Table[(KFunction1[expC+ 0.00000000001 EE[[i]]]-KFunction1[expC])/0.00000000001,{i, 1, numberT}]
Output = {0.0967742,-0.00196487,-0.00679117,-0.0101868,-0.0135823,-0.0221793,-0.0203735,-0.0254669}

%//MatrixForm

$$\begin{pmatrix} 0.0967742 \\ -0.00196487 \\ -0.00679117 \\ -0.0101868 \\ -0.0135823 \\ -0.0221793 \\ -0.0203735 \\ -0.0254669 \end{pmatrix}$$

uncertainty0=Sqrt[Abs[GradKFunction.CovMatrix.GradKFunction]]
output = 8.82167×10^{-7}

Summary

expC
output = {0.00161573, 0.00147061, 0.00140059,0.00122053, 0.00113663, 0.000979357, 0.00085633, 0.000696146}

stdC
output = {7.95493×10^{-6}, 7.30005×10^{-6}, 2.29438×10^{-5}, 6.66386×10^{-5}, 5.61723×10^{-6}, 7.95126×10^{-6}, 1.53281×10^{-5}, 1.52439×10^{-5}}

First-order model

bestk1
output = 0.0500537

fitting1
output = 1.49662×10^{-8}

uncertainty1
output = 0.000596741

MultipleListPlot[ExpData, ModelData1, PlotRange→{0,0.002}, PlotJoined→True]

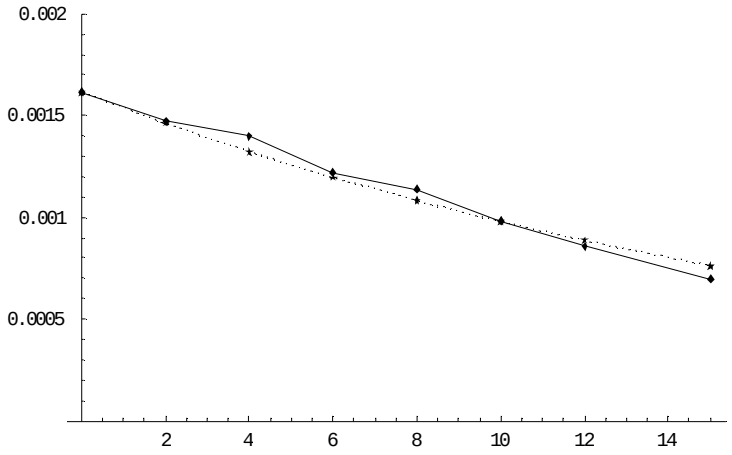

Zero-order model

bestk0
output = 0.0000621819

fitting0
output = 2.94435×10^{-9}

uncertainty0
output = 8.82167×10^{-7}

MultipleListPlot[ExpData, ModelData0, PlotRange→{0,0.002}, PlotJoined→True]

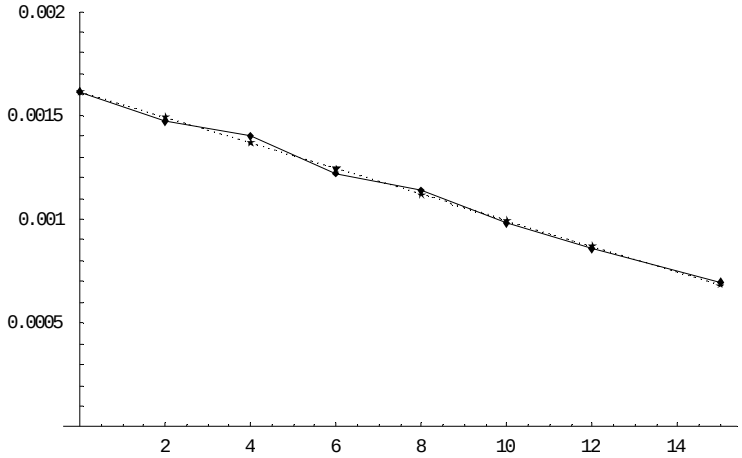

APPENDIX C

Estimation of the fraction of hydroxyl radicals reacting with isopropanol and acetone in homogeneous solution

This appendix is related to Chapter 3. It provides the details to estimate the fraction of hydroxyl radicals ($f_{OH^\bullet,i}$) that reacts with a system component, S_i. In our particular systems the component can be isopropanol, acetone or carbonate species. As we already stated before, the calculation assumes a strictly homogeneous kinetic system and only represents the efficiency at the start of the treatment.

As stated by Larson and Zepp (1988) [44] The equation used for the calculation of ($f_{OH^\bullet,i}$) is described by:

$$f_{OH^\bullet,\,i} = \frac{k(OH^\bullet + i)[S_i]}{\sum_i k(OH^\bullet + i)\,[S_i]}$$

Where $k(OH^\bullet + i)$ is the second-order rate constant for the reaction of hydroxyl radicals with the system component, $[S_i]$ is the molar concentration of the system component, and $\sum_i k(OH^\bullet + i)\,[S_i]$ represents the rate for $OH^\bullet$ scavenging in the system. In our photocatalytic systems, the major potential reactions of $OH^\bullet$ are with the organic model compound (isopropanol or acetone), bicarbonate, and carbonate anions.

Tables C.1 and C.2 show the computed values of $f_{OH^\bullet,i}$ for isopropanol and acetone in our photocatalytic systems.

[44] Larson, R. A.; Zepp, R. G. Reactivity of the carbonate radical with aniline derivatives. *Environ. Toxicol. Chem.* **1988**, 7, 265-274.

Table C.1. Calculation of the $f_{OH^\bullet,i}$ values for isopropanol in the presence of 0.01 M Na_2CO_3 at various initial pH values.

Potential $OH^\bullet$ scavenger	**$[S_i]$ (M)**	**$k(OH^\bullet+i)$ ($M^{-1}s^{-1}$)**	**$k(OH^\bullet+i)[S_i]$ (s^{-1})**	**$f_{OH^\bullet,i}$**
Kinetic system (pH 6.35)				
HCO_3^-	5.62×10^{-3}	8.5×10^6	4.7×10^4	0.02
isopropanol	1.54×10^{-3}	1.9×10^9	2.9×10^6	0.98
		$\sum_i k(OH^\bullet+i)[S_i] =$	2.9×10^6	
Kinetic system (pH 8.35)				
HCO_3^-	0.01	8.5×10^6	8.5×10^4	0.03
isopropanol	1.56×10^{-3}	1.9×10^9	2.9×10^6	0.97
		$\sum_i k(OH^\bullet+i)[S_i] =$	3.0×10^6	
Kinetic system (pH 10.36)				
HCO_3^-	5.0×10^{-3}	8.5×10^6	4.3×10^4	0.008
CO_3^{2-}	5.0×10^{-3}	3.9×10^8	2.0×10^6	0.38
isopropanol	1.62×10^{-3}	1.9×10^9	3.1×10^6	0.61
		$\sum_i k(OH^\bullet+i)[S_i] =$	5.1×10^6	
Kinetic system (pH 12.0)				
CO_3^{2-}	0.01	3.9×10^8	3.9×10^6	0.56
isopropanol	1.62×10^{-3}	1.9×10^9	3.1×10^6	0.44
		$\sum_i k(OH^\bullet+i)[S_i] =$	7.0×10^6	

Table C.2. Calculation of the $f_{OH^\bullet,i}$ values for acetone in the presence of 0.01 M Na_2CO_3 at various initial pH values.

Potential $OH^\bullet$ scavenger	**$[S_i]$ (M)**	**$k(OH^\bullet+i)$ ($M^{-1}s^{-1}$)**	**$k(OH^\bullet+i)[S_i]$ (s^{-1})**	**$f_{OH^\bullet,i}$**
Kinetic system (pH 6.35)				
HCO_3^-	5.62×10^{-3}	8.5×10^6	4.8×10^4	0.18
acetone	1.69×10^{-3}	1.3×10^8	2.2×10^5	0.82
		$\sum_i k(OH^\bullet+i)[S_i] =$	2.7×10^5	
Kinetic system (pH 8.35)				
HCO_3^-	0.01	8.5×10^6	8.5×10^4	0.28
acetone	1.70×10^{-3}	1.3×10^8	2.2×10^5	0.72
		$\sum_i k(OH^\bullet+i)[S_i] =$	3.1×10^5	
Kinetic system (pH 10.36)				
HCO_3^-	5.0×10^{-3}	8.5×10^6	4.3×10^4	0.01
CO_3^{2-}	5.0×10^{-3}	3.9×10^8	2.0×10^6	0.88
acetone	1.65×10^{-3}	1.3×10^8	2.1×10^5	0.10
		$\sum_i k(OH^\bullet+i)[S_i] =$	2.2×10^6	
Kinetic system (pH 12.0)				
CO_3^{2-}	0.01	3.9×10^8	3.9×10^6	0.95
acetone	1.58×10^{-3}	1.3×10^8	2.1×10^5	0.05
		$\sum_i k(OH^\bullet+i)[S_i] =$	4.1×10^6	

APPENDIX D

Effect of carbonate-bicarbonate alkalinity on the direct photolysis of acetone and isopropanol in aqueous solutions

This appendix provides the kinetic parameters (initial rate constants, k_{DP}) for the UV direct photolysis of acetone and isopropanol in the presence of 0.01 M Na_2CO_3 at different initial pH conditions. This table is related to Chapter 3.

Table D.1. Direct photolysis of isopropanol [(1.70-1.73) $x10^{-3}$ M] and acetone [(1.64-1.71) $x10^{-3}$ M] as a function of pH in the presence of 0.01 M Na_2CO_3.

Initial pH	k_{DP} (min^{-1})	
	Isopropanol	**Acetone**
6.42	$(7.4 \pm 0.1)\ x10^{-3}$	---
8.15	$(6.4 \pm 0.2)\ x10^{-3}$	$(2.8 \pm 0.1)\ x10^{-3}$
11.01	$(1.56 \pm 0.05)\ x10^{-3}$	$(2.2 \pm 0.2)\ x10^{-3}$
12.09	$(2.60 \pm 0.08)\ x10^{-3}$	$(3.3 \pm 0.2)\ x10^{-3}$